٥٦٢٨

IMPRIMATUR POUR LA THÈSE

Coordination Behaviour of Polydentate Aromatic N-donor Ligands: Ability to form Coordination Polymers

de Mme Marion Graf

UNIVERSITÉ DE NEUCHÂTEL

FACULTÉ DES SCIENCES

La Faculté des sciences de l'Université de Neuchâtel sur le rapport des membres du jury,

Mme et MM. les professeurs H. Stoeckli-Evans, R. Deschenaux et A. Williams (Genève)

autorise l'impression de la présente thèse.

Neuchâtel, le 4 mai 1995

Le doyen:

H.-H. Nägeli

For my family and friends

UNIVERSITE DE NEUCHATEL
FACULTE DES SCIENCES

"Coordination Behaviour of Polydentate Aromatic N-donor Ligands: Ability to form Coordination Polymers"

Thèse présentée à la Faculté des Sciences par

Marion Graf
(Dipl.-Chem.)

Chimiste diplômé de
Martin -Luther-Universität Halle-Wittenberg, Allemagne

pour l'obtention du grade
de Docteur ès Sciences

Institut de Chimie
de l'Université de
Neuchâtel

Novembre 1994

Thank

Specially I would like to thank my supervisor **Prof. H. Stoeckli-Evans** for the opportunity to study this subject, teaching the theory and practical applications of crystallography as well as for all support and help.

Furthermore I would like to thank

Prof. F. Stoeckli
for making available financial support

Dr. Gerd Rheinwald
for the introducing a drawing package for X-ray structures and helpful discussions about crystallography

Mdm. Dr. Meilleco Dai, Dr. S. Claude, Heinz Bursian
for recording n.m.r. spectra on the 400 MHz machine

Prof. A. Escuer and R. Vicente (Barcelona, Spain)
for magnetic investigations

Prof. W. Schläpfer (Fribourg)
for recording e.p.r. spectra

Antonia Neels
for collaboration in our laboratory and recording of some structure data sets

Dr. L. Jäger (Halle, Germany)
for supplying some pseudohalide compounds

and the **Swiss National Foundation** for financial support.

I have to thank especially my husband Dr. Hans-Christian Böttcher for all help and my little persevering doughter Pauline for all comprehension. My family I want to thank for making available the possibility to go this scientific way and for all assistance.

Index

Liste of Abbreviation:

b	broad
BEDT-TTF	bis(ethylendithio)tetrathiofulvalene
BDPQ	2,3-bis(2-pyridyl)benzoquinoxaline
bppz	2,3-bis(2-pyridyl)pyrazine
bpq	2,3-bis(2-pyridyl)quinoxaline
bpy	4,4'-bipyridine
bpyac	bis(4-pyridyl)acetylen
bzd	benzidine
ClDPQ	6-chloro-2,3-bis(2-pyridyl)-quinoxaline
COSY-	double-quantum-filtered correlation spectroscopy
d	doublet
dabco	1,4-diazabicyclo[2.2.2]octan
dpp	2,3-bis(2-pyridyl)-pyrazine
dppe	bis(diphenylphosphino)ethane
dppm	bis(diphenylphosphino)methane
dpq	2,3-bis(2-pyridyl)-quinoxaline
DSS	3-trimethylsilyl-1-propansulfonic acid sodiumsalt
pzd	pyrazinedicarboxylic acid
edta	ethylenediamintetraacetic acid
en	ethylendiamine
ET	BEDT-TTF
Fig.	figure
hfac	hexafluoroacetylacetonate
H_4pztc	pyrazine-2.3.5.6-tetracarboxylic acid
ida	iminodiacetate
m	multiplett
ma	malonate

NIT-R	2-substituted-4.4.5.5-tetramethylimidazoline-1-oxyl-3-oxide
ox	oxalate
pba	1,3-propylenebis(oxamate)
pbaOH	2-hydroxy-1,3-propylenebis(oxamate)
pc	phthalocyanine
p-dip	1,4-dicyano-benzene
ppd	p-phenylenediamine
p-py	p-pyridine
r.e.	reference electrode
s	strong
sh	shoulder
$sqacH_2$	squaric acid
t	triplet
Tab.	table
TAMP	tetrakis(aminomethyl)-2.3.5.6-pyrazine
TBAP	tetrabutylammoniumphosphate
T_c	Curie temperature
TCNQ	tetracyanochioodimethane
terpy	2,2':6',2"-terpyridyl
tppz	2.3.5.6-tetrakis(2-pyridyl)pyrazine
tptz	2.4.6-tris-(2-pyridyl)-1.3.5-triazine
tpymt	2.4.6-tris(2-pyrimidyl)-1.3.5-triazine
tren	2.2',2"-triaminotriethylamine
TTF	tetrathiofulvalene
tz	1.2.4.5-tetrazin
w.e.	working electrode

1. Introduction

Molecular-based ferromagnets, synthetic metallic conductors, non-linear optical materials, and ferroelectrics are some important applications of low dimensional coordination polymers. It should be possible to modify the bulk magnetic, electrical and optical properties of such materials by the careful design of the corresponding constituent molecules. A recent review by Chen and Suslick[1] presents examples of some applications mentioned above and focuses on the correlation between the molecular structure and the bulk properties of these materials. Generally, coordination polymers are conceivable by the combination of polydentate ligands with suitable transition metals.

At the University of Neuchâtel Werner Marty developed the original idea of using tetrasubstituted pyrazines as potentially bis(tridentate) chelating ligands with first row transition metals to form such coordination polymers. Marty wanted to form what he called a "columnane", in which the bridging ligands along the chain would be mutually perpendicular to one another. A number of coordination polymers have been formed from the reaction of transition metal salts with pyrazine-2.3.5.6-tetracarboxylic acid[2] (H_4pztc) and with tetrakis(aminomethyl)-2.3.5.6-pyrazine[3,4] (tamp). In this work we wanted to continue these investigations on the coordination behaviour of such polydentate N-donor ligands with she goal of obtaining the corresponding coordination polymers. At first the structural investigations by means of X-ray analysis methods should be undertaken to examine the coordination mode. Furthermore the study of the magnetic properties and the conducting properties of some Cu^{2+}-complexes and polymers should be investigated.

In the following some explanations of recent results in this interesting field of chemistry are given.

---

[1] C. T. Chen, K. S. Suslick, *Coord. Chem. Rev.*, 128 (1993) 293.

[2] P.-A. Marioni, Thèse de Doctorat, Université de Neuchâtel (1986).

[3] M. Ferigo, Thèse de Doctorat Université de Neuchâtel (1988).

[4] M. Ferigo, P. Bonhôte, W. Marty, H. Stoeckli-Evans, *J. Chem. Soc., Dalton Trans.*, (1994) 1549.

1.1. Coordination polymers as molecular magnets

During the last decade several types of light weight "molecular magnets" based on one-dimensional coordination polymers have been observed and summarized in some review articles[1,5,6]. Ferromagnetism, ferrimagnetism and antiferromagnetism all originate from the cooperative behaviour of magnetic spin within a solid. A great deal of research in this field of chemistry has been carried out by O.Kahn and co-workers. In one of their recent publications[7] they give a schematic representation of the non-zero magnetization of two dimensional array's of spins as shown in Fig. 1.

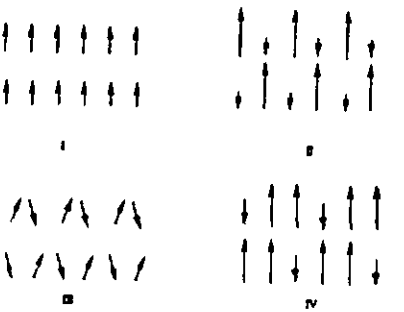

Fig. 1. Schematic representations of non-zero magnetization of two-dimensional arrays of spins.

I: The interactions between the nearest neighbours are ferromagnetic, the local spin tend to align along the same direction.

II: All interactions between the nearest neighbours are antiferromagnetic, resulting in a non-zero spin between centers.

III: All the spin carriers are similar and couple antiferromagnetically and result in a non-zero spin because of a small canting.

---

[5]J. S. Miller, A.J. Epstein, *Chem. Rev.* ,88 (1988) 201.

[6]M. Inoue, M. Kubo, *Coord. Chem. Rev.*, 88 (1988) 201.

[7]E. Bakalbassis, P. Bergarat, O. Kahn, S. Jeanniny, Y. Jeannin, Y. Dromzee, M.Guillot, *Inorg. Chem.*, 31 (1992) 625.

IV: A non-zero spin arises from a very complicated spin structure involving both ferromagnetic and antiferromagnetic couplings with canting as an additional possibility.

Gatteschi and co-workers[8] have synthesized metal complexes of nitronyloxide which can form linear chains after introducing additional bridging ligands to build polymers of the type $[\{M(hfac)_2(NIT\text{-}R)\}_x]$ (NIT-R=2-substituted-4,4,5,5-tetramethylimidazoline-1-oxyl-3-oxide; hfac = hexafluoroacetylacetonate with M = Mn^{2+}, Ni^{2+}, Cu^{2+}). The magnetic properties can be ferromagnetic (M = Cu^{2+}) or ferrimagnetic (M = Mn^{2+} or Ni^{2+}). The nitronyloxide units also provide an unmatched spin and this leads to a non compensated net moment. Covalent connections may also increase the magnetic interactions between the chains. One example is $[\{Cu(hfac)_2\}_3(NIT\text{-}pPy)_2]_x$ (pPy = p-pyridine) which forms one-dimensional polymer chains. The chain consists of dimeric units of $[\{Cu(hfac)_2\}_3(NIT\text{-}pPy)_2]$ bridged by $[Cu(hfac)_2]$ molecules, shown in Fig. 2.

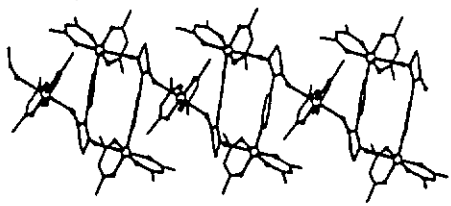

Fig. 2. The chain structure formed by dimeric units of $[\{Cu(hfac)_2\}_3(NIT\text{-}pPy)_2]$ bridged by $[Cu(hfac)_2]$ moieties.

---

[8]A. Canneschi, D. Gatteschi, J. Laugier, *J. Am. Chem. Soc.*, 109 (1987) 2191.

A. Canneschi, D. Gatteschi, P. Rey, R. Sessoli, *Inorg. Chem.*, 27 (1988) 1756.

A. Canneschi, D. Gatteschi, J.P. Renard, P. Rey, R. Sessoli, *Inorg. Chem.*, 28 (1989) 2940.

A. Canneschi, F. Ferrara, D. Gatteschi, P. Rey, R. Sessoli, *Inorg. Chem.*, 30 (1991) 3162.

C. Benelli, A. Canneschi, D. Gatteschi, P. Rey, L. Pardi, *Inorg. Chem.*, 31 (1992) 741.

Magnetic studies of this one-dimensional chain exhibit an antiferromagnetic behaviour. With this ligand also mixed valent compounds of the type $[Mn_2M(hfac)_6(NIT\text{-}pPy)_2]$, (M = Mn,Co,Ni) were obtained. No crystal structurel data have been reported. Interestingly, all these compounds give rise to spontaneous magnetization below 10 K.

Since 1987 the study of the magnetic behaviour by ordered biheterometallic systems has been published by O. Kahn and co-workers[9]. They synthesized and characterized the following coordination polymers by X-ray structure analysis and magnetic measurements: $[MnCu(pbaOH)(H_2O)_3]_x$(I), pbaOH = 2-hydroxy-1,3-propylene-bis(oxamate); $[\{MCu(pba)(H_2O)_3\}\cdot 2H_2O]_x$ (II) (M = Mn, Ni), pba = 1,3-propylenebis-(oxamate); $[MnCu(pbaOH)(H_2O)_2]_x$ (III). The X-ray structures of I and II show that both compounds have the same chain structure. Along the a-direction the shortest separations are of the type Mn-Mn and Cu-Cu instead of Mn-Cu. Both compounds have an antiferromagnetic coupled ordered bimetallic chain behaviour in the temperature range of $30 < T < 300$ K. Upon cooling below 30 K $\chi_M T$ increases much faster for II than for I and diverges around 5 K. I orders antiferromagnetically at 2.2 K and II orders ferromagnetically at 4.6 K. The temperature dependence of the magnetization was investigated for II along the three directions of the lattice. It was found that the c-axis is the easiest magnetization axis.The three-dimensional ordering of both compounds are given in Fig. 3. The relative position of the chains withio the lattice are slightly different and this is the reason for the different magnetic behaviour at low temperatures. It is known that the Curie temperature (T_c) in one-dimensional coordination polymers depends on the magnitude of both the intra and interchain interactions. If a large intrachain interaction exists a week interchain interaction results. The goal is to shift T_c towards higher temperatures through subtle chemical changes in the coordination sphere of the metal centers. A further fact to increase the dimensionality of the interactions to predict a

---

[9] Y. Pei, M. Verdaguer, O. Kahn, J. Sletten, J.P. Renard. *Inorg. Chem.*, *26 (1987) 138.*

Y. Pei, M. Verdaguer, O. Kahn, J. Sletten, J.P. Renard, *J. Am. Chem. Soc.*, **110** (1988) 782.

Y. Pei, M. Verdaguer, O. Kahn, J. Sletten, J.P. Renard, *J. Am. Chem. Soc.*, **108** (1986) 7428.

K. Nakatani, P. Bergerat, E. Codjovi, C. Mathoniere, Y. Pei, O. Kahn, *Inorg. Chem.*, 30 (1991) 3978.

spontaneous magnetization is to remove coordinated water. Warming **I** in the solid state at 100 °C affords a new compound **II** which contains one molecule of water less than in **I**.

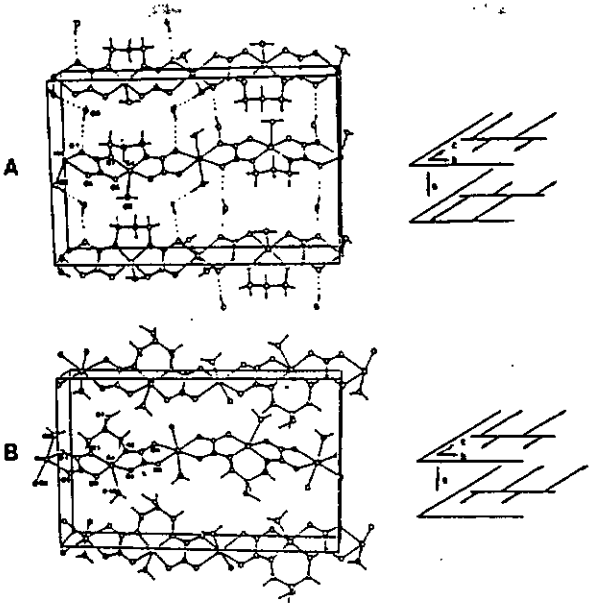

Fig. 3. Three neighboring chains in $[\{MnCu(pba)(H_2O)_3\}2H_2O]_x$ (A), and in $[MnCu(pba)(H_2O)_3]_x$ (B). Their magnetic spin topologies are shown schematically on the right

The structure consists of bimetallic chains. The shortest interchain separations are Mn-Cu instead of Mn-Mn or Cu-Cu. The Mn-Cu interaction through the oxamato bridge is indeed strongly antiferromagnetic. After removing the weekly bound water (2.417Å) the chains may be closer to each other and J_{inter} increases to some extent. The critical temperature has been raised considerably to 30 K. The structure of this powder is not known in detail, however.

1.2. Coordination polymers as molecular conductors

A second most important application of coordination polymers are molecular based synthetic conductors. Classical conductors are subdivided into three categories: electron conductors, ion

conductors and mixed conductors in which an electrical current is realized by electrons and ions simultaneously.

Synthetic molecular conductors consist of ligand systems (electron donors) and metal centers (electron acceptors), whereby the organic ligands can be arranged in stacks and the p-orbitals of the neighbour chains can overlap one another. Consequently a transport of electrons (by donor acceptor interactions between the chains) is conceivable. The temperature dependence of such compounds define a subdivision in conductors and semiconductor. The electrical conductivity of metallic substances increases with decreasing temperature, while that of a semiconductors decreases. The first organic solid with metallic conducting behaviour was TTF-TCNQ (TTF = tetrathiofulvalene, TCNQ = tetracyanochinodimethane)[10] shown in Fig. 4.

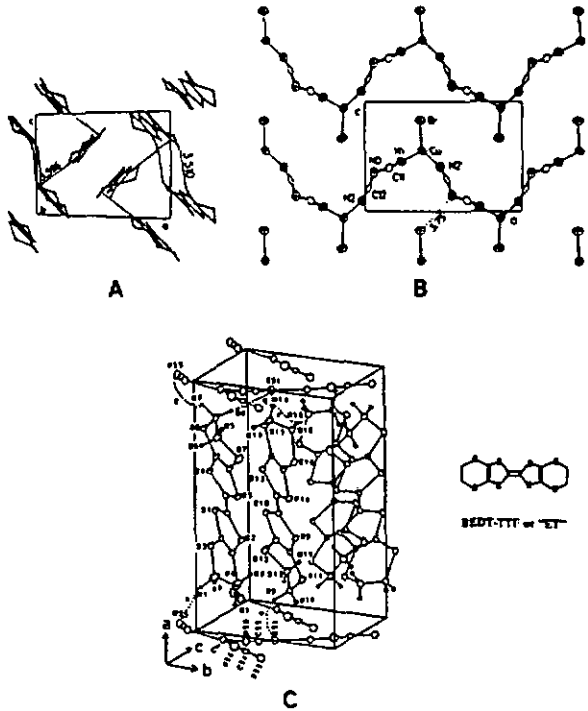

[10]P. Cassoux, L. Valade, H.Kobayashi, R.A. Clark, A.E. Underhill, *Coord. Chem. Rev.*, **110** (1991) 115.

Fig. 4. Crystal structures of (A) the ET donor layer in κ-$(ET)_2Cu[N(CN)_2]Br$, (B) polymeric anion layer of κ-$(ET)_2Cu[N(CN)_2]Br$, and (C) κ-$(ET)_2Cu[N(NCS)_2]$. Note the polymeric anion layers sandwich the ET layer in (C).

This class of one-dimensional stacks or two-dimensional sheet structures is based on π-conjugated organic molecules having a partial charge transfer between stacks. One of the most successful series of organic metals and superconductors is that of BEDT-TTF (BEDT=bis(ethylendithio)tetrathiofulvalene). In the compound [β-$(BEDT\text{-}TTF)_2X$] ($X=I_3^-$, IBr_2^-, AuI^-) the arrangement is a two-dimensional sheet structure separated by the counteranions, shown in Fig. 4. Many of the salts were found to be superconductors below transition temperatures that are relatively high, ca. 8.1 K. A further type of one-dimensional polymer conductor has direct overlap of d_{z^2}-orbitals of the metal atoms[1]. $[Pt(CN)_4]^{n-}$ and $[Ir(CO)_2Cl_2]^{n-}$ are cation deficient salts (with $n<1$) and have metal-metal distances shorter than 2.9 Å, as shown in Fig.5.

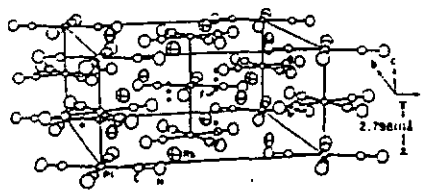

Fig. 5. Crystal structure of $Rb_2[Pt(CN)_4] \cdot 0.4$ THF

The room temperature conductivity can be a high as 2300 Ωcm^{-1} for $Rb_2[Pt(CN)_4] \cdot 0.4$ THF and 5.0 Ωcm^{-1} for $K_{0.58}[Ir(CO)_2Cl_2]$.

Phthalocyanine complexes have been studied intensively as coordination polymers. Phtalocyanine oxosilicon and oxogermanium polymers $[\{M(Pc)O\}_x]$[11] (M = Si, Ge) were first synthesized in the early 1960's by Joyner and Kenney. Similar fluoroaluminium and

[11]R.D. Joyner, M.E. Kenney, *Inorg. Chem.*, 1 (1962) 717.

fluorogallium compound[12,13] [M(Pc)X] (M = Al, Ga; X = F) have been obtained with high conductivity and a good thermal stability. Doping this compound with halogens or other ionic and organic acceptors, results in a dramatic enhancement of conductivity. A further family studied are the "shish kebab" stacked macrocyclic metal complexes.

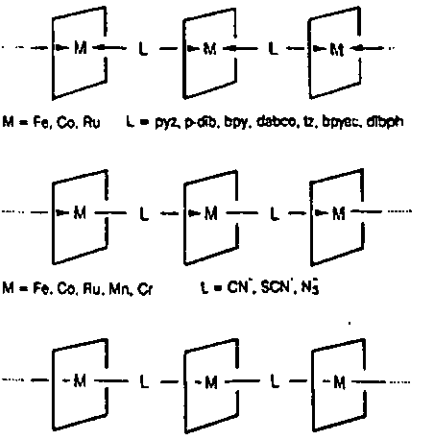

Fig. 6. Various "shish kebab" one-dimensional coordination polymers

Hanack et al[14] have prepared a large family of such phthalocyanine complexes of the type $[\{M(Pc)(L\text{-}L)\}_{\infty}]$. Various one-dimensional polymers are given in Fig. 6.

---

[12]P.M. Kuznesow, K.J. Wynne, R.S. Nohr, M.E. Kenney, *J. Chem. Soc., Chem. Commun.*, (1980) 121.

[13]P.M. Kuznesow, K.J. Wynne, R.S. Nohr, M.E. Kenney, P.G. Siebenman, *J. Am. Chem. Soc.*, **103** (1981) 4371.

[14]O. Schneider, M. Hanack, *Angew. Chem. Int. Et. Engl.*, **19** (1980) 392.

O. Schneider, M. Hanack, *Angew. Chem. Int. Et. Engl.*, **21** (1982) 79.

O. Schneider, M. Hanack, *Chem. Ber.*, **116** (1983) 2088.

B. N. Diel, T. Inabe, N.K. Jaggi, J.W. Lyding, O. Schneider, M. Hanack, C.R. Kannewurf, T.J. Mark, L.H. Schwart, *J. Am. Chem. Soc.*, **106** (1984) 3207.

W. Kobel, M. Hanack, *Inorg. Chem.*, **25** (1986) 103.

M. Hanack, S. Deger, A. Lange, *Coord. Chem. Rev.*, **83** (1988) 115.

Many of these complexes doped with iodine result in a dramatic increase of their conductivity, this depends on the interactions of the d_{π}-orbitals with π^* level of the bridging ligands.

In contrast to the numerous hitherto synthesized polymer compounds with the above mentioned properties their application in physical and technical fields is still at the beginning and a task for the future.

M. Hanack, A. Hirsch, H. Lejmann, *Angew. Chem. Int. Ed. Engl.*, 29 (1990) 1467.

M. Hanack, A. Gul, L.R. Subramanian, *Inorg. Chem.*, 31 (1992) 1542.

I.3. Examined polydentate N-donor ligands

The following three N-donor ligands have been investigated in the present work. First the ligand 2.3.5.6-tetra (2-pyridyl)pyrazine (tppz), which was synthesized by Goodwin and Lions[15] in 1959.

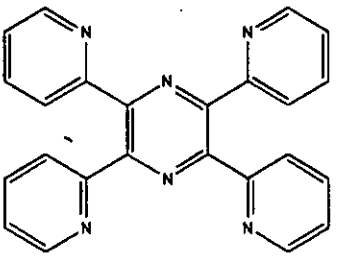

The six nitrogen atoms can be devided in two groups of three nitrogens and a bis-(tridentate) coordination should be possible. We were interested in the question of the ability of the nitrogen donor atoms to accommodate to a specific coordination sphere to form a polymer network by using tppz alone or in combination with other bridging ligands.

The second ligand studied was 2.4.6-pyrimidyl-1.3.5-triazine (tpymt):

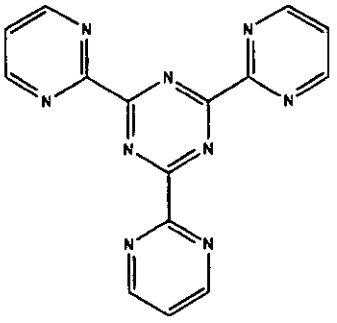

which should also offer the possibility of coordinating three metals in a tridentate terpyridine like form to build three dimensional coordination polymers. However it has received little

[15]H.A. Goodwin, F. Lions, *J. Am. Chem. Soc.*, 81 (1959) 6415.

attention from coordination chemists, probably because of the low yield of the first published synthesis. This was later partially increased by Case and Koft[16].

The third ligand, pyrazine 2.3.5.6-tetracarboxylic acid (H_4pztc), was first synthesized in 1887 by Wolff[17].

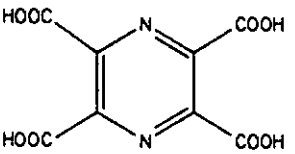

At that time a first indication was given that the acid could act as ligand in metal complexes. The reaction with $FeSO_4$ gave a colour change to deep violet[16]. The coordination behaviour of this ligand has been intensively investigated by P.-A. Marioni[2]. A series of transition metal salts have been reacted with tbe ligand under different conditions (see chapter 3). We carried out further reactions in the presence of divalent cations to obtain new coordination polymer structures and to investigate their conducting properties.

The reactions of these three ligands with metals salts and the investigations of the coordination behaviour are described in the following chapters.

---

[16]F.H. Case, E. Koft, *J. Am. Chem. Soc.*, 81 (1959) 905

[17]L. Wolff, *Ber. Dtsch. Chem. Ges.*, 20, (1887), 425.

L. Wolff, *Ber. Dtsch. Chem. Ges.*, 26, (1893), 721

2. Study of the coordination behaviour of 2.3.5.6-tetra(2-pyridyl)pyrazine (tppz) towards some transition metals

2.1. Introduction

This ligand was first synthesized by Goodwin and Lions[18] in 1959 by a condensation reaction of 2,2'-pyridoin with ammonium acetate. The reaction occurs at 180°C in a molten mixture of the two compounds, according to the following equation:

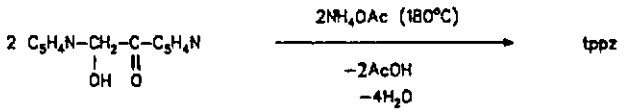

The recrystallization was undertaken from pyridine or from a mixture of pyridine/dichloromethane.

The ligand tppz should be able to coordinate in both a mono-and bis-tridentate fashion. It should also be possible by a bridging coordination mode to form di-or polynuclear complexes. However, to our knowledge no crystal structures of any metal complex of tppz had been published up to the beginning of 1993. We therefore desided to carry out some investigations on the coordination behaviour of this ligand.

Goodwin and Lions prepared some mononuclear tridentate complexes of iron, ruthenium, copper and cobalt, e.g. $[Fe(tppz)_2](ClO_4)_2 \cdot 4H_2O$, $[Fe(tppz)_2]I_2 \cdot 4H_2O$, $[Ru(tppz)_2](ClO_4)_2 \cdot 6H_2O$, $[Ni(tppz)_2](ClO_4)_2 \cdot H_2O$, $[Cu(tppz)(H_2O)](ClO_4)_2 \cdot 3H_2O$, $[Cu(tppz)Cl]Cl \cdot H_2O$, $[Cu(tppz)Cl]ClO_4$ and $[Co(tppz)_2](ClO_4)_3 \cdot 2H_2O$. However, the characterization was based on elemental analyses only. The metal to ligand ratio was in each case 1:1 or 1:0.5. In this context it was assumed that the pyrazine nucleus was unable to have both its nitrogen atoms acting simultaneously as donors.

---

[18] H.A. Goodwin, F. Lions, *J. Am. Chem. Soc.*, 81 (1959) 6415.

Reactions of tppz with some first row transition metal salts were also investigated by M. Lymann[19]. He worked with ligand to metal ratios of 1:0.5, 1, 2, respectively. Essentially, the characterization was undertaken by means of infrared spectra and u.v. measurements. In this diploma work there was no indications for the formation of binuclear complexes or columnane like arrangements.

Mono ligand complexes of the similar tridentate chelating ligand 2,3,5,6-tetrakis-(6-methyl)pyrazine (L) of the general formular $[MLX_2]$ where M= Mn, Fe, Co, Ni, Cu and where X may be Cl, Br, I, NCS, NCSe or NO_3, have beeo described by Goodwin and Sylva[20] in 1969. Infrared, visible and near-ultraviolet spectral, conductance and magnetic data were obtained for these complexes. Based on these data an attempt was made to assign coordination numbers to the metal atoms. Five and six coordination was assumed.

The structure of the monoclinic form of tppz, recrystallized from chloroform was published by Bock and co-workers[21] in 1992. In this case tbe two pyridine rings on either side of the central pyrazine ring are twisted out of its plane by 50° either up or down. The adjacent pyridice rings are twisted io opposite directions giving a N...N distance of 3.24 Å. This value exceeds the sum of two N-van der vaals radii of 1.55 Å and therefore the repulsion nitrogen lone pair interaction is reduced. We have also solved the structure of the monoclinic form, recrystallized from dichloromethane, with identical results.

In 1989 Escuer et al.[22] prepared a bexafluoroacetylacetonate copper complex of tppz and by means of elemental analyses data they proposed a dinuclear complex $[Cu_2(tppz)(hfacac)_4]$. Ruminski et al. have also synthesized and characterized some mono- and bimetallic complexes

---

[19]M. Lymann, Travail de diplome, Université de Neuchâtel, 1988.

[20]H.A. Goodwin, R.N. Sylva, *Inorg. Chim Acta*, 4 (1970) 197.

[21]H. Bock, T. Vaupel, C. Näther, K. Rupert, Z. Havlas, *Angew. Chem. Int. Ed. Engl.*, 31 (1992) 299.

[22]A. Escuer, T. Comas, J. Ribas, R. Vicente, X. Solans, C. Zanchini, D. Gatteschi, *Inorg. Chim. Acta.*, 162 (1989) 97.

of ruthenium[23], rhodium[24] and iron[25] with tppz, e.g. $[(NH_3)_3Ru(tppz)Ru(NH_3)_3](ClO_4)_4$, $[Rh(tppz)Cl_3]$, $[Cl_3Rh(tppz)RhCl_3]$, $Na_2[(CN)_3Fe(tppz)Fe(CN)_3]\cdot 6H_2O$.

From the literature some complexes are known in which tppz acts as a bridging ligand between two or three metal centers. However, there is a lack of crystal structural data for these compounds. For instance, the complex $[(terpy)Ru(tppz)Ru(terpy)](PF_6)_4$ was mentioned[26] and characterized by n.m.r. methods. Furthermore a series of monometallic, homo- and heterobimetallic as well as trimetallic complexes of ruthenium and osmium containing tppz were prepared[27], e.g. compounds like $[M_2(tppz)_3](PF_6)_4$, $[(terpy)M(tppz)M'(terpy)](PF_6)_4$ (M = M' = Ru, Os; M,M' = Ru,Os) and $[(terpy)Ru(tppz)Os(tppz)Ru(terpy)](PF_6)_4$. However, direct structural evidence of the di- and trimetallic nature is not given, only the results of the fast atom bombardement (FAB) mass spectra yielded hints for their composition.

The compound $[(terpy)Ru(tppz)Ru(terpy)](PF_6)_4$ was also synthesized by Collin et al.[28], however in this case the evidence for the dimetallic structure is better indicated by the mass spectra as described above. They found a peak for the mass $[(terpy)Ru(tppz)Ru(terpy)(PF_6)_4]^{2+}$ (m/z = 764). Spectrochemical and electrochemical investigations have been described and by means of these data a possible oxidation to the mixed valence species Ru^{2+}/Ru^{3+} is discussed.

The mixed metal complex $(Ru^{2+}/Ir^{3+})[(terpy)Ru(tppz)IrCl_3](PF_6)_2$ has been described by Vogler et al.[29] in 1993. The latter was prepared by reacting $[Ru(terpy)Cl_3]$ with $[Ir(tppz)Cl_3]$ and subsequent addition of KPF_6. An X-ray analysis of the mononuclear complex $[Ir(tppz)Cl_3]$

---

[23]R.R. Ruminski, J.L. Kipling, T. Cockroft, C. Chase, *Inorg. Chem.*, 28 (1989) 370.

[24]R.R. Ruminski, C. Letner, *Inorg. Chim. Acta*, 162 (1989) 175.

[25]R.R. Ruminski, J.L. Kipling, *Inorg. Chem.*, 29 (1990) 4581.

[26]R.P. Thumel, S. Chirayil, *Inorg. Chim. Acta*, 154 (1988) 77.

[27]C.R. Arana, H.D. Abruna, *Inorg. Chem.* 32 (1993) 194.

[28]J.P. Collin, P. Laine, J.P. Launay, J.P. Sauvage, A. Sour, *J. Chem. Soc. Chem. Comun., (1993) 434.*

[29]L.M. Vogler, B. Scott, J. Brever, *Inorg. Chem.*, 32 (1993) 898.

has been established. Consequently, this was the first structurally characterized compound containing tppz, Fig. 6a.

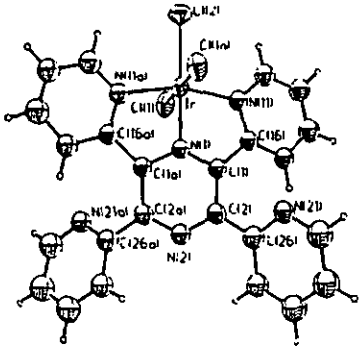

Fig. 6a Diagram of $[Ir(tppz)Cl_3]$ showing thermal ellipsoids.

The iridium atom has a distorted octahedral geometry. An twofold axis bisects the tppz ligand, the Ir atom and the equatorial Cl atom. The coordinated pyridintrings make an angle of 33.4° with the pyrazine ring.

Recently some investigations on compounds bearing the ligand tppz have been published by R.G. Brewer et al[30]. In this study the ligand is bound to only one metal center in a non bridging mode. The presence of the remote uncoordinated nitrogen atoms makes the development of polymetallic complexes utilizing this ligand possible. The studied compounds represent a new class of complexes which have the composition $[Os(tppz)L]^{2+}$, $[Os(tppz)(dppe)X]^{n+}$ and $[Os(tppz)(PPh_3)X]^{n+}$ (L = terpy, tppz; dppe = bis(diphenylphosphino)ethane; X = Cl^-, CH_3CN).

---

[30]R. G. Brewer. G.E. Jensen. K.J. Brewer. *Inorg. Chem.*, 33 (1994) 124.

Furthermore complexes like $[(terpy)Ru(tppz)Co(PPh_3H_2]^{3+}$, $[(NC)_3Fe(tppz)CoH_2L]$, (L = PPh_3, PEt_2Ph) have been mentioned[31] but there are no remarks on the synthesis and the characterization of this compounds.

C. Arana et al.[32] tested some transition metal complexes containing tridentate ligands which are active in the electrocatalytic reduction of carbon dioxide. Under an atmosphere of nitrogen and carbon dioxide the compounds $[M(tppz)]_2(PF_6)_2$ (M=Fe, Co, Ni) were tested by cyclovoltammetric measurements in the potential range of 0 to 2.0V in DMF/0.1M TBAP.

The novel ligand 6',6"-Bis(2-pyridyl)-2,2':4,4":2",2"-quarterpyridine (L) was synthesized by E.C. Constable et al.[33] in 1990.

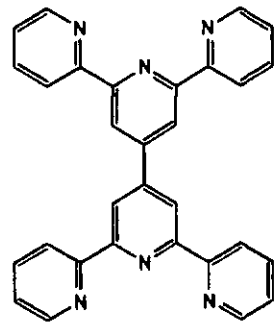

The coordination behaviour of this "back to back" analogue to tppz was investigated. The diruthenium(II) complex $[(terpy)RuLRu(terpy)]^{4+}$ has been shown to exhibit no Ru-Ru interactions and contains two non-interacting $Ru(terpy)_2$ units.

A connection of polydentate ligands to di- or polymetallic systems is possible by introducing bridging ligands like oxalate (ox) or iminodiacetate (ida). For instance, this is known for some Cu^{2+} complexes of terpy, which is a comparable tridentate system as present in tppz. M. Julve

---

[31]J.D. Peterson, L.W. Morgan, I.Hsu, M.A. Biladeau, S. E. Ronco, *Coord. Chem. Rev.*, 111 (1991) 319.

[32]C. Arana, S. Yan, M. Keshavarz-K, K.T. Potts, H.D. Abruna, *Inorg. Chem.*, 31 (1992) 3680.

[33]E.C. Constable, M.D. Ward, *J.Chem. Soc. Dalton Trans.*, (1990) 1405.

and co workers[34] have determined the X-ray structures of two new complexes e.g. the dimer $[\{Cu(terpy)(H_2O)\}_2(ox)][\{Cu(terpy)\}_2(ox)](ClO_4)_4 \cdot H_2O$ and the monomer $[Cu(terpy)(H_2O)(ox)] \cdot 4H_2O$. The dimer structure contains two different centrosymmetrical Cu^{2+} dinuclear dicationic units, uncoordinated perchlorate groups and water of crystallization. In both dinuclear units the terpyridyl group is terminal and the oxalate acts as an asymmetrical bis(chelating) bridge. However the complex contains one five-fold and one six-fold coordinated Cu^{2+} atom. Interestingly, R. P. Bonomo[35] et al. obtained a polymeric compound in which Cu(terpy) units are bridged with units of ida, $[Cu(terpy)(ida)]_\infty$, see Fig.7.

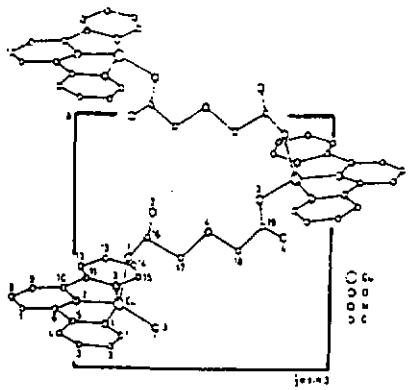

Fig. 7. Molecular structure of $[Cu(terpy)(ida)]_\infty$.

The Cu^{2+} atoms have a distorted trigonal bipyramidal geometry, the six-coordinate environment was also proved by e.s.r. measurements and visible absorption spectra.

The above discussed papers shows that there is a lack of structural data to demonstrate the flexibility of the ligand tppz. Up to now no examples of a two fold coordination in the form of a bridging mode has been proved by X-ray structure analysis. Evidence for such a bridging function has only been given by mass spectroscopic experiments.

---

[34] I. Castro, J. Faus, M. Julve, A. Gleizes. *J. Chem. Soc. Dalton Trans.*, (1991) 1937.

[35] N.B. Bresciani-Pahor, G. Nardin, R.P. Bonomo, E. Rizzarelli, *J. Chem. Soc. Dalton Trans.*, (1984) 2625.

2.2 Characterization of the free ligand tppz and reaction with HCl

The structure of the monoclinic form of tppz recrystallized from $CHCl_3$ (tppz-II,Fig. 8b) was determined by Bock and co-workers[21] as mentioned above. At the same time B. Greaves[36] obtained also the monoclinic form of the free ligand, recrystallized from CH_2Cl_2.

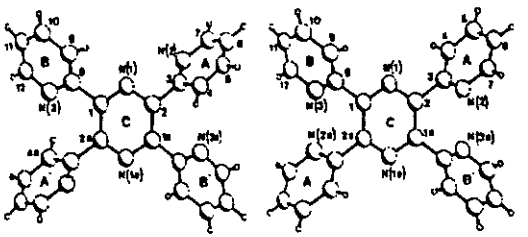

Fig. 8. Pluto plot of the tetragonal (a, tppz-I) and the monoclinic (b, tppz-II) form of tppz.

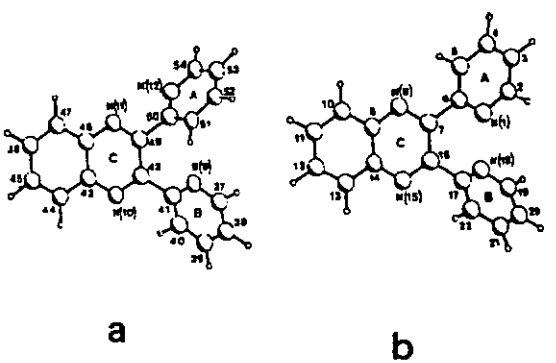

Fig. 9. Pluto plot of a), bpq-I and b), bpq-II.

---

[36]B. Greaves, H. Stoeckli-Evans, *Acta Cryst.*, C48 (1992) 2269.

From a reaction of tppz with $ZnCl_2$ (metal to ligand ratio of 1:1 in $EtOH/H_2O$) a small amount of a mononuclear Zn^{2+}-complex and a new tetragonal form of tppz (tppz-I, Fig. 8a) was isolated. In tppz-II the pyridine N atoms are inclined towards the pyrazine ring C by 48.9(1) and 51.7(1)°, respectively, and to one another by 62.4(1)°. The similar compound 2.3-bis(2-pyridyl)quinoxaline (bpq) has also been observed in two formes (Fig. 9). In bpq-I[37] the pyrazine ring is almost planar (twist angle 0.035°), whereas in bpq-II[38] the pyrazine ring is twisted by 5.7°. This twisting in the pyrazine ring has also been observed for complexes of tppz with some first row transition metals which will be described later. It has also been found that the orientation of the pyridine rings in 2.3bis(2-pyridyl)pyrazine (bppz).[39] is similar to that in tppz-II and bpq-II. A comparison of the similar dihedral angles between the pyridine ring A and B and the pyrazine ring C, as well as the intramolecular distances, are given in Table 1.

One can see that the geometry in tppz-I and in bpq-I are very similar, more so than in tppz-II, bpq-II and bppz. The largest differences concern the shortest intramolecular contacts. For example, the distance N(3)-C(4a) with 3.297Å in tppz-I compared to 3.180Å for the distance N(9)-C(51) in bpq-I. The same tendency is observed in tppz-II, bpq-II and bppz. For example, the distance N(2)-N(3a) of 3.237Å in tppz-II is significantly larger than the distance N(2)-N(2a) of 2.962Å in bppz. This difference is also reflected in the dihedral angle of 31.69° between the rings A and C in bpq-II which is much smaller than that in tppz-II (48.9°) or in bppz (42.2°), see Tab. 1.

---

[37]K.V. Goodwin, W.T. Pennington, J.D. Petersen, *Acta Cryst.*, C46 (1990) 898.

[38]S.C. Rasmussen, M.M. Richter, E. Yi, H. Place, *Inorg. Chem.*, 29 (1990) 3926.

[39]N.-T. Huang, W.T. Pennington, J.D. Petersen, *Acta. Cryst.*, C47 (1991) 2011.

Tab.1. Comparison of various dihedral angles (°) and short intramolecular distances (Å) in tppz-I and bpq-I, tppz-II, bpq-II and bppz

Angles	tppz-I	bpq-I	tppz-II	bpq-II	bppz
∠ AB	60.4	58.9	62.4	60.6	54.1
∠ AC	59.0	54.0	48.9	31.7	42.2
∠ BC	46.4	45.2	51.7	46.4	42.2
Distances					
N(1)-N(2)	2.907	2.830			
N(1)-C(9)	2.912	2.910			
N(3)-C(4a^{i})	3.297	3.180			
n(1)-C(4)			2.939	2.854	2.859
N(1)-C(9)			2.958	2.941	2.859
N(2)-C(3a^{ii})			3.237	3.017	2.962

Symmetry operations: i) 1.5-x,0.5-y, 1.5-z; (ii) 2-x, -y, -z.

The reason for the existence of these two forms could be reflected in the influence of the different solvents used for recrystallization. In accordance with these X-ray analysis results we found also by means of u.v. solid state measurements, using ethylenglycol as dispersion medium, that these two formes of tppz exist. Two different absorptions were observed: for the monoclinic form at 325 and for the tetragonal form at 345 nm. Furthermore, dynamic n.m.r. studies were undertaken. ^{15}N n.m.r. investigations show for tppz a temperature dependent behaviour concerning the shift of the signal of the pyridine rings, see Fig. 10. Whereas the signal for the pyrazine ring is unchanged from -10 to 55°C, the signal for the pyridine rings are shifted downfield at higher temperatures (-10°C : 230 ppm; 25°C : 232 ppm; 55°C : 233 ppm). Therefore a movement of the pyridine rings at elevated temperatures is assumed.

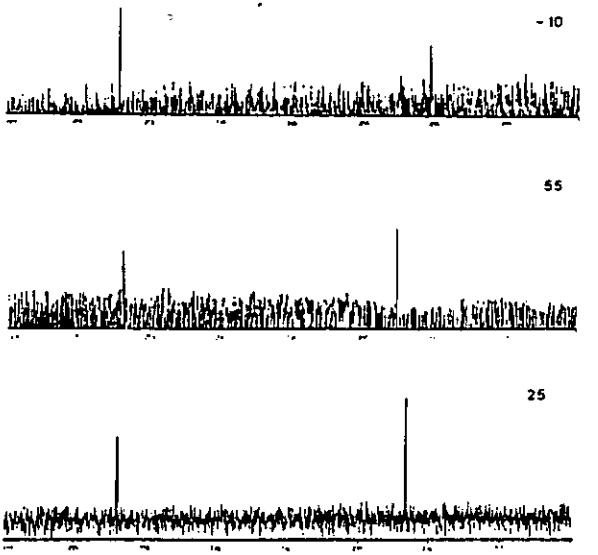

Fig. 10. ^{15}N n.m.r. spectra of tppz recrystallized from CH_2Cl_2, recorded in $CDCl_3$ at -10, 25 and 55°C.

For a further characterization of tppz the question of different hydrochlorides was of interest. As described by Bock and co-workers[21] a two-fold hydrochloride is obtainable. Contrary, we could isolate a four-fold hydrochloride in a reaction of tppz with 2M HCl after recrystallization from water. This hydrochloride salt crystallized with two molecules of water as tppz·4HCl·$2H_2O$ (1)[40]. A picture of the molecular structure is given in Fig.11 and important bond distances and angles are given in Table 2.

[40]M. Graf, H. Stoeckli-Evans, manuscript in preparation.

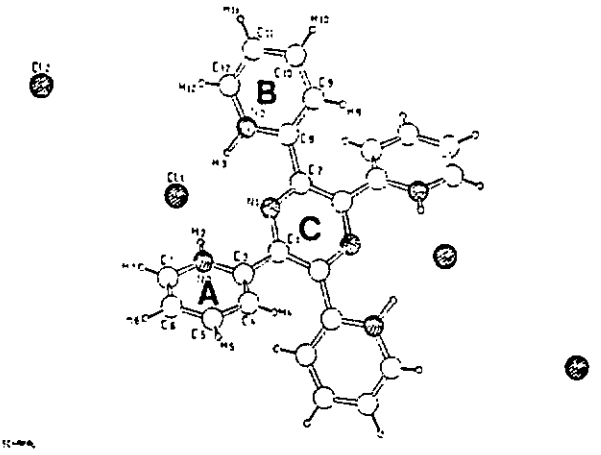

Fig. 11. SCHAKAL[41] plot of tppz·4HCl·2H_2O.(1)

Tab.2. Important bond distances (Å) and angles (°) of tppz·4HCl·2H_2O (1)

H(2)-Cl(1)	2.143(3)	H(3)-Cl(2)	6.39(3)
H(3)-Cl(1)	2.08(3)	N(2)-N(3)	4.521(3)
H(2)-Cl(2)	6.783(24)	Cl(1)-Cl(2)	5.784(19)
Cl(1)-H(2)-N(2)	163.8(21)		
Cl(1)-H(3)-N(3)	167.6(22)		

Interestingly, in this centrosymmetric structure two chloride ions are situated near the N(3) and N(2) atom with distances N(H2)-Cl(1) 2.14(3) and N(H3)-Cl(1) 2.08(3)Å, whereas the other two chloride ions are situated far away from the two protonated N atoms with distances N(H2)-Cl(2) 6.783(24) and N(H3)-Cl(2) 6.39(3) Å, probably by reason of crystal packing effects. The angles Cl(1)-H(2)-N(2) and Cl(1)-H(3)-N(3) are both greater than 150° and are an indication for a relative strong H^+...Cl^- bond. The shortest intramoleculare distance (N...N) is

[41]E. Keller, SCHAKAL 88, a Fortran Program for the Graphical Representation of Molecular and Crystallographic Models, University Freiburg, 1988.

between N(2)-N(3) with 4.521(3)Å. The Cl(1)···Cl(2) distance is 5.784(19)Å. In our hydrochloride the dihedral angle of pyridine ring A relative to the pyrazine ring C is 37.69(14)° and B to C is 40.73(13)°, whereas the dihedral angle between the rings A and B is 60.65(8)°. A comparison of 1 and the two formes of the tppz is given in Table 3.

Tab. 3. Dihedral angles (°) of the pyridine rings relativ to the central pyrazine ring C

Angle	tppz (monoclinic)	tppz (tetragonal)	tppz·4HCl·2H$_2$O
A^B	62.4	60.4	60.65(8)
A^C(C')	48.9	59.0	37.69(14)
B^C(C')	51.7	46.4	40.73(13)

The proton n.m.r. spectrum of the hydrochloride 1 recorded in D_2O/DSS, (see experimental), shows four signals indicating four equivalent pyridine rings. The location of the HCl protons proved impossible (sample measured in $CDCl_3$). An expected downfield shift in comparison with the free ligand was observed. U.v. measurements in water as solvent show a noticeable shift of the two characteristic bands for the ligand λ_{1max}=297 and λ_{2max}=320 nm compared to the spectrum of the free tppz (λ_{max}=265, 308 nm). Bock and co-workers[21] obtained from a reaction of tppz with aqueous 1N HCl and after recrystallization from CH_3CN a twofold hydrochloride in which the diagonally oppositing pyridine rings are protonated. They formed bydrogen bridges, N-H···Cl, to the two electron-rich chloride anions. The unprotonated pyridine rings rotate into planarity with the pyrazine ring (from 50° to 16°). Furthermore an anion exchange with tetraphenylborate [Li[B(C_6H_5)$_4$] in acetonitrile was studied. The structure determination of this compound indicated drastic changes. The dihedral angles of the pyridine rings relative to the pyrazine ring were reduced to 21° and 26°, respectively. A movement in the direction of a more planar system was assumed.

M.Y. Khuhawar[42] studied 2,2'- pyridyl substituted pyrazine and dihydropyrazine compounds using CCl_4 as solvent, nujol and KBr disc techniques. Different regions of strong absorptions are assigned. For tppz we found identical results as described here. A close resemblance between 1390-1600 cm^{-1} was observed with bands at 1393vs, 1435w, 1477w, 1486w, 1567s and 1588vs cm^{-1} corresponding to ν(C=C), ν(C=N) stretching vibrations in the pyridine and pyrazine rings. The spectrum shows clearly the two characteristic bands at 1567s and 1588vs cm^{-1} which are separated by 21 cm^{-1}. Absorptions in the region from 1300 to 1600 cm^{-1} (corresponding to plane hydrogen bonding modes and ring vibrations), in the region from 625 to 1000 cm^{-1} (mainly corresponding to the (C-H) out of plane deformations), ring breathing vibrations near 700 $cm^{-1}$and overtones of lower frequencies were also observed. A very strong band at 785 cm^{-1} could be assigned to the corresponding C-H groups. The infrared spectrum for the hydrochloride of tppz indicates a shift in the absorption of the characteristic doublet in the ν(C=C, ν(C=N) region. The very intensive band at 1612 cm^{-1} is shifted by 24 cm^{-1} to higher wave numbers and the strong band at 1543 is also shifted by 24 cm^{-1} to lower wave numbers. The very strong band for the free ligand at 1393 cm^{-1} is shifted for the hydrochloride salt to 1379 cm^{-1}. by 14 cm^{-1}. The intensive band at 776 cm^{-1} is shifted by 9 cm^{-1} in comparison to the spectrum of the free ligand. Elemental analyses agrees also with the results found by means of X-ray structure analysis.

Bock and co-workers[21] investigated the two step reduction of tppz under aprotic conditions as well as in solutions containing Li^+ and Na^+ conducting salt cations. Under protic conditions two one electron reductions are coupled with a protonation to dihydropyrazine. Under aprotic conditions after the pickup of two electrons a dianion could be discussed which is suitable to form a contact-ion-pair in the presence of $(C_4H_9)N^+$, Na^+ or K^+. A reversible redox process was observed, the anion/cation complex $[M^-M^+]$ is persistent at room temperature.

---

[42]M.Y. Khuhawar , *Pakistan. J.Sci. Ind. Res.*, 26 (1983) 301.

2.3. Coordination behaviour of Co(II) and Ni(II) complexes of tppz

Complexes of Co^{2+} exist in many structural varieties. The prefered coordination sphere is commonly the tetrahedron or the octahedron. An octahedral coordination sphere is classically known for $[Co(NH_3)_6]^{2+}$ or $CoCl_2$. For Co^{3+} complexes the most stable coordination sphere is octahedral (E.A.N. rule), classical complexes are $[Co(en)Cl_2]^+$, $[Co(CN)_6]^{3+}$, $[CoF_6]^{3+}$ and CoF_3. By means of elemental analyses data, Goodwin and Lions proposed an octahedral coordination sphere for the complex $[Co(tppz)_2](ClO_4)_3 \cdot 2H_2O$ however no structural proof has been given up to now. In view of this fact we carried out a number of reaction attempts with several cobalt salts. Ligand to metal ratios of 1:1 or 1:2 yielded no defined products by crystallization or precipitation. However from a reaction of $CoCl_2 \cdot 6H_2O$ with tppz (molar ratio 6:1) we obtained after crystallization from EtOH fine red needles of compound **2**.

$$CoCl_2 \cdot 6H_2O + tppz \rightarrow [Co(tppz)Cl(H_2O)_2]Cl + 4H_2O \quad (2)$$

We assume a mononuclear complex $[Co(tppz)Cl]Cl \cdot 2H_2O$ probably with a octahedral coordination mode. The FAB-mass spectrum indicates the fragment m/e = 482 for $[Co(tppz)Cl]^+$ (100%) and the fragment m/e = 446 for $[Co(tppz)]^+$. The elemental analysis supports the composition of this assumption. U.v. measurements in water solution show a typical coordination shift of the ligand. The two bands for tppz are bathochromically shifted at λ_{1max}=295 and λ_{2max}=325 nm. To introduce further bridging ligands we carried out some reactions with sodium salts of chelating ligands like ida, edta, 2-carboxypyrazine, 2,3-dicarboxypyrazine, 2,5-dicarboxypyrazine, 2,6-dicarboxypyrazine as well as diimine, dppm, pyrazine, 2,3,5,6-tetramethylpyrazine and 1,1'-dimethyl-4,4'-bipyridinium dichloride. However from all of these reactions no well defined complexes could be isolated. From a reaction of $CoCl_2 \cdot 6H_2O$ with tppz and disodium malonate we obtained well formed red needles suitable for X-ray diffraction studies.

$$CoCl_2 \cdot 6H_2O + tppz + Na_2ma \rightarrow [Co(tppz)(ma)(H_2O)] \cdot 4H_2O + H_2O + 2NaCl \quad (3)$$

We found a mononuclear complex in which both of the chelate functions of one malonate molecule and additionally one water molecule are coordinated to form a nearly octahedral coordination sphere, see Fig.12. The Co-O(malonate) distances are 1.964(8)Å for Co(1)-O(1) and Co(1)-O(2) 2.077(7)Å, respectively. The Co-N(pyrazine) distance is 2.092(8)Å. Crystallographic data have been published for several pyrazinecarboxylates and pyrazinedicarboxylates by Richard[43] and O'Conner[44] and co-workers. A selection of important bond distances is given in Table 4.

Tab. 4. Co-O(oxalate) and Co-N(pyrazine) distances (Å) of some carboxylate and dicarboxylate complexes

$[Co(2,3\text{-pyd})\cdot 2H_2O]$			
Co-O(2)	2.069(4)	Co-N(1)	2.173(4)
Co-O(3)	2.037(4)	Co-N(2)	2.135(4)
$[Co\{C_4N_2(COO)_2(COOH)_2(H_2O)\}_2]$			
Co-O(8)	2.057(1)	Co-N(1)	2.109(1)
$[Co(C_4N_2COO)_2(H_2O)_2]\cdot 2H_2O$			
Co-O(1)	2.084(1)	Co-N(1)	2.135(1)
$[Co(C_4N_2COO)_2(H_2O)_2]$			
Co-O(1)	2.093(1)	Co-N(1)	2.102(1)

The Co-N(pyrazine) distance in $[Co(tppz)(ma)(H_2O)]\cdot 4H_2O$ is shorter than the same distances in the above described compounds. The Co-O(malonate) bondlengths are comparable. The Co-N(pyridyl) distances, further important bond lengths and angles are given in Table 5. Up to now there is a lack of crystallographic data for such closely related compounds. The central pyrazine ring is considerably distorted. The dihedral angle beetwen planes C'[C(1), N(1), C(4)] and C"[(2), N(2), C(3)] is 9.4(6)°. Larger and smaller twist angles have been observed in

[43] P. Richard, D. Tran Qui, E.F. Bertaut, *Acta Cryst.*, B29 (1973) 1115.

[44] C. J. O'Conner, E. Sinn, *Inorg. Chem.*, 20 (1981) 545.

complexes of tppz and will be described later. A comparison of dihedral angles of mononuclear complexes of tppz is given in Table 6.

In the X-ray structure of the complex $[Co(terpy)_2]Br_2 \cdot 3H_2O$[45]; all six nitrogens are bonded to the cobalt, the central Co-N distances are shorter than the other distances (1.89, 2.10 Å) and also shorter than the Co-N(pyrazine) distances in our malonate complex. A Co-N distance of 1.863(7), 1.853(7) Å was found for the central nitrogen atoms and 1.921(7)-1.937(7) Å for the distal nitrogen atoms in the dimeric complexe $[Co(terpy)_2]Cl_3$[46]. For the complex $[Co(terpy)_2]I_2 \cdot 2H_2O$ a Co-N (central) bondlength of 1.942(7)Å was found and a Co-N distance of 2.104(5) Å(distal)[47].

The elemental analysis results for this complex is in agreement with the composition found by X-ray diffraction. U.v. measurements in water solution indicate a typical coordination shift of the ligand. We found the two characteristic bands for the ligand at 300 and 320 nm. The infrared spectrum exhibits a very strong band for the ν(COO) at 1573 cm^{-1} and a typical band pattern for the tppz was observed. In the ν(C=C), ν(C=N) region we found bands at 1477m; 1400s,sh; 1386s,sh and 1300m cm^{-1}.

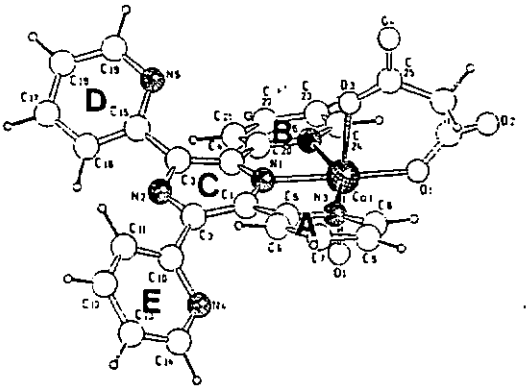

Fig. 12. SCHAKAL plot of $[Co(tppz)(ma)(H_2O)] \cdot 4H_2O$

[45]E.N. Maslen, C.L. Raston, A.H. White, *J. Chem. Soc., Dalton Trans.*, (1974) 1803.

[46]B.N. Figgis, E.S. Kucharski, A. H. White, *Aust. J. Chem.*, 36 (1983) 1563.

[47]B.N. Figgis, E.S. Kucharski, A. H. White, *Aust. J. Chem.*, 36 (1983) 1527.

Tab. 5. Selected distances (Å) and angles (°) of $[Co(tppz)(ma)(H_2O)]\cdot 4H_2O$

Co(1)-O(1)	1.964(8)	Co(1)-N(1)	2.092(8)
Co(1)-O(2)	2.077(7)	Co(1)-N(3)	2.127(8)
Co(1)-O(5)	2.141(8)	Co(1)-N(6))	2.135(8)
O(1)-Co(1)-O(3)	88.9(3)	O(3)-Co(1)-N(6)	93.0(3)
O(1)-Co(1)-O(5)	89.8(3)	O(5)-Co(1)-N(1)	88.5(3)
O(1)-Co(1)-N(1)	173.6(3)	O(5)-Co(1)-N(3)	90.8(3)
O(1)-Co(1)-N(3)	110.5(3)	O(5)-Co(1)-N(6)	88.8(3)
O(1)-Co(1)-N(6)	99.5(3)	N(1)-Co(1)-N(3)	75.7(3)
O(3)-Co(1)-O(5)	178.0(3)	N(1)-Co(1)-N(6)	74.3(3)
O(3)-Co(1)-N(1)	88.1(3)	N(3)-Co(1)-N(6)	150.0(3)
O(3)-Co(1)-N(3)	88.1(3)		

Tab. 6. Collection of dihedral angles (°) of several mononuclear complexes of tppz

angles	$[Co(tppz)(ma)(H_2O)]\cdot 4H_2O$	$[Ni(tppz)(ox)(H_2O)]\cdot 5H_2O$	$[Zn(tppz)Cl_2]$
A^B	11.8(5)	7.3(3)	13.5(1)
A^C(C')	20.9(5)	23.6(3)	7.8(2)
B^C(C')	18.9(4)	17.5(3)	21.0(1)
D^E	41.3(4)	51.5(3)	37.0(1)
D^C"	36.6(4)	53.3(3)	22.8(2)
E^C"	40.4(4)	30.8(3)	43.9(2)
A^D	57.5(5)	73.9(3)	37.6(1)
A^E	52.5(5)	50.7(3)	61.9(1)
B^D	32.3(4)	69.8(3)	50.9(1)
B^E	57.5(5)	43.3(3)	74(1)
C'^C"	9.4(6)	9.0(4)	10.6(2)

Ni^{2+} complexes exist also in a large variety of different coordination polyhedra. An octahedral coordination sphere is known for instance in $[Ni(H_2O)_2(NH_3)_4]^{2+}$, $[Ni(NH_3)_6]^{2+}$ and $[Ni(en)_3]^{2+}$. We carried out a number of reactions (molar ratio 1:1 or 1:2) of Ni^{2+} salts with tppz however we could oot obtain well defined products. From a reaction of tppz with an excess of $Ni(NO_3)_2 \cdot 6H_2O$ (1:6) we obtained well formed red brown needles of 4.

$$2Ni(NO_3)_2 \cdot 6H_2O + tppz + 3H_2O \rightarrow [Ni_2(tppz)(H_2O)_6](NO_3)_4 \cdot 3H_2O \quad (4)$$

X-ray diffraction studies show a bis(tridentate) dinuclear complex, see Fig.13. Hence, for the first time, a metal of the 3d row coordinates in a bis(tridentate) manner with tppz. Six molecules of water are coordinated around the nickel atoms and the nitrates acts as counterions to give the composition $[Ni_2(tppz)(H_2O)_6](NO_3)_4 \cdot 3H_2O$[48]. The coordination sphere of tbe nickel atoms can be described as nearly octahedral. The central pyrazine ring in this molecule is highly distorted. The dihedral angle between planes C'[C(1), N(1), C(4)] and C"[C(2), N(2), C(3)] is 10.9(10)°. The Ni...Ni separation in this binuclear complex is 6.6446(18)Å and the central Ni-N(pyrazine) distances are 2.025(7)Å and 1.998(7)Å. The Ni-N(pyridine) distances are larger. The Ni-O(water) distances together with further important bond lengths and angles are given in Table 7. The pyridine rings A and B coordinated to Ni(1) are inclined to one another by 9.8(4)° and by 24.1(3)° and 28.0(3)° relatively to the central pyrazine ring C. The pyridine rings D and E are coordinated to the Ni(2) atom and are inclined to one another by 9.8(3)° and by 22.6(3)° and 24.4(3)° relative to the central pyrazine ring. The shortest intramolecular distances are between C(6)...C(11) witb 3.141(17)Å and H(6)...H(11) separated by 2.302Å, as well as C(16)...C(21) with 3.249(16)Å and H(16)...H(21) are separated by 2.588Å.

[48]To be published.

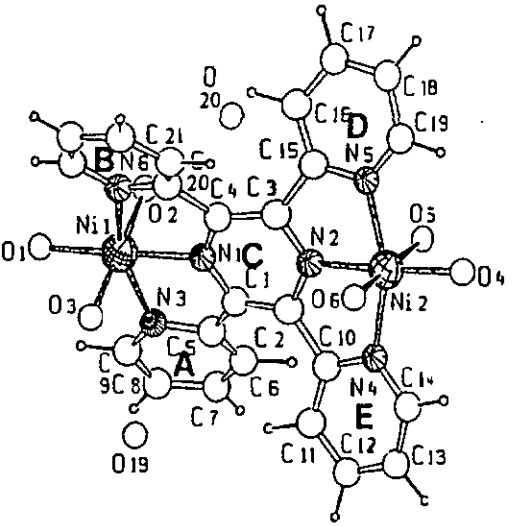

Fig. 13. SCHAKAL plot of $[Ni_2(tppz)(H_2O)_6](NO_3)_4 \cdot 3H_2O$.

Tab. 7. Selected distances (Å) and angles (°) of $[Ni_2(tppz)(H_2O)_6](NO_3)_4 \cdot 3H_2O$

Ni(1)-O(1)	2.025(7)	Ni(1)-N(1)	2.025(7)
Ni(1)-O(2)	2.051(7)	Ni(1)-N(3)	2.099(8)
Ni(1)-O(3)	2.096(6)	Ni(1)-N(6)	2.090(7)
Ni(2)-O(4)	2..036(6)	Ni(2)-N(2)	1.998(7)
Ni(2)-O(5)	2.121(6)	Ni(2)-N(4)	2.076(7)
Ni(2)-O(6)	2.098(7)	Ni(2)-N(5)	2.061(7)
N(1)-Ni(1)-N(3)	78.4(3)	N(3)-Ni(1)-O(1)	101.7(3)
N(1)-Ni(1)-N(6)	78.5(3)	N(3)-Ni(1)-O(2)	90.7(3)
N(1)-Ni(1)-O(1)	179.2(3)	N(6)-Ni(1)-O(1)	101.4(3)
N(1)-Ni(1)-O(2)	90.6(3)	N(6)-Ni(1)-O(2)	92.2(3)
N(1)-Ni(1)-O(3)	91.8(3)	N(6)-Ni(1)-O(3)	86.8(3)
N(2)-Ni(2)-N(4)	77.8(3)	N(4)-Ni(2)-O(5)	90.7(3)
N(2)-Ni(2)-N(5)	79.3(3)	N(4)-Ni(2)-O(6)	91.9(3)

Tab. 7 (continuation)

N(2)-Ni(2)-O(5)	90.8(3)	N(5)-Ni(2)-O(4)	98.8(3)
N(2)-Ni(2)-O(6)	92.4(3)	N(5)-Ni(2)-O(5)	90.5(3)
N(4)-Ni(2)-O(4)	104.2(3)	N(5)-Ni(2)-O(6)	88.2(3)

Cortes[49] and co-workers published the structural data for the complex $[Ni(terpy)Cl(H_2O)_2]Cl$. The Ni atom is hexa-coordinated forming with one chloride and two water molecules, a distorted octahedron. The Ni-N distance to the central nitrogen is 1.981Å the bond lengths to the other two nitrogens are 2.096 and 2.097Å. Similar distances were found for the complex bis(4'-phenyl-2,2':6', 2"-terpyridine)nickel(II) chloride decahydrate[50].

The infrared spectra indicate a coordination shift of the ligand, the vibrations for the nitrate anions were found in a broad absorbtion which overlaps a large part of the spectrum. U.v. measurements in water solution also indicate the coordination of the ligand. Bands were observed at 295 and 350 nm. Attempts to coordinate bridging ligands as described for the cobalt complexes were unsuccessful. Furthermore from a reaction of tppz with Ni-oxalate in a molar ratio of 1:6 we obtained only the mononuclear complex.

$$Ni(ox) + tppz + 6H_2O \rightarrow [Ni(tppz)(ox)(H_2O)]\cdot 5H_2O \quad (5)$$

The Ni atom has an octahedral coordination sphere. One molecule of water is coordinated with a Ni(1)-O(5) distance of 2.094(5)Å and one molecule of oxalate with Ni-O(oxalate) distances of Ni(1)-O(1) 2.063(5) and Ni(1)-O(3) with 2.003(5)Å. The central Ni-N(pyrazine) distance is 1.997(6)Å whereas the Ni-N(pyridine) distances are 2.096(6) and 2.088(6)Å, respectively. Up to now no structural data for such similar Ni systems are known in the literature. The central pyrazine ring in the molecule is distorted by 9.0(4)°. The pyridine rings A and B, coordinated to the Ni atom, are inclined to one another by 7.3(3)°. The uncoordinated pyridine rings D and E are inclined to one another by 51.5(3)°. This is larger than the same dihedral angle found for

[49]R. Cortes, M. I. Arriortua, T. Rojo, X. Solans, C. Miravilles, B. Beltran, *Acta Cryst.*, C (1985) 1733.

[50]E.C. Constable, J. Lewis, M. C. Liptrot, P.R. Raithby, *Inorg. Chim. Acta.*, 178 (1990) 47.

the similar complex [Co(tppz)(ma)(H_2O)·]4H_2O, see Table 6. Pyridine rings D and E are inclined to the central pyrazine ring C by 53.3(3)° and 30.8(3)°, respectively. The pyridine ring D has the largest dihedral angle relatively to the pyrazine ring when compared with the dihedral angles of uncoordinated pyridine rings in mononuclear complexes, see Tab. 8 and Fig. 14.

Tab. 8. Selected distances (Å) and angles (°) of molecule A of [Ni(tppz)(ox)(H_2O)]·5H_2O

Ni(1)-O(1)	2.063(5)	Ni(1)-N(1)	1.997(6)
Ni(1)-O(3)	2.003(5)	Ni(1)-N(3)	2.096(6)
Ni(1)-O(5)	2.094(5)	Ni(1)-N(6)	2.088(6)
O(1)-Ni(1)-O(3)	81.62.(22)	O(3)-Ni(1)-N(6)	104.71(23)
O(1)-Ni(1)-O(5)	92.11(21)	O(5)-Ni(1)-N(1)	92.11(21)
O(1)-Ni(1)-N(1)	96.55(22)	O(5)-Ni(1)-N(3)	91.30(20)
O(1)-Ni(1)-N(3)	90.81(20)	O(5)-Ni(1)-N(6)	89.95(21)
O(1)-Ni(1)-N(6)	91.52(21)	N(1)-Ni(1)-N(3)	77.90(25)
O(3)-Ni(1)-O(5)	89.74(21)	N(1)-Ni(1)-N(6)	78.16(25)
O(3)-Ni(1)-N(1)	176.59(23)	N(3)-Ni(1)-N(6)	156.1(3)
O(3)-Ni(1)-N(3)	99.20(23)		

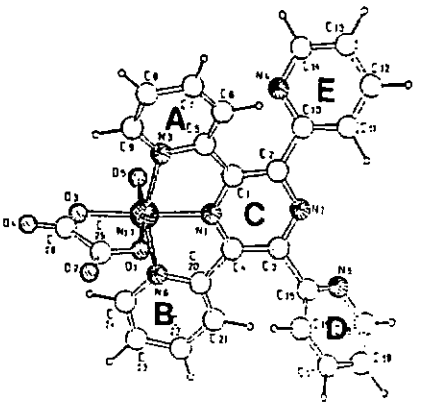

Fig. 14 SCHAKAL plot of the molecule A of [Ni(tppz)(ox)(H_2O)]·5H_2O.

The infrared spectrum indicates coordination for the ligand as well as for the oxalate. There is a very strong absorption band for ν(C=O) at 1635 cm^{-1} with a shoulder for the ν(C=N) vibration in this region. In the u.v. spectrum, recorded in water solution, the bands for the ligand were found at 290 and 350 nm.

2.3.1. Coordination behaviour of Ni(II) complexes of tppz with pseudohalides and a squaric acid derivative

Pseudohalides represent an interesting class of inorganic anions. All are negatively charged, polyatomic, mesomeric stabilized and monoanions. A summary of important pseudohalides are given in Table 9.

Tab. 9. Listing of important pseudohalides[51]

Structural type	representative
AB^-	CN^-
ABC^-	N_3^-, CNO^-, NCO^-, NCS^-, $NCSe^-$, $NCTe^-$
$A(BC)_2^-$	$N(CN)_2^-$, $P(CN)_2^-$
$A(BC)_3^-$	$C(CN)_3^-$,
$A(BC)_n^-(n>3)$	$Co(CO)_4^-$, $Mn(CO)_5^-$

The ability to coordinate with complexes of tppz with three of the representative pseudohalides, NCS^-, $C(CN)_3^-$ and $N(CN)_2^-$, were tested. Numerous comparisons as well as the formation of corresponding mixed complexes show that there are marked analogies between thiocyanate and halide complexes in both their stability and structural features[51]. It is considered that the thiocyanate ion is a stronger donor ligand than the halide ions. In this case the SCN^- should form more stable complexes than the corresponding halide ions. In fact,

[51] A.M. Golub, H. Köhler, *Chemie der Pseudohalogenide*, Deutscher Verlag der Wissenschaften, Berlin 1979.

however, this was only observed for metals such as cobalt, nickel, zinc and indium. Based on the charge distribution data given for the SCN^- anion, there are several possibilities for the coordination behaviour of the SCN-group. Some examples are given below.

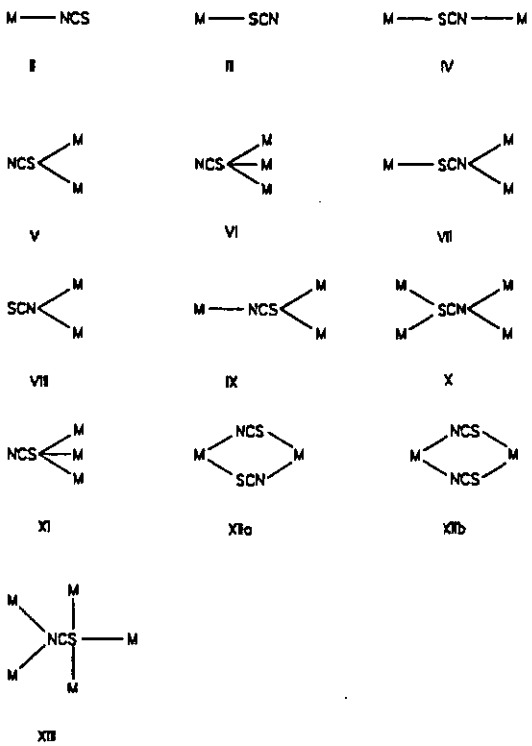

Not all of these types have been detected by X-ray structure analyses[51]. According to the conception of Pearson a SCN-group coordinated through the nitrogen represents a hard base, whereas a sulphur-coordinated SCN is considered as a soft base. Therefore it is assumed that soft acids coordinate via sulphur and hard acids prefer the nitrogen. On the other hand it is established that the divalent cations from Fe to Zn build a middle class which may react with both hard and soft bases. The limitation of Pearson's classification are indicated by many results.

The possibility of the coordination XIIa was found by Rojo et all [52, 53]. They obtained from a reaction of $[Ni(terpy)Cl(H_2O)_2]Cl{\cdot}H_2O$ with KSCN or KSeSCN (1:3) the dimeric complex $[\{Ni(terpy)(NCX)_2\}_2]$ (X = S, Se). The X-ray structure analysis indicates that both of the complexes are isomorphous (triclinic cells and the same space group). Interestingly, the two Ni atoms are bridged by two thiocyanato ions and the two others act as terminal ligands, Fig. 15.

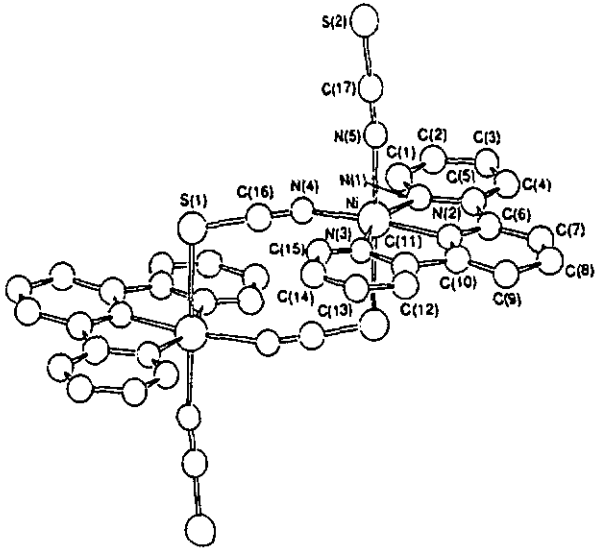

Fig. 15. Molecular structure of the dimeric complex $[\{Ni(terpy)(NCS)_2\}_2]$.

The Ni-Ni separation in the complex is 5.633(3) Å. The two thiocyanato ligands of the bridging unit are coplanar being related by an inversion center. The Ni(II) ions are below and above (±0.056 Å) the coordination sphere of the four nitrogen atoms. The complexes exhibits a ferromagnetic exchange interaction. The electronic spectra of the sulphur compound exhibits three bands at 10600, 17200 and 24300 cm^{-1} which could assigned to the d→d transition

---

[52]T. Rojo, R. Cotés, L. Lezama, M.I. Arriortua, K. Urtiaga, G. Villeneuve, *J. Chem. Soc., Dalton Trans.*, (1991) 1779.

[53]T. Rojo, R. Cotés, L. Lezama, J.L. Mesa, , G. Villeneuve, *Inorg. Chim. Acta*, 162 (1989) 11.

$[^3A_{2g}\rightarrow{}^3T_{2g}, {}^3A_{2g}\rightarrow{}^3T_{1g}(F), {}^3A_{2g}\rightarrow{}^3T_{1g}(P)]$ in an octahedral coordination sphere for the d^8 ion. Infrared spectra contain the bands for the [νCN] at 2100 and 2130 cm^{-1}.

Furthermore we carried out a reaction of $[Ni_2(tppz)(H_2O)_6](NO_3)_6\cdot 3H_2O$ with NH_4SCN (molar ratio 1:4) in water solution at 70°C.

$$[Ni_2(tppz)(H_2O)_6](NO_3)_4\cdot 3H_2O + 4NH_4SCN \rightarrow [Ni_2(tppz)(SCN)_4(H_2O)_2] + 7H_2O + 4NH_4NO_3 \quad (6)$$

From the reaction mixture a red powder precipitated very quickly. By the elemental analysis results we assume the composition $[Ni_2(tppz)(SCN)_4(H_2O)_2]$ (6). The compound is sparingly soluble in all common solvents and recrystallization from a large amount of several solvents gave only very fine crystals which were not suitable for X-ray diffraction studies. From infrared measurements (KBr) we obtained the information that in the solid state a coordination of SCN^- takes place. The characteristic bands of the thiocyanate (in NH_4SCN) are found for ν(CN) at 2050 sh, vs; ν(CS) at 752 m and ν(SCN) at 477 m cm^{-1}. The position of the bands corresponding to the ν(CN) stretching vibrations can illustrate the coordination mode to the metal ions. The ν(CN) frequencies of the various types increase in the order SCN^- < M-NCS < M-SCN < M-NCS-M. In the case when bridging SCN groups are present, νCN may increase by 70-120 cm^{-1} compared with that of the SCN ion (2050 cm^{-1}).

We found a broad band with a shoulder in the spectrum of the complex shifted by 50 cm^{-1} to higher wave numbers (2100vs cm^{-1}). This could be an indication of M-NCS coordination mode. In the reflectance spectra (compound diluted with MgO) we found the three expected d→d transition bands $[^3A_{2g}\rightarrow{}^3T_{2g}, {}^3A_{2g}\rightarrow{}^3T_{1g}(F), {}^3A_{2g}\rightarrow{}^3T_{1g}(P)]$ for octahedral (O_h) symmetry at 11363, 13333 and 24390 cm^{-1}.

The anion dicyanamide ($N(CN)_2^-$), which was also used also offers the possibility to act as bridging ligand to form coordination polymers. The very close relationship of the dicyanamide ion to the cyanates is a consequence of the pseudohalide character of the NCN-group. Alkali dicyanamides are easily obtained by treating alkaline cyanamide solution with cyanogen

bromide[54];[55] ($NaNHCN + BrCN + NaOH \rightarrow NaN(CN)_2 + NaBr + H_2O$). The sodium dicyanamide trimerized at higher temperatures to tricyanomelamine a homologe to the cyanuric acid. The addition of one molecule of alcohol resulted in the formation of N-cyano-O-ethyl-isourea, and in the presence of Zn^{2+} or Cu^{2+} a catalyzed addition of another molecule of alcohol[56] occurs. Today a number of dicyanamide complexes are known (Table 10). Dicyanamide has a low basicity like tricyanomethanide and thiocyanate but it is a good complexing ligand. In generally this compound is capable of forming covalent as well as coordinative bonds via the cyano nitrogen or the amide nitrogen. See the mode of bondings:

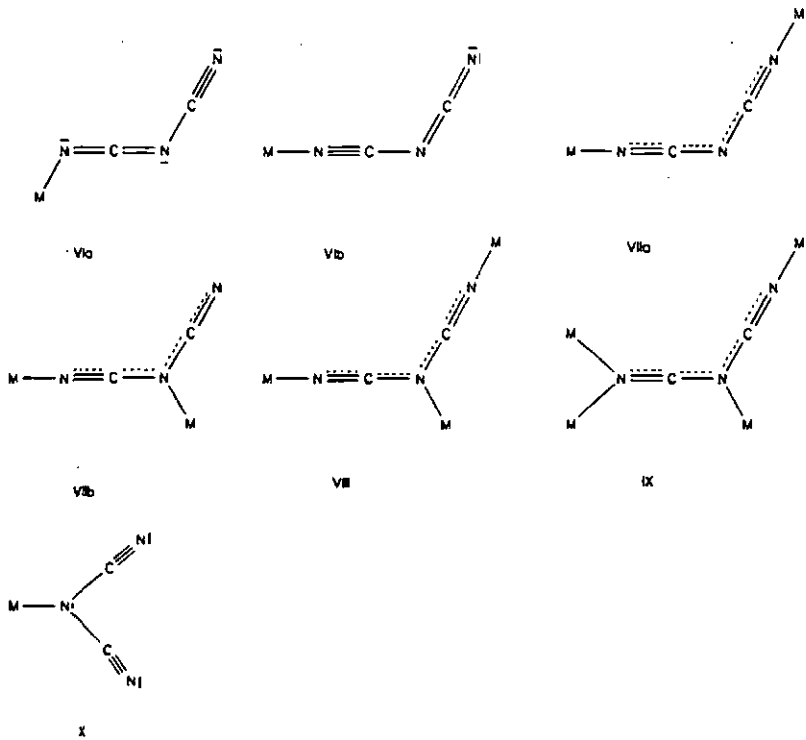

[54]B.L. Evans, A.D. Joffe, P. Gray, *Chem. Rev.* 59 (1959) 515.

[55]W. Beck, P. Swoboda, K. Feldl, R.S. Tobias, *Chem. Ber.* 104 (1971) 533.

[56]T.A. Turney, G.A. Wright, *Chem. Rev.* 59 (1959) 497.

MO calculations gave a much higher charge density (-1.155) for the cyano-N atoms than for the amide-N (-0.677), which shows the ambivalent character of this ligand.

The bonding situation in dicyanamide derivatives is reflected in a typical way by the infared spectra, see Tab. 10: When the dicyanamide behaves as a multidentate bridging ligand (coordination polymers are frequently observed), then generally a shift of the ν(CN) stretching vibration bands towards higher wavenumbers is observed.

Tab. 10. Summary of the ν(CN) stretching vibrations of dicyanamide in several bonding modes (recorded in KBr or nujol)[51]

compound	ν(CN)	bond type
$[Zn\{N(CN)_2\}_4]^{2-}$	2140vs, 2210m, 2235s	VI
$[Co\{N(CN)_2\}_2(NCS)_2]^{2-}$	2168vs, 2230m	VI
$[Co\{N(CN)_2\}_4]^{2-}$(sol)	2185s, 2230m	VI
$[Cd\{N(CN)_2\}_4]^{2-}$	2160vs, 2210m, 2230s	VI
$(C_6H_5)_2P(O)NCNCN$	2190vs, 2260s	VI
$(C_6H_5)_2P(O)N(CN)_2$	2260s	X
$[(CH_3)_2Sn\{N(CN)_2\}_2]_n$	2210···2225s, 2256	VII
$[Ni\{C_5H_5N)_2\}\{N(CN)_2\}_2]_n$	2200vs, 2255m	VII
$[Ni\{N(CN)_2\}_3^-]_n$	2185s, 2250m	VII
$[Ni\{N(CN)_2\}_2]_n$	2210s, 2260sh	VIII

We studied the reaction of $[Ni_2(tppz)(H_2O)_6](NO_3)_4\cdot 3H_2O$ with $KN(CN)_2$ and obtained small orange red crystals which were soluble in a large amount of water.

$$[Ni_2(tppz)(H_2O)_6](NO_3)_4\cdot 3H_2O + 2KN(CN)_2 \rightarrow [Ni_2(tppz)\{N(CN)_2\}_2(H_2O)_4](NO_3)_2 + 5H_2O + 2KNO_3. \quad (7)$$

The infrared spectrum (KBr) of $KN(CN)_2$ contains the following characteristic bands: 915 w [νs(C-N)]; 1327 s νas(C-N); 2152 vs νs(CN); 2222m; νas(CN); 2262s;

$\nu s+\nu as(CN)$. In the spectrum of the complex we found in the $\nu(CN)$ region four vibration bands at 2284 s, 2128m, 2171 vs and 2218 s cm^{-1}. Here we found an additional signal which could be an indication of two different types of bonding modes in the complex. Elemental analysis results agree with the composition $[Ni_2(tppz)(N(CN)_2)_2(H_2O)_4](NO_3)_2$. The reflectance spectra exhibits three bands at 11353, 19607 and 26666 cm^{-1}. The bands have been ascribed to a d→d transition near to O_h symmetry [$^3A_{2g}\rightarrow{}^3T_{2g}$, $^3A_{2g}\rightarrow{}^3T_{1g}(F)$, $^3A_{2g}\rightarrow{}^3T_{1g}(P)$].

The ligand tricyanmethanide is also a very interesting molecule because it coordinate polydentate. This ligand can be obtained from a reaction of 1,1-dicyano-2-amino-2-alkoxyethene with potassium hydroxide[57]. In the following scheme the possible bonding modes are given.

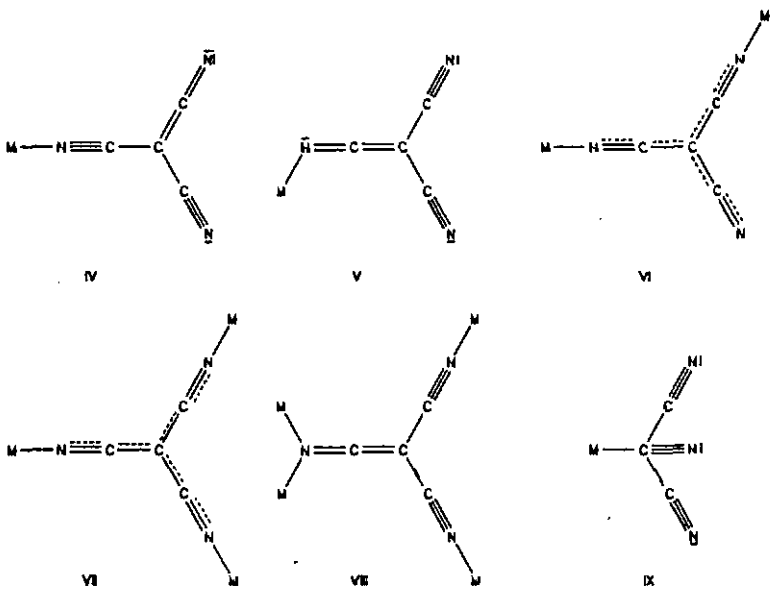

[57]W. J. Middleton, V.A. Engelhardt, *J. Am. Chem. Soc.* ,80 (1958) 2788.

MO calculations show, in agreement with the above mentioned results that the cyano nitrogens are much more negative (-1.114) than the central carbon atom (-0.374)[58], but tricyanmethanide is able to form bonds of different types:

Because of a high degree of the ionic charge delocalization the three cyano N-atoms are equally capable of establishing coordinative bonds. This enables tricyanomethanide to act not only as a monodentate but also preferably as a bi-and tridentate ligand bridging function. A tetradentate coordination was shown by an X-ray structure analysis of the dimethyl-thallium tricyanomethanide[59]. Infrared spectra of complexes containing the $C(CN)_3^-$ ligand enable one to predict a coordination type analogous to Fig. 16. A combination with the ^{15}N n.m.r. spectroscopy allowed a more realistic characterization.

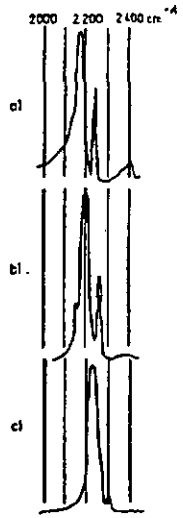

Fig. 16. Comparison of the ν(CN) stretching vibrations of coordinatively mono-, bi and tridentate Ni(II) complexes containing tricyanomethanide. a: $[Ni\{NCC(CN)_2\}_2(py)_4]$; b: $[Ni\{NCC(CN)_2\}_2(py)_2]$; c: $[Ni\{NCC(CN)_2\}_2]$.[51]

---

[58]J.H. Enemark, R.H. Holm, *Inorg. Chem.*, 3 (1964) 1516.

[59]Y.M. Chow, D. Britton, *Acta Cryst.*, B31 (1975) 1934.

We carried out a reaction of $[Ni_2(tppz)(H_2O)_6](NO_3)_6 \cdot 3H_2O$ with $KC(CN)_3$ in a molar ratio of 1:2 and obtained an orange powder which precipitated very quickly.

$$[Ni_2(tppz)(H_2O)_6](NO_3)_4 \cdot 3H_2O + 2KC(CN)_3 \rightarrow [Ni(tppz)_2](C(CN)_3)_2 \cdot 2H_2O + Ni(NO_3) \quad (8) \quad + 2KNO_3 + 7H_2O$$

After recrystallization from a methanol/water solution we obtained very fine orange plates. The infrared spectrum contains the characteristic bands for the tricyanmethanide at 2157vs, sh cm^{-1}. This is an indication that $C(CN)_3^-$ acts as counter ion in a non-coordination mode. In the ν(C=C), ν(C=N) region the characteristic bands for the coordinated tppz are present at 1599 m, sh; 1569 m; 1542 w; 1480 m; 1469m; 1446m and 1403s cm^{-1}. By means of elemental analysis results we propose the composition $[Ni(tppz)_2](C(CN)_3) \cdot 2H_2O$. It is assumed that two molecules of tppz are coordinated in an octahedral coordination sphere around the nickel atom. This was structurally proved for a similar zinc complex. FAB mass spectroscopy gave the following typical fragments which are a further indication for the predicted arrangement:

Tab. 11. FAB-mass spectrum (70eV) of $[Ni(tppz)_2](C(CN)_3) \cdot 2H_2O$

m/e	rel. intensity (%)	fragment
925	28	$[\{(Ni(tppz)_2\}\ (C(CN)_3)]^+$
835	45	$[Ni(tppz)_2]^+$
447	98	$[Ni(tppz)]^+$

The reflectance spectra of the diluted compound (MgO) exhibits three bands at 12345, 20202 and 25316 cm^{-1}. The bands have been ascribed to a d→d transitioo near to O_h symmetry [$^3A_{2g} \rightarrow {}^3T_{2g}$, $^3A_{2g} \rightarrow {}^3T_{1g}(F)$, $^3A_{2g} \rightarrow {}^3T_{1g}(P)$]. The n.m.r. spectra in DMSO solution shows the decomposition of the complex. We found four signals for the free ligand at 9.47 (m), 9.10 (m), 7.60 (m) and 6.10 (m) ppm.

Furthermore, we carried out a reaction of $[Ni_2(tppz)(H_2O)_6](NO_3)_4 \cdot 3H_2O$ with a manganese complex of squaric acid ($sqacH_2$) (ratio 1:1) $[Mn(H_2O)_4(sqacH)_2]$; synthesized by Wang[60].

$$[Ni_2(tppz)(H_2O)_6](NO_3)_4 \cdot 3H_2O + [Mn(H_2O)_4(sqacH)_2] \rightarrow [Ni_2(tppz)(H_2O)_6](sqac)_2 \cdot 2.5H_2O \quad (9)$$
$$+ Mn(NO_3)_2 + 2HNO_3 + 4.5H_2O$$

From this reaction we obtained a red brown powder and after recrystallization from methanol/water solutions we isolated well formed block like crystals suitable for X-ray diffraction studies. The squaric acid molecules act as counter ions in the new compound $[Ni_2(tppz)(H_2O)_6](sqac)_2 \cdot 2.5H_2O$[48]. During the reaction the manganese complex decomposed. The new complex possess crystallographic C_i symmetry and we found an interesting molecular arrangement. The four oxygen atoms of the squaric acid are hydrogen bonded to the six coordinated water molecules of the binuclear nickel complex to form a polymeric network. Additionally the water molecules of crystallization are hydrogen bonded to each other and to two oxygen atoms of the squaric acid. The C-C and C-O distances demonstrate the charge delocalization in the molecule, Table 12.

Tab. 12. Collection of C-C and C-O distances (Å) of the squaric acid molecule molecule

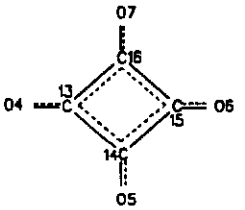

C(13)-C(14)	1.453(11)	C(15)-C(16)	1.477(11)
C(14)-C(15)	1.450(11)	C(16)-C(13)	1.455(11)
C(13)-O(4)	1.265(9)	C(15)-O(6)	1.250(9)
C(14)-O(5)	1.263(10)	C(16)-O(7)	1.237(10)

[60]Yi Wang, personal communication.

This could be the reason for the strong hydrogen bonding network. The Ni-N(pyrazine) distance in the centrosymmetric bis(tridentate) complex (2.011(6) Å) is shorter than the Ni-N(pyridine) distances (2.085(6), 2.084(7)Å). These values are comparable with those found for the corresponding nitrate complex. The Ni(1)...Ni(1)^{a} separation is 7.488(19)Å and the separation of the Ni(1) atom to Ni(1)^{b}, Ni(1)^{c} and Ni(1)^{d} are 7.2430(20), 8.468(21) and 6.632(18)Å respectively. The Ni-O(water) distances are given in Table 13. The pyridine rings A and B are inclined to one another by 4.9(3) and to the central pyrazine ring C by 73.0(3) and 70.0(3)°, respectively. The central pyrazine ring is distorted and the dihedral angle between plane C'^C" is 10.7(3)°. Only the protons of the water molecule O(3) were located. The distance O(3)-HW(31) is 0.81(6) and the distance of HW31...O(5)^{b} of the squaric acid was found to be 1.86(6)Å, whereas the distance between both oxygens O(3)-O(5)^{b} is 2.678(8)Å. The angle O(3)-HW(31)...O(5)^{b} is 168°.We found further imponant distances of O(5)^{c} and O(5)^{d} to HW(32) with 2.21(8) and 2.21(7)Å. All distances which are indications for hydrogen bridging bonds are collected in Tab. 13. The protons of O(1) and O(2) were not located and for this reason short O-O distances are given to demonstrate the interactions in the crystal.

Tab. 13. Selected distances (Å) of $[Ni_2(tppz)(H_2O)_6](sqac)_2 \cdot 2.5H_2O$

Ni(1)-N(1)	2.011(6)	Ni(1)-O(1)	2.101(6)
Ni(1)-N(2)	2.085(6)	Ni(1)-O(2)	2.110(6)
Ni(1)-N(3)	2.084(7)	Ni(1)-O(3)	1.968(6)
O(5)^{b}-O(3)	2.678(8)	O(5)^{d}-O(3)	2.706(8)
O(6)^{b}-O(2)	2.724(8)	O(4)^{d}-O(1)	2.678(9)
O(5)^{b}-HW(31)	1.860(6)	O(5)^{d}-HW(32)	2.210(7)
O(7)-O(1)^{a}	2.713(8)	O(4)-OW(8)^{c}	2.831(9)
O(6)-O(2)	2.691(8)	O(7)-OW(9)^{a}	2.874(13)
OW(9)-OW(10)	3.000(3)	OW(8)-OW(9)^{h}	2.826(13)
OW(9)-OW(10)^{k}	2.440(3)	OW(8)-OW(5)^{g}	2.952(9)
OW(10)-OW(10)^{k}	1.570(5)		

Symmetry operations: [a] 1.5-x, y, o 5-z; [b]2-x, 1.5-y, 0.5-z; [c]0.5+x, 1-y, 0.5+z; [d]x, 0.5+y, 0.5-z; [g]1-x, 1.5-y, 0.5-z; [h]-0.5+x, 0.5-y, z; [k]1-x, 1-y, -z..

A demonstration of the hydrogen bonded network between the oxygen atoms of the squaric acid molecules and the protons of the coordinated water molecules are given in Fig 17 and a demonstration of the packing in Fig. 17a.

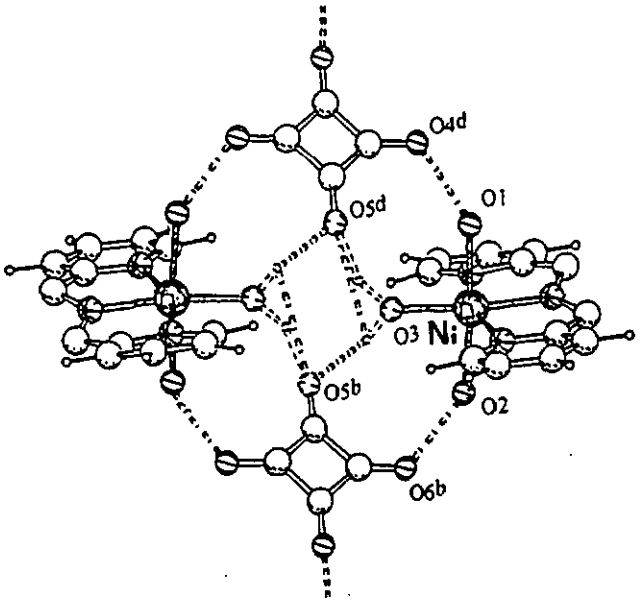

Fig. 17. Demonstration of the hydrogen bridges between the oxygen atoms of the squaric acid molecules and the water molecules in the complex $[Ni_2(tppz)(H_2O)_6]^{2-}$, water molecules of crystallization are omitted for clarity.

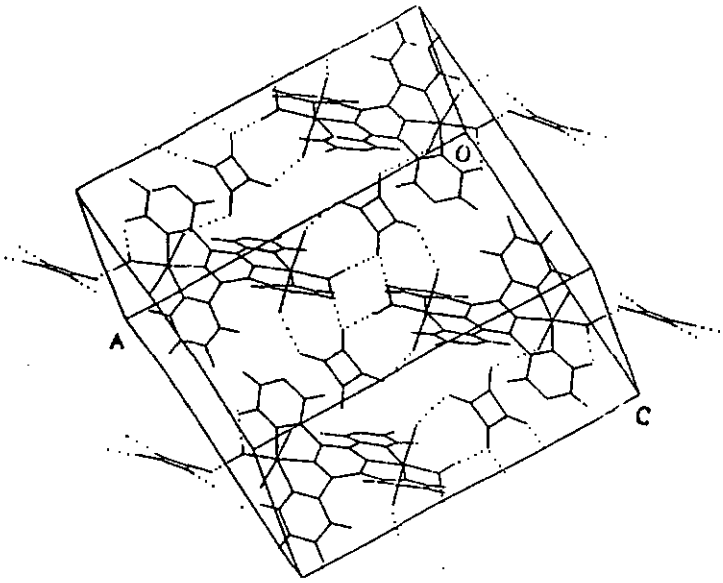

Fig 17a. Demonstration of packing in the crystal of the hydrogen bonded polymer $[Ni_2(tppz)(H_2O)_6](sqac)_2 \cdot 2.5H_2O$.

Because of the close arrangement of nickel atoms in the crystal packing of the starting material **4** and the hydrogen bonded polymer **9** magnetic investigations are in progress and will be published [61].

[61] To be published.

2.4. Structural and magnetic properties of Cu(II) complexes of tppz

Copper in the oxidation state (II) reacts with ammonia in aqueous medium under stepwise addition to $[Cu(NH_3)(H_2O)]^{2+}$ ... $[Cu(NH_3)_4(H_2O)_2]^{2+}$. A coordination of five or six molecules of ammonia is generally difficult due to the Jahn-Teller-effect. Therefore, a coordination of tppz with Cu^{2+} to build a polymer structure is nearly impossible, for this reason we introduced further bridging ligands.

From a reaction of tppz with two equivalents of $Cu(ClO_4)_2$ in a $EtOH/H_2O$ mixture at 90°C we obtained green square rods.

$$Cu(ClO_4)_2 \cdot 6H_2O \quad + \quad tppz \quad \rightarrow \quad [Cu_2(tppz)(H_2O)_4](ClO_4)_4 \cdot 2H_2O \qquad (10)$$

X-ray structure analysis showed that this is a dinuclear complex and the ligand coordinates in a bis-tridentate[62] manner. The complex possesses crystallographic C_i symmetry and the central pyrazine ring is planar, see Fig. 14. The pyridine rings A and B are inclined to one another by 34.3(2) and by 21.3(3) and 21.7(3)°, respectively, to the central pyrazine ring C. The shortest C...C intramolecular distance is between atoms C(4) and C(9a) with 3.089Å. Protons H(4) and H(9a) are separated by 2.316 Å. The coordination sphere of the copper atom can be described as a distorted square pyramidal, the copper atom being displaced by -0.008(3)Å from the plane through atoms N(1), OW(1) and OW(2), with atoms N(2) and N(3) displaced by -1.982(5) and 1.953(5)Å, respectively, and the N(2)-Cu-N(3) angle equal to 158.57(15)°. The central Cu-N(pyrazine) distance is slightly longer than the central Cu-N(pyridine) distance in the copper terpy complexes[63], [64], [65] while the Cu-N(pyridine) distances are significantly shorter (*c.* 0.04Å),

---

[62]M. Graf, B. Greaves, H. Stoeckli-Evans, *Inorg. Chim. Acta*, 204 (1993) 239.

[63]W. Henke, S. Kremer, D. Rheinen, *Inorg. Chem.*, 22 (1983) 2858.

[64]T. Rojo, M. Vlasse, D. Beltran-Porter, *Acta Cryst.*, C39 (1983) 194.

[65]T. Rojo, R. Cortes, L. Lezama, J.L. Mesa, J. Via, M.I. Arriortua, *Inorg. Chim. Acta*, 185 (1989) 91.

see Table 14. The Cu...Cu separation in the dinuclear complex is 6.497(2)Å (symmetry operation: 2-*x*, 1-*y*, -*z*), selected bond distances are given in Tab.15.

Tab. 14. Selected distances (Å) in Cu(II) complexes of tppz and terpy

	$[Cu_2(tppz)(H_2O)_4]$	$[Cu(terpy)Cl_2]$	$[Cu(terpy)Cl_2](H_2O)$	$[Cu(terpy)(NCO)(H_2O)](NO_3)$
Cu-N(1)	1.962(3)	1.952	1.952	1.942
Cu-N(2)	2.007(4)	2.056	2.0442.	2.047
Cu-N(3)	1.999(4)	2.052	2.039	2.043
Cu-Cl(1)		2.252	2.221	
Cu-Cl(2)		2.469	2.554	
Cu-OW1	1.955(3)			
Cu-NCO				1.893
Cu-OW2	2.209(4)			2.210
Cu...Cu	6.497(2)[a]	5.54	4.01	3.950

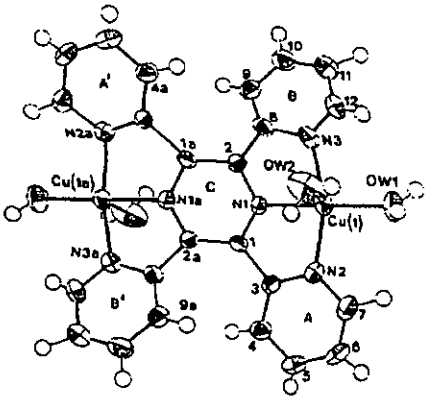

Fig. 18. SCHAKAL plot of $[Cu_2(tppz)(H_2O)_4](ClO_4)_4$.

Tab. 15. Selected distances (Å) and angles (°) of $[Cu_2(tppz)(H_2O)_4](ClO_4)_4$

Cu(1)-N(1)	1.962(3)	Cu(1)-OW(1)	1.9553(3)
Cu(1)-N(2)	2.007(4)	Cu(1)-OW(2)	2.209(4)
Cu(1)-N(3)	1.999(4)	Cu(1)-Cu(1[a])	6.497(2)
N(1)-Cu(1)-N(2)	80.42(15)	N(2)-Cu(1)-OW(1)	99.71(16)
N(1)-Cu(1)-N(3)	80.18(15)	N(2)-Cu(1)-OW(2)	94.42(16)
N(1)-Cu(1)-OW(1)	174.74(15)	N(3)-Cu(1)-OW(1)	88.77(17)
N(1)-Cu(1)-OW(2)	94.04(19)	N(3)-Cu(1)-OW(2)	95.95(18)
N(2)-Cu(1)-N(3)	158.57(15)	OW(1)-Cu(1)-OW(2)	91.20(19)

Symmetry operation: [a]2-x, 1-y, -z.

In the infrared spectrum (KBr) we found the corresponding (νC=C, C=N) stretching vibrations as a characteristic pattern at 1630s and 1601vs cm^{-1} which indicates a shift of the free ligand of 42 and 34 cm^{-1}. Further bands in this region are found at 1499w, 1477s, 1424m, 1417w, 1390w cm^{-1}. U.v. measurements in water as solvent also indicates the coordination of the ligand (λ_{1max}=300 and λ_{2max}=362 nm). The elemental analysis is in agreement with the composition shown by X-ray analysis.

E.p.r. studies of mixed hexafluoroacetylacetonate complexes of copper(II) are reported with some diimine ligands in[22] by Escuer et al. in 1989. The room temperature e.p.r. spectra of the polycrystalline monomeric compounds $[CuL(hfacac)_2]$, with L= dpp, dpq, bdpq, dMedpq and Cldpq are axial with $g_{\|}$, $g_{\perp}$ values shown in Table16.

Tab. 16. Room temperature polycrystalline e.p.r. spectra of several copper compounds

Compound	$g_{\|\|}$	$g_{\perp}$	$A_{\|\|}$ (G)
$[Cu(hfacac)_2DPP]$	2.30	2.09	
$[Cu(hfacac)_2DPQ]$	2.31	2.07	140
$[Cu(hfacac)_2DMeDPQ]$	2.31	2.08	140
$[Cu(hfacac)_2BDPQ]$	2.30	2.08	
$[Cu(hfacac)_2]ClDPQ]$	2.31	2.09	
$[(hfacac)_2Cu$-(tppz)-$Cu(hfacac)_2]$	2.32	2.09	

The powder spectrum of the binuclear complex $[(hfacac)_2Cu(tppz)Cu(hfacac)_2]$[22] is only slightly different to the mononucleat complexes, indicating that no exchange interaction is operative betweeo the two metal ions.

From a similar reaction in the presence of 2M HCl we obtained large green lozenge type crystals.

$$2Cu(ClO_4)_2 + tppz + 2HCl \rightarrow [Cu(tppzH)Cl]_2(ClO_4)_4 \quad (11)$$

The X-ray structure analysis showed that tbe copper atom is five-fold coordinated and the complex forms a dimer with a bridging Cu...Cl^a distance of 2.682(3)Å, a Cu...Cu^a bridging separation of 3.446(3)Å and a bridging angle Cu-Cl(1)...Cu^a of 88.49(7)°, see Fig. 15. In 1993 E. Spodine et al.[66] published the structure of the dimeric five-coordinated Cu^{2+} complex $[Cu(DPM)Cl_2]_2$ with asymmetrical bridging Cl atoms. Tbe Cu-Cl bond lengths were 2.315(1) and 2.629(1)Å in this case. In $[Cu(tppzH)Cl]_2(ClO_4)_4$ the dimers are stacked up the a axis with a short Cu...Cu^b inter-stacking distance of only 3.854(4) Å, see Table 11 and Fig.16. The coordinated part of the ligand is less planar than that found for Cu(terpy)

[66]E. Spondine, J. Manzur, M.T. Garland, J.P. Fackler, Jr., R.J. Staples, B. Trzinska-Bancroft, *Inorg. Chim. Acta*, 203 (1993) 73.

complexes[67, 68, 63-65]. The torsion angles N(1)-C(1)-C(3)-N(2) and N(1)-C(2)-C(8)-N(3) are 2.3 and 13.7°, respectively, compared to a maximum value of 8.93° and a minimum value of 0.03° in the Cu(terpy) complexes considered. However, this system is more planar than in the zinc complex described later, where the same torsion angles are -5.8 and -17.8°, respectively. The pyrazine ring is considerably distorted. The dihedral angle between planes C'[C(1), N(1), C(4)] and C"[C(2), N(2), C(3)] is 8.0(2)°. Larger and smaller twist angles have been observed in the pyrazine rings in complexes of rhodium (12.3 and 15.3°)[69], a ruthenium (12.8°)[70] and a copper complex (3.9 and 8.0°)[71] containing the similar ligand 2.3-bis(2-pyridyl)-quinoxaline (bpq) and the zinc complex described later. The coordinated pyridine rings (A and B) are inclined to one another by 1.9(2)° and to plane C' by 13.7(3) and 13.0(3)°, respectively. The uncoordinated pyridine rings (D and E) are inclined to one another by 49.8(2)° and to plane C" by 38.2(4) and 41.8(3)°, respectively. The copper coordination is best described as distorted square pyramidal ($\tau = 0.27$); the copper atom being displaced by 0.172(2)Å from the best plane through atoms N(1), N(2), N(3) and Cl(1) (planar to within 0.002(2)Å). Atom Cl(1^B) occupies the apical position at 2.682(3)Å from atom Cu(1), showing a typical Jahn-Teller distortion. The central Cu-N(pyrazine) distance [1.943(4)Å] is similar to the central Cu-N(pyridine) distance observed in a number of mononuclear Cu(terpy) complexes[63-65] and in two dimeric Cl-bridged Cu(terpy) complexes[67,68] and a NCO bridged Cu(terpy) complex[63]. The lateral Cu-N(pyridine) distances are also similar to those observed in the above mentioned compounds, see Tab.18. The pyridine ring involving atom N(6) is protonated and hydrogen bonded to a perchlorate O atom, see Table17.

---

[67]T. Rojo, M.I. Arriotua, J. Ruiz, J. Darlet, G. Villeneuve, D. Beltran-Porter, *J. Chem. Soc., Dalton Trans.*, (1987) 285.

[68]J.-V. Folgado, P. Gomez-Romero, F. Sapina, D. Beltran-Porter, *J. Chem. Soc., Dalton Trans.*, (1990) 2325.

[69]S.C. Rasmussen, M.M. Richter, E.Yi.H. Place, K.J. Brewer, *Inorg. Chem.*, 29 (1990) 3926.

[70]D.P. Rillema, D.G. Taghdiri, D.S. Jones, C.D. Keller, L.A. Wrol, T.J. Meyer, H.A. Levy, *Inorg. Chem.*, 26 (1987) 578.

[71]V.K. Goodwin, W.T. Pennington, J.D. Petersen, *Acta Cryst., C*, 46 (1990) 898.

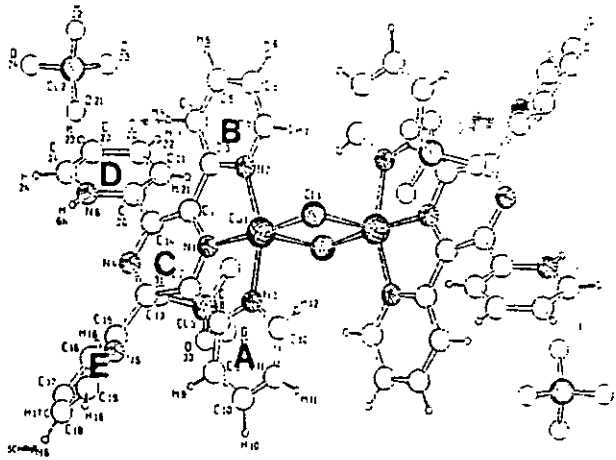

Fig. 19. SCHAKAL plot of the molecular structure of $[Cu(tppzH)Cl]_2(ClO_4)_2$ (11).

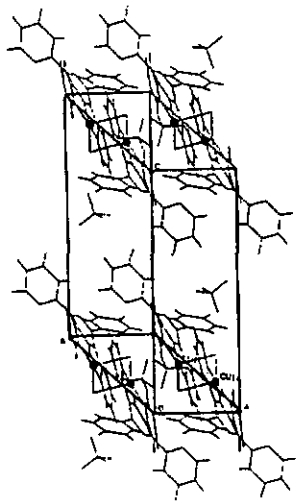

Fig 19a. PLUTO[72] packing diagram of $[Cu(tppzH)Cl]_2(ClO_4)_4$ (11).

---

[72]E.J. Gabe, Y. Le Page, J.P. Charland, F.L. Lee, P.S. White, NRCVAX-an Interactive program System for Structure analysis, *J. Appl. Crystallogr.* 22 (1989) 384.

Tab. 17. Selected distances (Å) and angles (°) of $[Cu(tppzH)Cl]_2(ClO_4)_2$ (11)

Cu(1)-Cl(1)	2.2359(16)	Cu(1)-N(2)	2.013(4)
Cu(1)-Cl(1[a])	2.682(3)	Cu(1)-N(3)	2.022(4)
Cu(1)-N(1)	1.943(4)	Cu(1)···Cu(1[a])	3.446(3)
N(6)-H(6N)	0.71(6)	Cu(1)···Cu(1[b])	3.854(4)
H(6N)···O(34[c])	2.18(6)	N(6)···O(34[c])	2.869(7)
Cl(1)-Cu(1)-Cl(1[a])	91.51(7)	Cl(1[a])-Cu(1)-N(3)	95.48(11)
Cl(1)-Cu(1)-N(1)	170.59(11)	N(1)-Cu(1)-N(2)	79.82(14)
Cl(1)-Cu(1)-N(2)	99.11(11)	N(1)-Cu(1)-N(3)	79.86(15)
Cl(1)-Cu(1)-N(3)	99.58(11)	N(2)-Cu(1)-N(3)	158.05(14)
Cl(1)-Cu(1)-N(1)	97.90(12)	Cu(1)-Cl(1)-Cu(1[a])	88.49(7)
Cl(1)-Cu(1)-N(2)	95.43(11)	N(6)-H(6N)···O(34[c])	163.00(6)

[a]2-x, 1-y, -z; [b]1-x, 1-y, -z; [c]-1+x, y, z.

Tab. 18. Selected distances (Å) in Cu(II) complexes of tppz and terpy

	$[Cu(tppzH)Cl]_2$	$[Cu(terpy)Cl_2]_2$	$[Cu(terpy)(NCO)=(H_2O)]_2(PF_6)_2$	$[\{Cu(terpy)Cl_2\}=CuCl_2]_2$
Cu-N(1)	1.943(4)	1.909	1.933	1.938
Cu-N(2)	2.013(4)	2.021	2.038	2.021
Cu-N(3)	2.022(4)	2.017	2.028	2.014
Cu-Cl(1)	2.236(2)	2.218		2.221
Cu-Cl(1)	2.682(3)[b]	2.723		2.613
Cu-NCO			1.906	
Cu-OW			2.298	
Cu...Cu	3.446[b]	3.510	3.678	3.595

Symmetry operations: [b]2-x, 1-y, -z.

The infrared spectra (KBr) indicates the presence of the coordinated ligand. In the region of the ν(C=N), ν(C=C) vibrations we found the characteristic doublet split into four bands at 1626m, 1614vs, 1601s and 1589m cm^{-1} probably by reason of the coordinated and uncoordinated pyridine rings of tppz, respectively. Further bands in this region are present at 1541w, 1549w, 1533m, 1469m, 1460m, 1442m, 1403m cm^{-1}. The strong band for the perchlorate vibration overlaps a large part of the spectrum. U.v. measurements in water solution indicate the coordination of the ligand. We found the absorption bands for tppz at 300 and 360 nm.

Cyclovoltammetric measurements were undertaken in acetonitrile solutions. The working electrode was a platinum microelectrode and Ag/0.01 M $AgNO_3$ was used as reference electrode. The reversible half-wave potential of ferrocene was measured and amounted to 91 mV. The background electrolyte was 0.1 M tetrabutylammoniumhexafluorophosphate (TBAP) solution. The cyclovoltamograms were scanned at 5, 20 and 50V/s between +0.5 and -1.5 V. The two reduction waves for the ligand are outside of this potential range. For the chloride-bridged dimer two reduction peaks E_1 = 0.006 V and E_2 = -0.396 V as well as one oxidation peak at -0.143 V were observed, the cyclovoltammogram is given in Fig.20. Therefore, we assume a stepwise reduction from a Cu^{2+}-Cu^{2+} species to Cu^{2+}-Cu^{+} and from Cu^{2+}-Cu^{+} to Cu^{+}-Cu^{+} complex. A peak to peak separation of 0.4 V is observed. This behaviour was also found for the $[Cu(DPM)Cl]_2$ complex mentioned above[66]. For the oxidation we found only one wave which is less pronounced than the reduction waves. The cyclovoltammograms recorded with scan rates of 5 , 20 and 50 V/s, (see Fig.20a) may indicate a kinetically hindered process. For the reduction we found with a 20 V scan rate the potential E_1= -0.015 V, E_2= -0.436 V and at 50 V scan rate for E_1=-0.048 V and E_2= -0.476 V. A determination of the potential for the oxidation at higher scan rates is impossible. A comparison of electrochemical behaviour with the other copper complexes containing tppz was impossible due to the very poor solubility of these compounds in acetonitrile.

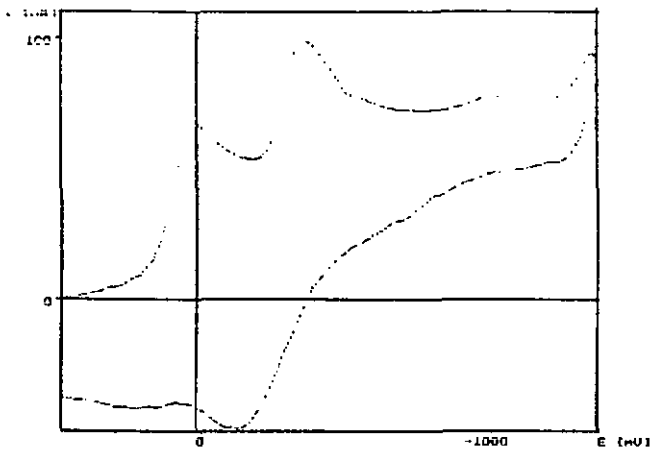

Fig. 20. Cyclic voltammogram for $[Cu(tppzH)Cl]_2(ClO_4)_2$ in CH_3CN solution, scan speed 5V/s, 0.1M TBAP, w.e.: platinum microelectrode; r.e.: Ag/0.01 M $AgNO_3$, $E_{1/2(ferrocene)}$91 mV/s.

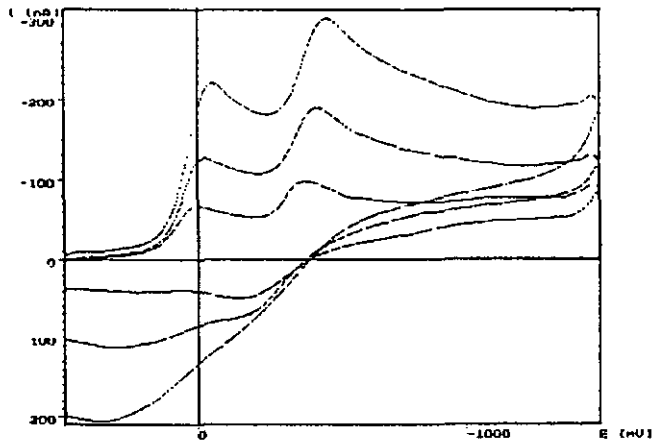

Fig. 20a. Cyclic voltammogram for $[Cu(tppzH)Cl]_2(ClO_4)_2$ in CH_3CN solution; scan speed, 5 V/s, 20 V/s and 50 V/s; 0.1M TBAP; w.e. platinum microelectrode; r.e.: Ag/0.01 M $AgNO_3$, $E_{1/2(ferrocene)}$ 91 mV/s.

The reaction of tppz with an excess of $CuCl_2$ (metal to ligand ratio 6:1) in water/ethanol at 90°C yields a compound crystallizing in the form of dark green crystals 12.

$$2CuCl_2 \cdot 2H_2O + tppz + H_2O \rightarrow [Cu_2(tppz)Cl_4] \cdot 5H_2O \quad (12)$$

Crystal structure analysis showed that it is a dinuclear complex which crystallizes with five molecules of water. Reaction attempts with ligand to metal ratios 1:1 or 1:2 resulted in a mononuclear complex which crystallized as fine plates not suitable for X-ray analysis. The expectation of chloride bridges in this complex, which could give the possibility of forming coordination polymers, failed. In this case the central pyrazine ring is distorted by 10.18(24)°, see Fig.21. In comparison with the corresponding Cu-N distances of the complex $[Cu(terpy)Cl_2]$ all Cu-N bond lengths are slightly longer, see Table 14. The Cu(1)-Cu(2) separation in the dinuclear complex is 6.565Å and the shortest interstacking distances between Cu(1)-Cu(1a) and Cu(2)-Cu(2a) are 4.425 and 4.375Å. The Cu-Cl(2) and Cu-Cl(3) distances (2.4987(16)Å, 2.5386(15)Å) are significantly longer than the distances between Cu-Cl(1) and Cu-Cl(4) of 2.2281(15) and 2.2093(14)Å because of the Jahn-Teller-effect (chloride atoms are situated nearly in the plane with the ligand). The pyridine rings A, B, D and E are inclined relative to the central pyrazine ring C by 20.70(18)°, 16.47(18)° ,17.14(17)° and 26.72(17)°, further important dihedral angles are given in Table 18a.

Tab. 18a. Dihedral angles (°) between the pyrazine ring C and the pyridine rings of Cu^{2+} complexes of tppz

angle	$[Cu_2(tppz)(H_2O)_4]^{4+}$	$[Cu(tppzH)Cl]_2$	$[Cu_2(tppz)Cl_4]$
A^B	34.3(2)	1.9(2)	6.43(20)
A^C(C')	21.3(3)	13.7(3)	20.70(18)

Tab.18a. (continuation)

B^C(C')	21.7(3)	13.0(3)	16.47(18)
D^E		49.8(2)	12.83(18)
D^C"		38.2(4)	17.14(17)
E^C"		41.8(3)	26.72(17)
A^D		46.8(2)	37.65(19)
A^E		62.4(2)	47.14(19)
B^D		48.1(2)	32.69(18)
B^E		61.9(2)	43.18(18)
C'^C"	0	8.0(2)	10.18(24)

The shortest C...C intramolecular distance are those between atoms C(6)-C(11) 3.164Å and C(16)-C(21) 3.119Å. The protons H(6)-H(11); H(16)-H(21) are separated by 2.444Å and 2.242, respectively. We found the angle N(3)-Cu(1)-N(6) to be 156.07(17)° and for N(4)-Cu(2)-N(5) 155.59(17)°. The coordination sphere of the copper atom can be described as distorted square pyramidal ($\tau_{Cu(1)} = 0.25$; $\tau_{Cu(2)} = 0.2$). Selected bond distances are given in Table 19.

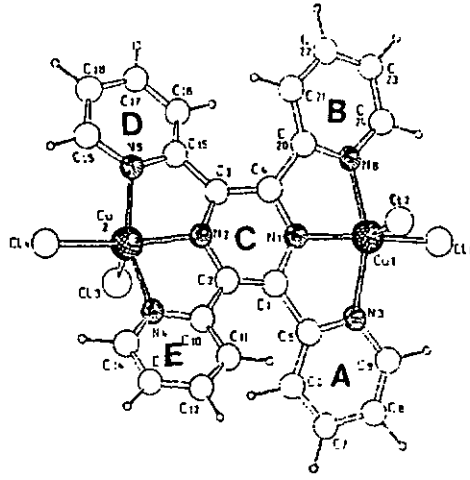

Fig. 21. SCHAKAL plot of $[Cu_2(tppz)Cl_4]$ (12).

Tab. 19. Selected distances (Å) and angles (°) of $[Cu_2(tppz)Cl_4]\cdot 5H_2O$ (12)

Cu(1)-N(1)	1.980(4)	Cu(2)-N(2)	1.982(4)
Cu(1)-N(3)	2.025(5)	Cu(2)-N(4)	2.023(4)
Cu(1)-N(6)	2.025(4)	Cu(2)-N(5)	2.022(4)
Cu(1)-Cl(1)	2.2281(15)	Cu(2)-Cl(3)	2.5386(15)
Cu(1)-Cl(2)	2.4987(16)	Cu(2)-Cl(4)	2.2093(14)
Cu(1)-Cu(2)	6.565	Cu(1)-Cu(1[a])	4.425
Cu(2)-Cu(2[b])	4.375		
Cl(1)-Cu(1)-Cl(2)	103.14(6)	Cl(3)-Cu(2)-Cl(4)	105.23(6)
N(1)-Cu(1)-N(3)	79.66(17)	N(2)-Cu(2)-N(4)	79.86(16)
N(1)-Cu(1)-N(6)	78.76(17)	N(2)-Cu(2)-N(5)	78.85(17)
N(1)-Cu(1)-Cl(1)	161.63(13)	N(2)-Cu(2)-Cl(3)	87.37(13)
N(1)-Cu(1)-Cl(2)	95.20(13)	N(2)-Cu(2)-Cl(4)	167.40(13)
N(3)-Cu(1)-N(6)	156.07(17)	N(4)-Cu(2)-N(5)	155.59(17)
N(3)-Cu(1)-Cl(1)	99.21(13)	N(4)-Cu(2)-Cl(3)	98.38(13)
N(3)-Cu(1)-Cl(2)	96.27(14)	N(4)-Cu(2)-Cl(4)	98.34(12)
N(6)-Cu(1)-Cl(1)	98.00(12)	N(5)-Cu(2)-Cl(3)	92.44(13)
N(6)-Cu(1)-Cl(2)	95.88(13)	N(5)-Cu(2)-Cl(4)	99.81(13)

Symmetry operation: [a] 2-x,1-y,-z; [b] 1-x,1-y,-z.

For further characterization u.v. spectra, infrared measurements and elemental analyses were made. The u.v. data in water as solvent indicate a coordination of the ligand, two bands are present at 306 and 363 nm. In the infrared spectrum we found in the ν(C=C), ν(C=N) region bands at 1596s; 1585s,sh; 1568s cm^{-1} an additional band and shoulder was also observed. A reason for this could probably be the influence of the distorsion in the pyrazine ring. Further bands in this region were present at 1390s, 1403ws, 1445s, 1465s, 1475m, 1520w,

1540w cm^{-1}. With the componds **10**, **11** and **12** magnetic investigations were carried out[73]. For paramagnetic compounds a ferromagnetic or antiferromagnetic exchange interaction possible. The qualitative temperature dependence of the magnetic susceptibility is given in Fig. 22.

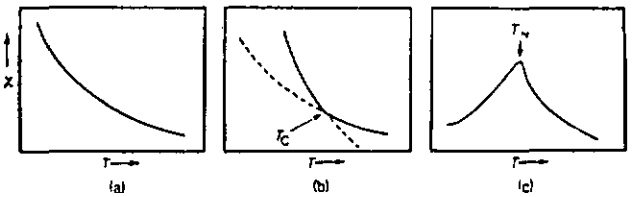

Fig. 22 Temperature dependent behaviour of the magnetic susceptibility.

a) simple paramagnetism, b) ferromagnetism. T_C= Curie temperature

c) antiferromagnetism, T_N = Néel temperature

The molar susceptibility of polycrystalline samples of the complexes $[Cu_2(tppz)Cl_4]\cdot 5H_2O$ and $[Cu_2(tppz)(H_2O)_4](ClO_4)_4\cdot 2H_2O$ were investigated, see in Fig. 23-26. It was found that the χ_M value ($2.62\cdot 10^{-3}$ for **12** and $2.31\cdot 10^{-3}$ cm^3mol^{-1} for **10** at room temperature) increases when the temperature decreases, reaching a maximum at ca 30 K for **12** and 50 K for **10**, with χ_M values of $1.33\cdot 10^{-2}$ and $8.50\cdot 10^{-3}$ cm^3mol^{-1}, respectively. Below this temperature, the curve decreases continuously for **12** whereas for **10** a minimum in the susceptibility was observed due to the presence of a small amount of paramagnetic impurities. The position of the maxima indicates moderate antiferromagnetic coupling between the copper (II) ions through the pyrazine bridge. The experimental susceptibility data were fitted to the classical expression for a [CuCu] pair derived from the Hamiltonian $H = -JS_1S_2$, by minimizing the function $R = S(\chi_M^{calcd} - \chi_M^{obs})2/\Sigma(\chi_M^{obs})2$ and the best fit parameters were $J = -34.2$ cm^{-1}, $g = 2.05$, and $J = -61.1$ cm^{-1}, $g = 2.13$ for **12** and **10** respectively. E.p.r. spectra show a rhombic spectra

[73]Manuscript in preparation.

for 12 with three well defined signals at g_1 = 2.06, g_2 = 2.10 and g_3 = 2.20. For 10 the spectrum is axial, with $g_{||}$ = 2.20 and $g_{\perp}$ = 2.10 and a half-field signal at g = 4.3.

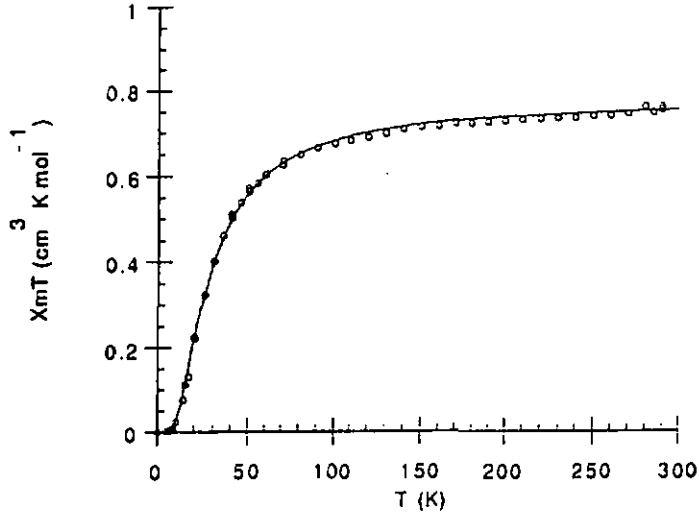

Fig. 23. The molar susceptibility (XmT vsT) plots of the complex $[Cu_2(tppz)Cl_4]\cdot 5H_2O$.

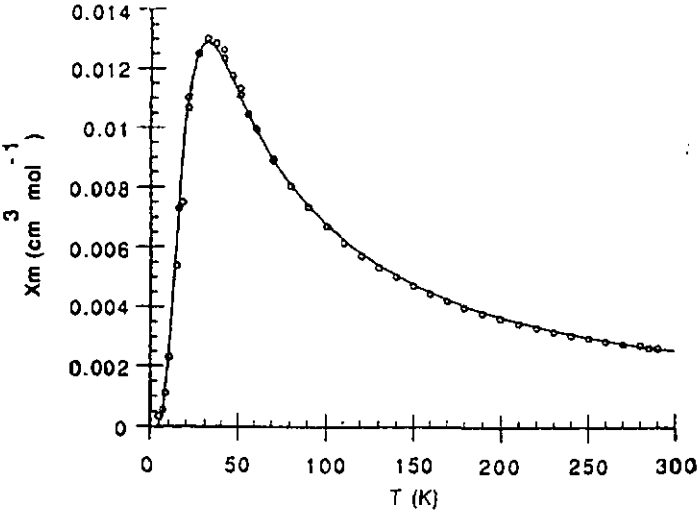

Fig. 24. The molar susceptibility (Xm vsT) plots of the complex $[Cu_2(tppz)Cl_4]\cdot 5H_2O$.

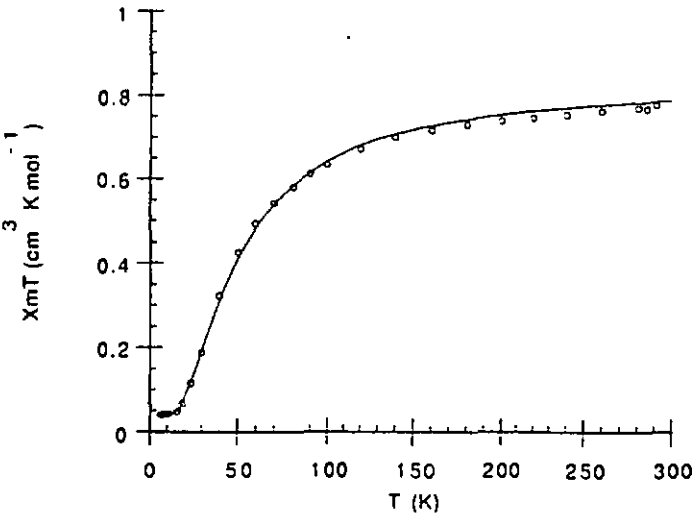

Fig.25. The molar susceptibility (XmT vsT) plots of $[Cu_2(tppz)(H_2O)_4](ClO_4)_4 \cdot 2H_2O$.

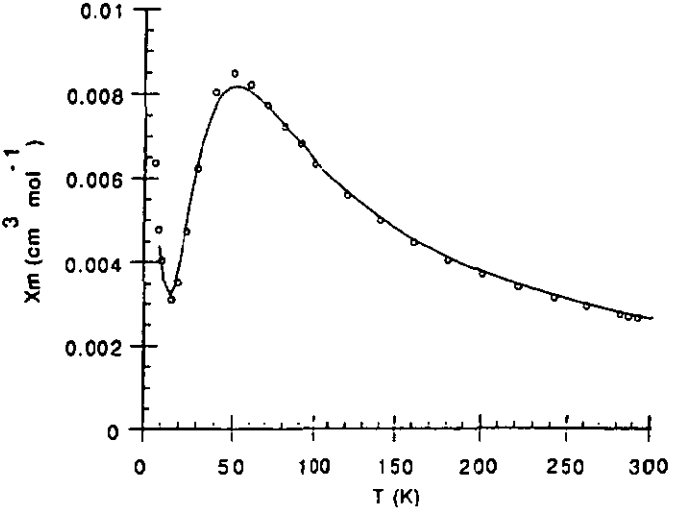

Fig.26. The molar susceptibility (Xm vsT) plots of $[Cu_2(tppz)(H_2O)_4](ClO_4)_4 \cdot 2H_2O$.

Superexchange mechanisms in polynuclear copper(II) complexes with bridging ligands such as pyrazine are a controversial subject and several poorly compatible points of view have been pointed out in the past two decades. The main point in the discussion of a possible superexchange mechanism is the kind of pathway either, "σ" (ligand σ orbitals overlap with the d orbitals of the metal) or "π" (ligand π orbitals overlap with the d orbitals of the metal), which allow an interaction. The two alternative mechanisms have MOs of the adequate symmetry and energy to interact with the symmetric and antisymmetric combination of the atomic orbitals of the copper atoms that contain the unpaired electron, $d_{z^2}(s)$ and $d_{z^2}(a)$ or $d_{x^2-y^2}(s)$ and $d_{x^2-y^2}(a)$ depending on the geometry of the coordination polyhedron of the copper atom. The discussion will be centered on square pyramidal coordination and further references assume the d x^2-y^2 combinations and the notated d_s and d_a.

The early proposal on the π pathway, developed from spectroscopic evidence, was made by Hatfield[74] et al. (1976): superexchange should occur through the π network by means of the overlap of the d_s and d_a combinations of the d_{xy} atomic orbitals with the HOMO π_s (b_{1g}) and its antisymmetric analogue π_a (b_{3u}) that gives the corresponding the φ_s and φ_a molecular orbitals.

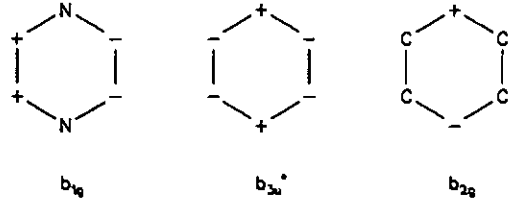

b_{1g} b_{3u}^* b_{2g}

A schematic simplified molecular orbital diagram of a spin coupled pair of copper ions interacting with the spin transmitting orbitals of the pyrazine ligand is shown in Fig.26.

A modification was introduced in 1976 by the same authors[75], when they consider as a second factor the interaction of the $d_{xy}(a)$ with the σ_a bonding MO (b_{2g}) of the pyrazine bridge.

---

[74]H.W. Richardson, W.E. Hatfield, *J. Am. Chem. Soc.*, 98 (1976) 835.

[75]H.W. Richardson, J.R. Wasson, W.E. Hatfield, *Inorg. Chem.*, 16 (1977) 484.

It should be noted that in this model, the antiferromagnetic character of the compounds must be weak: the b_{1g} and b_{3u} MOs have no density on the nitrogen atoms and the overlap will be in efficient and for the interaction between $d_{xy}(a)$ and b_{2g} it is assumed that only some unpaired spin density lies in the d_{xy} orbitals by mixing with the ground state $d_{x^2-y^2}$ orbitals.

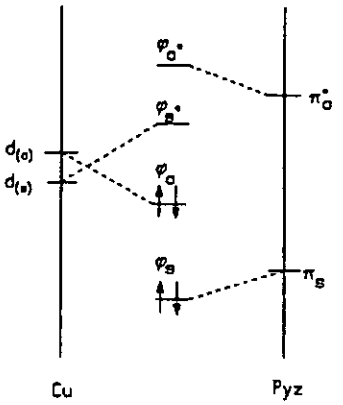

Fig. 26 Simplified molecular orbital diagram depicting a spin coupled pair of copper ions interacting with the spin transmitting orbitals of the ligand

Previously, Hendrickson[76] had proposed the interaction of the ds, a with the highest σ occupied MOs of the bridge, taking as reference the dinuclear copper complexes[77] $[Cu_2(tren)_2(ppd)]X_4$, where X = NO_3^-, ClO_4^-, PF_6^- and ppd as the bridging ligand p-phenylenediamine, for which the superexchange parameters are in the -70.2/-39.6 range ($H = -JS_1S_2$). The related p-benzidinediamine bridge, bzd, despite the large Cu-Cu separation, gives an antiferromagnetic coupling of the same order as for pyrazine. In these complexes the interaction should be propagated by the highest σ MO of the ppd or bzd ligands. Comparative MO calculations on ppd, pzd and pyrazine shows that these MOs are mainly a symmetric

---

[76]M.S. Haddad, D.N. Hendrickson, J.P. Cannady, R.S. Drago, D.S. Bieksza, *J. Am. Chem. Soc.* 101 (1979) 898.

[77]T.R. Feldhouse, D.N. Hendrickson, *Inorg. Chem.*, 17 (1978) 2636.

combination of nitrogen lone-pair orbitals with minor contributions of the C-ring atoms for pyrazine and comparable C-ring contributions for ppd or bzd. The low antiferromagnetic coupling for pyrazine compounds is explained by the poor 2p contribution argument and from the fact that ppd or bzd are stronger bases than pyrazine.

More recently, Oshio[78] et al. suggested that even through the σ pathway the antiferromagnetic interaction should be low in accordance with the experimental values reported to now as a consequence of the small J_{ab} two center Coulomb repulsion integral value, which should be low due to the long Cu-Cu distance. In the Hatfield model the dihedral angle between the coordination plane of the copper atoms and the pyrazine plane is determinant in the interaction (antiferromagnetic interaction needs a tilted position of the pyrazine plane with respect to the copper plane and increases with the dihedral angle), whereas for the σ pathway this dihedral angle is not relevant. All the pyrazine polynuclear derivatives reported to date show a common fact: all of them show negligible or weak antiferromagnetic coupling.

This experimental fact does not permit an unambiguous definition of the superexchange pathway. The copper tppz dinuclear compounds are relevant in this context due to their comparatively high antiferromagnetic behaviour. In our case the dihedral angles between the pyrazine ring and the basal coordination plane of the copper atoms are roughly 10° and according to the Hatfield model should be weakly coupled. It is also significant that the value of J = -61.1 cm-1 obtained for compound 10, which is not compatible with the weak interactions predicted in the π model directly derived of the poor overlap between ds,a and the φs,a MOs of the pyrazine and consequently, should be assumed that the superexchange is propagated through the σ system.

The magnetic behaviour of the complex $[Cu(tppzH)Cl]_2(ClO_4)_4$ was also investigated in order to determine the extent of magnetic interactions which can occur. The temperature dependent magnetic data for the polycristalline sample are shown in Fig. 27 and 27a. The molar suceptibility was recorded in a temperature range from 0 to 180K. It was found that the molar susceptibility increases when the temperature decreases. From this behaviour a ferromagnetic

---

[78]H. Oshio, U. Nagashima, *Inorg. Chem.*, 29 (1990) 3321.

exchange interaction was implied. At 10 K an Xm value of $1.275\ 10^{-1}$ was observed and at 160K a value of $5 \cdot 10^{-3}$ cm^3mol^{-1} was observed.

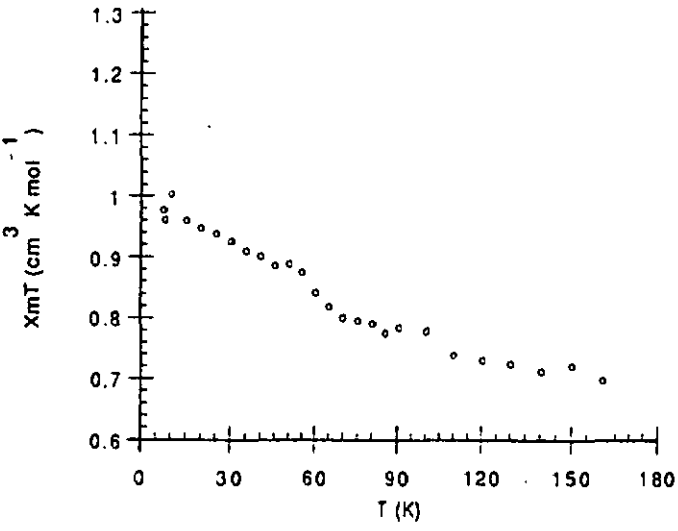

Fig. 27. The molar susceptibility (XmT / vsT) plots of $[Cu(tppzH)Cl]_2(ClO_4)_2$.

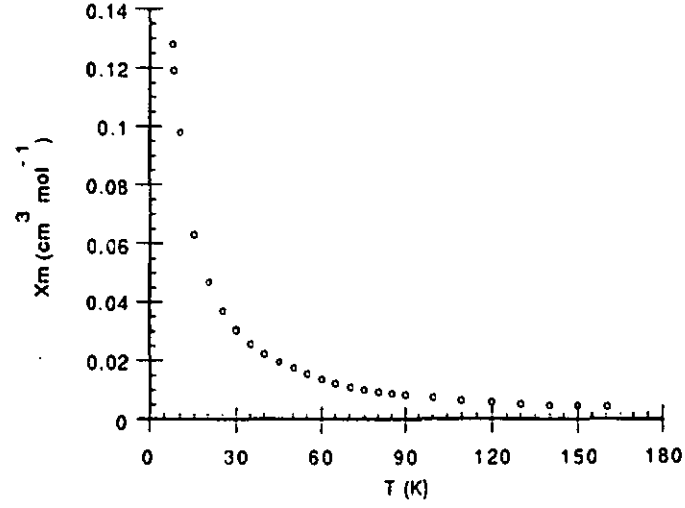

Fig. 27a. The molar susceptibility (Xm / vsT) plots of $[Cu(tppzH)Cl]_2(ClO_4)_2$.

For $[Cu(tppzH)Cl]_2(ClO_4)_4$ no e.p.r. spectrum of the solid was observed, that is an indication of a strong coupling between two different Cu(II) ions. This is characteristic for many systems with Cu(II) ions bridged by chloride ions. The e.p.r. spectrum in water solution indicated a single Cu(II) complex with characteristic four hyperfine lines. The values $g_o \approx 2.138$ and $A_{iso} \approx 75$ G were determined and are characteristic for Cu(II) ions in an axial coordination sphere. Furthermore there are indications that in solution the chloride bridges are broken. The chloride ligand is probably replaced by water. The e.p.r. spectrum of this complex in frozen solution shows a powder spectrum of an isolated Cu(II) ion. The g and A tensor are axial within the precision of the measurement, that is an indication for an axial coordination sphere. In the spectrum some indication of a nitrogen hyperfine splitting can be seen. The value $g_{\|}$ is found to be 2.138, $g_{\perp} = 2.053$ as well as $A_{\|} = 170$ G. $A_{\perp} = 14$ G. These values indicate a nitrogen (three) oxygen (N_3O) coordination in the plane.

We carried out a number of reaction attempts to introduce bridging ligands with the goal of obtaining coordination polymers. As starting materials we used the complex $[Cu_2(tppz)(H_2O)_4](ClO_4)_4$ and added the sodium salts of chelating ligands such as ida, edta, 2-carboxypyrazine, 2,3-dicarboxypyrazine, 2,5-dicarboxypyrazine, 2,6-dicarboxypyrazine, diimine, dppm, pyrazine, 2,3,5,6-tetramethylpyrazine, 1,1'-dimethyl-4,4'-bipyridinium dichloride, urea, N,N-dimethylthiourea and N,N-diisopropylurea. Furthermore attempts were made in which several componeets were mixed, e.g. a metal salt solution with the correspooding chelating ligands and tppz. From these reactions no mixed ligand complexes could be isolated. With the less bulky ligand oxalate Julve et al.[34] obtained dimeric copper complexes with terpy and determined the structure by X-ray diffraction, see Fig.28.

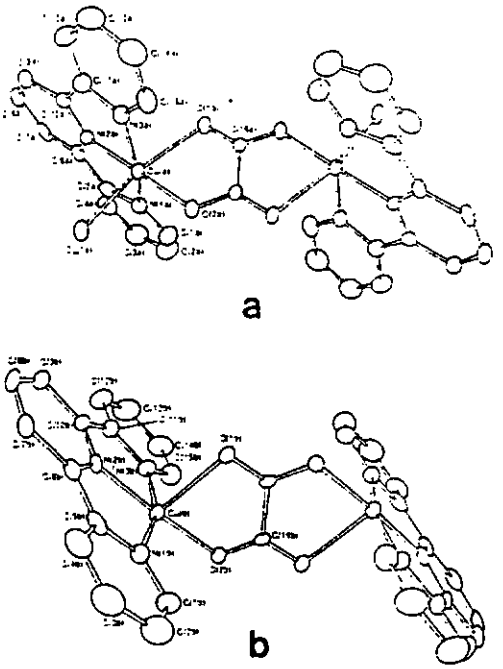

Fig. 28. Cationic dinuclear $[\{Cu(terpy)(H_2O)\}_2(ox)]^{2+}$ (a) and $[\{Cu(terpy)\}_2(ox)]^{2+}$ (b) units of $[\{Cu(terpy)(H_2O)\}_2(ox)][\{Cu(terpy)\}_2(ox)](ClO_4)_4 \cdot 2H_2O$.

The coordination geometry around each copper atom in **a** is distorted octahedral and in **b** distorted elongated tetragonal. In a similar manner we synthesized the complex $[\{Cu_2(tppz)(ox)(H_2O)_2\}(ClO_4)_2]_x$ from a reaction of $Cu(ClO_4)_2$ with tppz and lithium oxalate which crystallized as fine green needles. The same results were observed by starting from the binuclear copper complex and reacting it with disodium oxalate.

$$[Cu_2(tppz)(H_2O)_2](ClO_4)_4 + Na_2ox \xrightarrow[-2NaClO_4]{H_2O\ (60°C)} [\{Cu_2(tppz)(ox)(H_2O)_2\}(ClO_4)_2]_n$$

$$tppz + 2Cu(ClO_4)_2 + Na_2ox \xrightarrow[-2NaClO_4]{H_2O\ (60°C)} [\{Cu_2(tppz)(ox)(H_2O)_2\}(ClO_4)_2]_n$$

(13)

Because of the planarity of the central pyrazine ring in the complex $[Cu_2(tppz)(H_2O)_4](ClO_4)_4 \cdot 2H_2O$ the possibility for the formation of coordination polymers should be considered. Therefore we propose the following polymer structure:

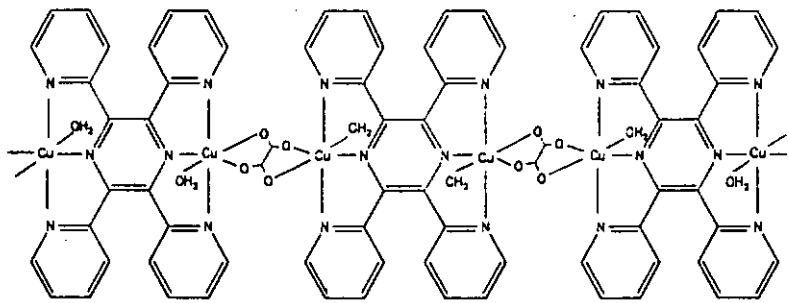

This is also in agreement with the X-ray structure results of the similar constituent complex containing terpy[14]. It was impossible to isolate suitable crystals for X-ray analysis. The characterization was effected by means of infrared, u.v. spectra, FAB-mass spectroscopy, elemental analysis, and e.p.r. spectra. In the infrared spectrum we found the ν(C=C), ν(C=N) absorption bands for the coordinated ligand. At 1659 cm^{-1} a very strong broad band for the νas(C=O) vibration and at 1620 $cm^{-1}$for the νs(C=O) vibration are present. This indicates significantly the bridging coordination mode of the oxalate anion. In the oxalate bridged dimeric terpyridyl complex the corresponding bands are found at 1640 and 1600 cm^{-1}. The very intensive perchlorate bands overlap a large part of the spectrum. The u.v. measurements in water solution show the two bands at 300 and 363 nm, we assume this for the aquoion $[Cu_2(tppz)(H_2O)_4]^{4+}$. To find a further indication of the coordination environment CuL_6 we recorded the reflectance spectra in the solid state. For a five-fold coordination sphere a band

maximum with a shoulder is known. In the literature[79] are explained the reflectance spectra of two representatives for a trigonal bipyramidal and square pyramidal coordination sphere of the Cu(II) complexes $[Cu(tren)(NH_3)](ClO_4)_2$ and $K[Cu(NH_3)_5](PF_6)_3$ in combination with extended Hückel calculations. We found in all further mentioned spectra of copper complexes only a maximum band without a shoulder which is indicative of an octahedral coordination mode. We observed a d→d transition band $^2E_g \rightarrow {}^2T_{2g}$ at 14671 cm^{-1}, this is an indication of octahedral symmetry of the CuN_6 cation. E.p.r. spectra of the solid, Fig.29, and in solution, Fig. 30, were recorded. The powder spectrum indicates an axial coordination sphere. Furthermore a Cu-Cu interaction in the solid is assumed. The values $g_{||} = 2.236$ and $g_{\perp} = 2.065$ are determined. In solution a characteristic spectrum of an isolated Cu^{2+} ($g_{iso} = 2.093$, $A_{iso} = 75.0G$) ion is given.

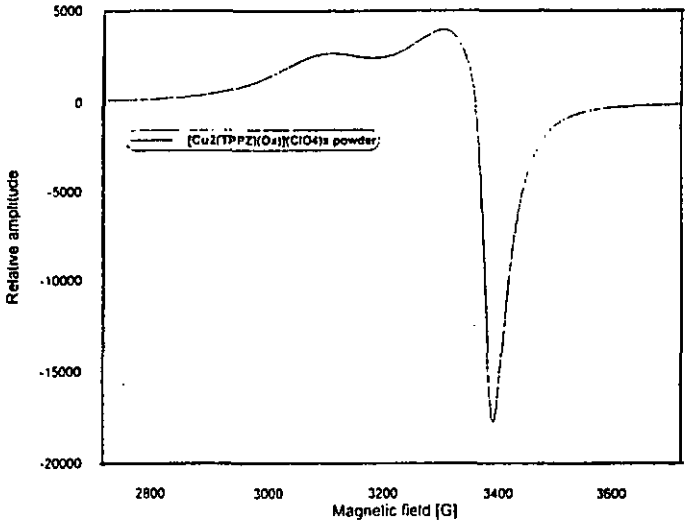

Fig. 29. E.p.r. spectrum of $[\{Cu_2(tppz)(ox)(H_2O)\}(ClO_4)_2]_x$ in the solid state.

[79]M. Duggan, N. Ray, B. Hathaway, *J. Am Chem. Soc.* (1980) 1342.

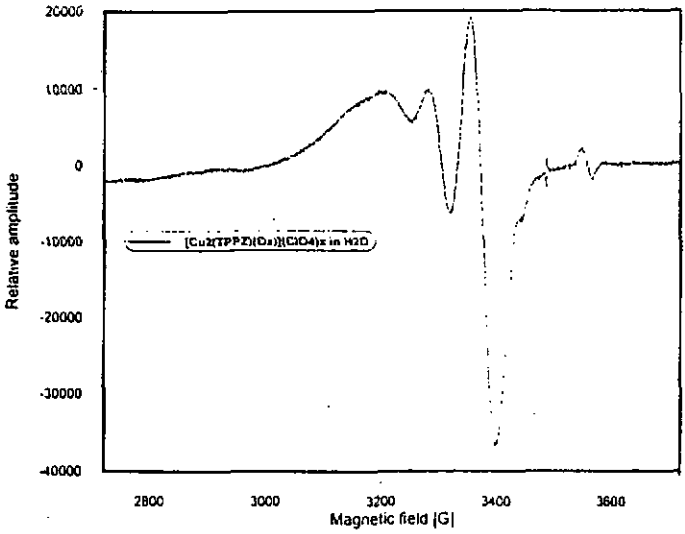

Fig. 30.E.p.r. spectrum of $[\{Cu_2(tppz)(ox)(H_2O)\}(ClO_4)_2]_x$ in water solution.

The FAB-mass spectrum also supported the composition of the monomer unit. We found the molpeak (M^+) of m/e = 836 with an intensity of 38% and a typical fragmentation for this type of complexe is given in Table 20.

Tab. 20. FAB mass spectrum (70eV) of $[\{Cu_2(tppz)(ox)(H_2O)\}(ClO_4)_2]_x$.

m/e	rel. intensity (%)	fragment
836	38	$[Cu_2(tppz)(ox)(H_2O)_2](ClO_4)_2^+$
800	10	$[Cu_2(tppz)(ox)](ClO_4)_2]^+$
602	18	$[Cu_2(tppz)(ox)]^+$
514	50	$[Cu_2(tppz)]^+$
451	72	$[Cu(tppz)]^+$

Because of the lack of structural data no magnetic investigations could be carried out with **13**. Oxalato bridged complexes of bipy were very well investigated by H. Oshio[80] and co-workers in 1992. The design of the homonuclear ferromagnetic chain $[Cu(bpy)(ox)]\cdot 2H_2O$ as well as structural and magnetic properties were described. The oxalate anions are centrosymmetric and act as quadridentate bridging ligands, whereas the oxygen atoms coordinate to each copper atom both from the equatorial ($d_{x^2-y^2}$ orbital) and axial (d_{z^2} orbital) positions. The ferromagnetic behaviour can be readily understood by considering the fact that the spin density on the copper atom is spread over the oxalato groups, as confirmed by the all-electron ab inito unrestricted Hartree-Fock calculation for $[Cu(ox)_2]^{2-}$. The spin on the terminal oxygen atom, which coordinates to the adjacent copper atoms from its d_{z^2} direction, induces spin on that d_{z^2} orbital. The orthogonality of the primary spin orbital ($d_{x^2-y^2}$) and induced spin orbital (d_{z^2}) causes the ferromagnetic interaction. O. Kahn[81] gave an overview of the magnetic properties of different oxalato bridged complexes. The fundamentals of this field of chemistry are explained there.

We carried out reactions of $[Cu_2(tppz)(H_2O)_4](ClO_4)_4$ with terpy in a $EtOH/H_2O$ solution at 70°C with a molar ratio of 1:2.

$$[Cu_2(tppz)(H_2O)_4](ClO_4)_4\cdot 2H_2O + terpy \rightarrow [Cu(H_2O)_2(tppz)Cu(terpy)](ClO_4)_4 + 4H_2O \quad \textbf{(14)}$$

After short reaction time a bright green product precipitated from the solution. The compound has a very low solubility in all common solvents. The FAB-mass spectrum exhibits the highest fragment at m/e=783 for $[Cu(H_2O)_2(tppz)Cu(terpy)]^+$ or $[(tppz)Cu(tppz)]^+$. Further fragmentations are given in Table 21.

---

[80]H. Oshio, U. Nagashima, *Inorg. Chem.*, **31** (1992) 3295.

[81]O. Kahn, *Angew. Chem.*, 97 (1985) 837.

Tab. 21. FAB mass spectrum (70eV) of $[Cu(H_2O)_2(tppz)Cu(terpy)](ClO_4)_4$

m/e	rel. intensity (%)	fragment
783	12	$[Cu(H_2O)_2(tppz)Cu(terpy)]^+$
684	45	$[(terpy)Cu(tppz)]^+$
550	98	$[Cu(tppz)(ClO_4)]^+$
529	35	$[(terpy)Cu(terpy)]^+$
451	80	$[Cu(tppz)]^+$
296	88	$[Cu(terpy)]^+$

Because of the very low solubility further purification was impossible. The infrared spectrum exhibits a remarkable change in comparison to the spectrum of $[Cu_2(tppz)(H_2O)_4](ClO_4)_4$. We found bands in the ν(C=C), ν(C=N) region at 1598m, 1578m, 1500w, 1476m, 1452m, 1395m and 1323m cm^{-1}. The strong band of the perchlorate covers a broad part of the spectrum. In the reflectance spectra we found one band at 14916 cm^{-1} for a d→d transition. We assume in this binuclear complex a five-and a six-fold coordination [CuN_3O_2, CuN_6]. An overlapping effect could be the reason for the single broad maximum band at 14916 cm^{-1}. More information could be given X-ray diffraction studies, but no suitable crystals could be isolated.

An example of lower symmetry relation theo O_h was found by Henke and Reinen[82]. They investigated the complex $[Cu(terpy)_2](NO_3)_2$ by X-ray analysis and electronic absorbtion spectroscopy. In the reflectance spectra two bands at 6550 and 14500 cm^{-1} are present. The explanation for the existence of these two d→d transitions is the lower symmetry than O_h. The splitted term scheme demonstrates the transition from $^2E_g \rightarrow {}^2T_{2g}$ and a second transition to the splitting terms of the antibonding $^2T_2$-levels. E.p.r. measurements could only be undertaken in the solid state due to the very low solubility. A broad axial spectrum was observed. No resolved hyperfine structure for the copper ions was obtained. Probably Cu-Cu

[82]W. Henke, D. Reinen, *Z. Anorg., Allg. Chem.*, 436 (1977) 187.

interactions in the solid are present, the value $g_{||}$=2.254 and $g_{\perp}$=2.101 were determined, see Fig.31.

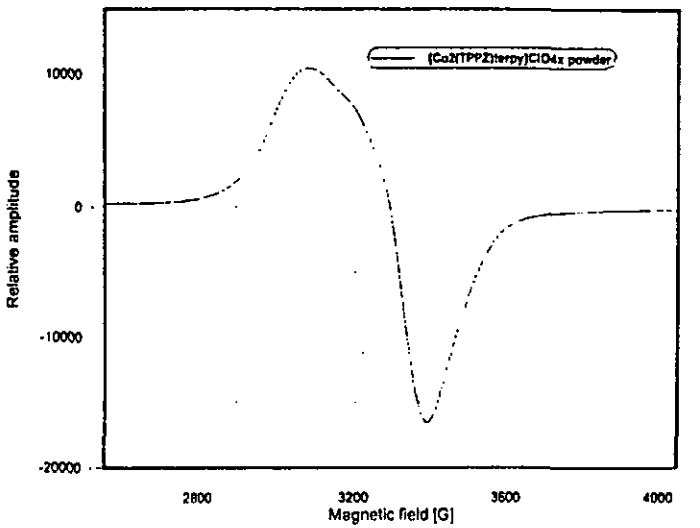

Fig. 31. E.p.r. spectrum of $[Cu(H_2O)_2(tppz)Cu(terpy)](ClO_4)_4$.

By a reaction of $[Cu_2(tppz)(H_2O)_4](ClO_4)_4$ with H_4pztc (molar ratio of 1:1) we wanted to introduce a further bridging ligand.

$$[Cu_2(tppz)(H_2O)_4](ClO_4)_4 \cdot 2H_2O + H_4pztc \rightarrow [\{Cu_2(tppz)(H_2pztc)(H_2O)_2\}(ClO_4)_2]_x + 2HClO_4 + 4H_2O \quad (15)$$

This reaction was also carried out in several buffer mediums but the result was in each case the precipitation of a green insoluble product from the solution. The characterization was effected by means of elemental analysis, infrared methods and mass spectroscopy. We propose the following structure.

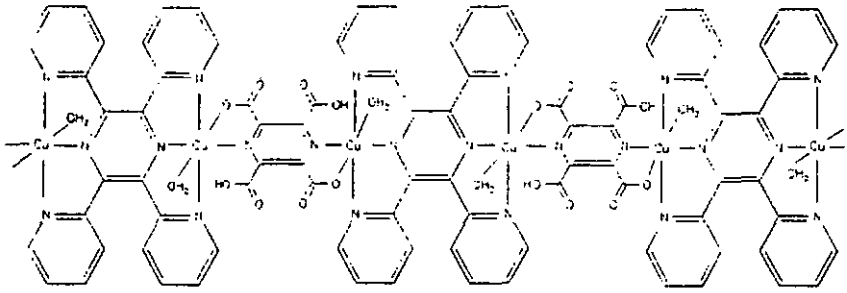

The calculated elemental analysis corresponding to this structure is C=38.13; H=2.18; N=11.12 and Cu=12.6%. We found for C=38.48; H=3.16; N=11.32 and for Cu=13.2%. The infrared spectrum indicates a coordination of tppz and H_4pztc. The characteristic strong bands for the protonated and deprotonated carboxylate groups are present at 1720 and 1656 cm^{-1}. We found a broad band for the [ν(O-H)] of the water molecules at 3455 cm^{-1} and the following bands in the ν(C=C), ν(C=N) region: 1291 m, 1405 s, 1424 s, 1478 m, 1495 w and 1598 s cm^{-1} which are characteristic for coordinated tppz. In the reflectance spectra we found one transition band at 13935cm^{-1} which is an indication of a $^2E_g \rightarrow {}^2T_{2g}$ transition in an octahedral coordination sphere. Thermogravimmetric measurements indicate a stepwise loss of mass between 24-73 °C corresponding to two molecules of water and 73-151 °C as well as 151-208°C corresponding to two molecules of CO_2.

2.5. Structural and n.m.r. iovestigations of Zn(II) complexes with tppz

The Zn^{2+} has filled d-orbitals, therefore no ligand field stabilization effects are possible. The stereochemistry depends only on the size as well as the electrostatic and covalent bonding forces. A coordination number from two to eight is possible. The coordination behaviour of Zn^{2+} with tppz is described in the following context.

As mentioned above the reaction of tppz with $ZnCl_2$ in a molar ratio of 1:1 results in the formation of the tetragonal form of the free ligand tppz and mononuclear Zn(II) complex[62]. During reactions with increased metal to ligand ratios (1:2, 1:6, 1:8) in a large amount of solvent and single heating we could isolate the mononuclear complex [Zn(tppz)Cl_2] (16). The

crystal structure analysis indicated that the Zn atom lies in the plane through atom N(1), Cl(1) and Cl(2) while atoms N(2) and N(3) are displaced by -2.097(3)Å and 2.024(3)Å either side of this plane, see Fig.33. The Zn- N (pyrazine) distance of 2.156(2)Å is found to be longer than the central Zn pyridine distance in the corresponding terpyridine complex (Tab.23). The coordination sphere around the Zn atom can be described as a square pyramidal. Important bond distances and angles are given in Table 22.

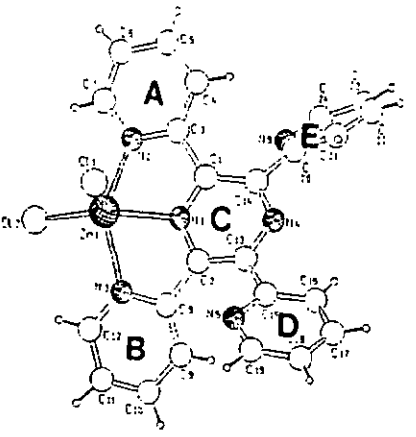

Fig. 32. SCHAKAL plot of [Zn(tppz)Cl_2] (17).

Tab. 22. Selected distances (Å) and angles (°) of [Zn(tppz)Cl_2] (17)

Zn(1)-Cl(1)	2.2759(10)	Zn(1)-N(2)	2.204(3)
Zn(1)-Cl(2)	2.2365(9)	Zn(1)-N(3)	2.175(3)
Zn(1)-N(1)	2.1561(24)		
Cl(1)-Zn(1)-Cl(2)	115..08(4)	Cl(2)-Zn(1)-N(2)	101.36(7)
Cl(1)-Zn(1)-N(1)	98.56(8)	Cl(2)-Zn(1)-N(3)	96.53(7)
Cl(1)-Zn(1)-N(2)	95.93(7)	N(1)-Zn(1)-N(2)	73.11(9)
Cl(1)-Zn(1)-N(3)	106.60(8)	N(1)-Zn(1)-N(3)	73.31(9)
Cl(2)-Zn(1)-N(1)	146.35(8)	N(2)-Zn(1)-N(3)	141.80(10)

Tab 23. Selected distances (Å) and angles (°) of [Zn(tppz)Cl_2] and [Zn(terpy)Cl_2]

	[Zn(tppz)Cl_2]	[Zn(terpy)Cl_2]
Zn-N(1)	2.156(2)	2.112
Zn-N(2)	2.204(3)	2.196
Zn-N(3)	2.178(3)	2.196
Zn-Cl(1)	2.276(1)	2.274
Zn-Cl(2)	2.237(1)	2.274

As in the other complexes the ligand is considerably distorted. Here the pyrazine ring has a twist conformation with a dihedral angle between the planes C' and C" of 10.6(2)° The coordinated pyridine rings A and B are inclined to one another by 13.5(1)°. For further characterization a two-dimensional n.m.r. experiment was undertaken. The proton n.m.r. spectrum shows clearly the eight expected signals for the eight different protons. To carry out an exact assignment of the signals a COSY- 45 experiment was undertaken, the correlation diagram is given in Fig.33. In the spectrum we observed the expected couplings for the uncoordinated ring proton a couples with the protons b and c, b with a, c, d and proton c with a, b, d as well as the proton d with protons c and b. At the coordinated side of the complex proton e couples with protons f and g, proton f with e, g, h, g couples with h, f and e, and h with g and f. The u.v. spectrum in water solution exhibits the two bands for the ligand at 295 and 315 nm. The infrared spectrum (KBr) indicates the coordination of the ligand. The characteristic doublet is shifted to higher wave numbers (1593vs, 1573sh cm^{-1}), further signals in the ν(C=C), ν(C=N) region were found at 1540m, 1475m, 1456m, 1444w, 1405vs, 1305m cm^{-1}. The elemental analysis is in agreement with the found composition.

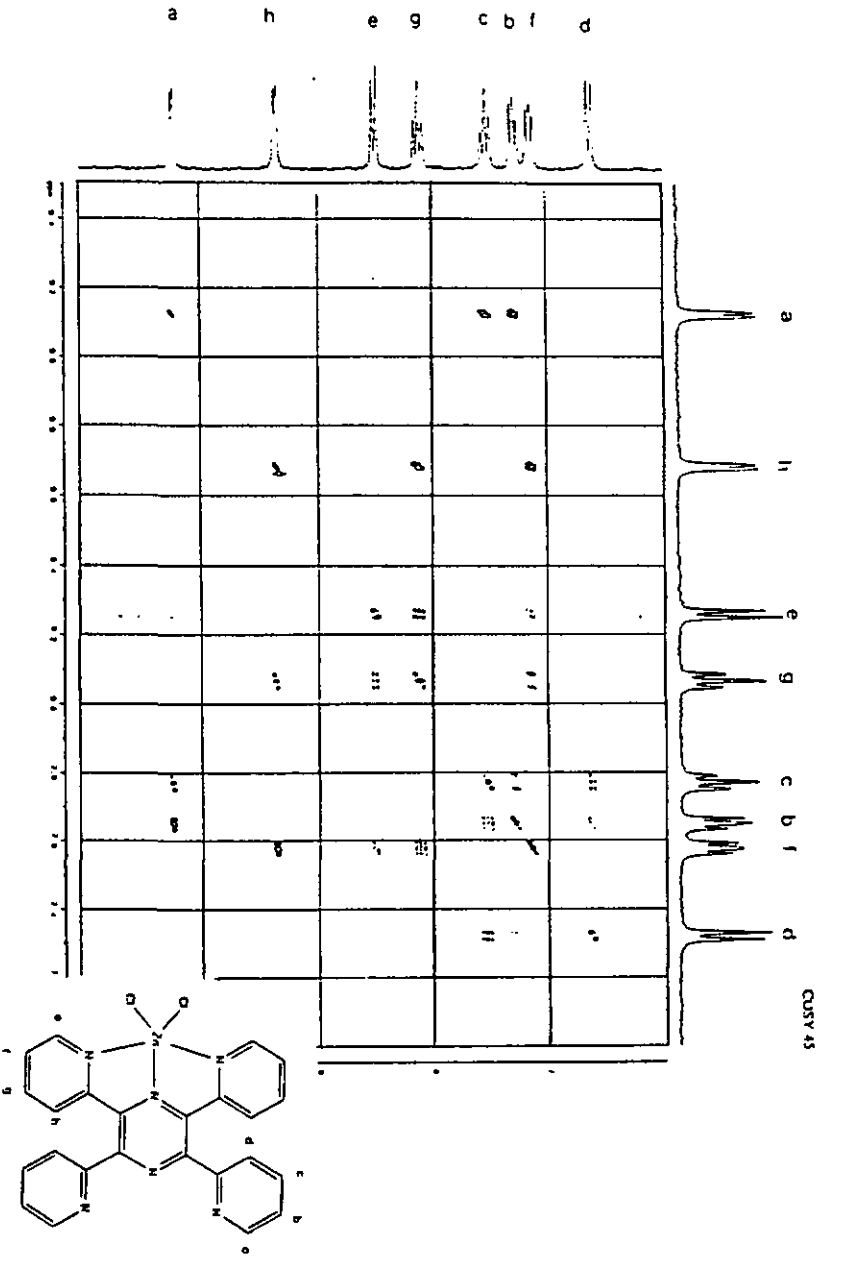

Fig. 33. COSY-45 spectrum of $[Zn(tppz)Cl_2]$.

In a reaction of an excess of $ZnCl_2$ with the ligand tppz (L20) in a minimum of solvent mixture ethanol/water (1:1) and after heating several times the dinuclear complex $[Zn_2(tppz)Cl_4]$ **(17)** was isolated. The coordination sphere around the zinc atoms can be described square pyramidal, the numbering scheme is shown in Fig.34. The angle N(3)-Zn(1)-N(6) is 146.72(20)° and N(4)-Zn(2)-N(5) is 141.11(21)°. Here we found also a twist conformation in the pyrazine ring with a dihedral angle between planes C' and C" of 12.0(5)°. In comparison to the dinuclear copper complex **(10)** (10.18°) and the binuclear nickel complex **(4)** (10.9) these planes are more twisted. The pyridine rings A, B, D and E are inclined relative to the central pyrazine ring C by 29.62(23)°, 16.81(23), 14.8(3)° and 28.83(24)°, respectively. Pyridine ring B and D are inclined to one another by 31.60(3)°, pyridine ring A and E by 58.25(24), see Tab.26. The shortest intramolecular C···C distances are those between the atoms C(6)...C(11) with 3.146(10)Å and C(16)..C(21) with 3.151(10)Å as well as between proton H(6)-H(11) and H(16)-H(21) at 2.3641(3)Å and 2.3172(3)Å, respectively. The distance between Zn(1)-N(1) (pyrazine) of 2.182(5)Å and the Zn(2)-N(2) (pyrazine) distance of 2.210(5)Å are longer than the same distance in the mononuclear zinc complex [2.156(2)Å]. In contrast, the Zn-N(pyridine) distances are shorter than in the mononuclear complex. The Zn-Zn separation in the dinuclear complex is 6.9450(13)Å, see, Tab. 24.

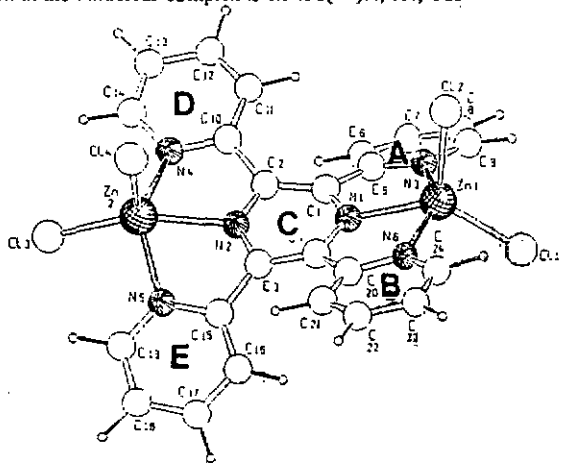

Fig. 34. SCHAKAL plot of $[Zn_2(tppz)Cl_4]$.(17).

Tab. 24. Selected distances (Å) and angles (°) of $[Zn_2(tppz)Cl_4]$ (17)

Zn(1)-N(1)	2.182(5)	Zn(2)-N(2)	2.210(5)
Zn(1)-N(3)	2.147(5)	Zn(2)-N(4)	2.159(6)
Zn(1)-N(6)	2.134(6)	Zn(2)-N(5)	2.153(6)
Zn(1)-Cl(1)	2.2513(19)	Zn(2)-Cl(3)	2.2546(20)
Zn(1)-Cl(2)	2.2757(20)	Zn(2)-Cl(4)	2.2587(20)
Zn(1)-Zn(2)	6.9450(13)		
Cl(1)-Zn(1)-Cl(2)	116.26(8)	Cl(3)-Zn(2)-Cl(4)	111.97(8)
N(1)-Zn(1)-N(3)	73.66(20)	N(2)-Zn(2)-N(4)	72.55(20)
N(1)-Zn(1)-N(6)	73.47(20)	N(2)-Zn(2)-N(5)	73.10(20)
N(1)-Zn(1)-Cl(1)	132.83(16)	N(2)-Zn(2)-Cl(3)	148.90(15)
N(1)-Zn(1)-Cl(2)	110.83(15)	N(2)-Zn(2)-Cl(4)	99.11(15)
N(3)-Zn(1)-N(6)	146.72(20)	N(4)-Zn(2)-N(5)	141.11(21)
N(3)-Zn(1)-Cl(1)	98.82(15)	N(4)-Zn(2)-Cl(3)	99.72(17)
N(3)-Zn(1)-Cl(2)	95.25(16)	N(4)-Zn(2)-Cl(4)	100.71(17)
N(6)-Zn(1)-Cl(1)	99.55(15)	N(5)-Zn(2)-Cl(3)	100.28(16)
N(6)-Zn(1)-Cl(2)	101.12(15)	N(5)-Zn(2)-Cl(4)	102.18(17)

To carry out an exact assignment of the protons a COSY-45 n.m.r. spectrum was recorded, see Fig. 35. Because of the bis(tridentate) coordination mode we observed four signals for the equivalent protons. It can be seen that proton d couples with proton c and b , proton b with a,c and d; proton a with b and c; proton c with b and d, resulting in the proposed assignment. U.v. measurements in water solution shows the two bands of the ligand at 295 and 315 nm. The infrared spectra of the binuclear complex show no significant differences in comparison to the spectra of the mononuclear complex $[Zn(tppz)Cl_2]$. The proposed composition is in agreement with the elemental analysis.

In a reaction of an excess of $ZnCl_2$ with the ligand tppz (1:20) in a minimum of solvent mixture ethanol/water (1:1) and after heating several times the dinuclear complex $[Zn_2(tppz)Cl_4]$ (17) was isolated. The coordination sphere around the zinc atoms can be described square pyramidal, the numbering scheme is shown in Fig.34. The angle N(3)-Zn(1)-N(6) is 146.72(20)° and N(4)-Zn(2)-N(5) is 141.11(21)°. Here we found also a twist conformation in the pyrazine ring with a dihedral angle between planes C' and C" of 12.0(5)°. In comparison to the dinuclear copper complex (10) (10.18°) and the binuclear nickel complex (4) (10.9) these planes are more twisted. The pyridine rings A, B, D and E are inclined relative to the central pyrazine ring C by 29.62(23)°, 16.81(23), 14.8(3)° and 28.83(24)°, respectively. Pyridine ring B and D are inclined to one another by 31.60(3)°, pyridine ring A and E by 58.25(24), see Tab.26. The shortest intramolecular C···C distances are those between the atoms C(6)...C(11) with 3.146(10)Å and C(16)...C(21) with 3.151(10)Å as well as between proton H(6)-H(11) and H(16)-H(21) at 2.3641(3)Å and 2.3172(3)Å, respectively. The distance between Zn(1)-N(1) (pyrazine) of 2.182(5)Å and the Zn(2)-N(2) (pyrazine) distance of 2.210(5)Å are longer than the same distance in the mononuclear zinc complex [2.156(2)Å]. In contrast, the Zn-N(pyridine) distances are shorter than in the mononuclear complex. The Zn-Zn separation in the dinuclear complex is 6.9450(13)Å, see, Tab. 24.

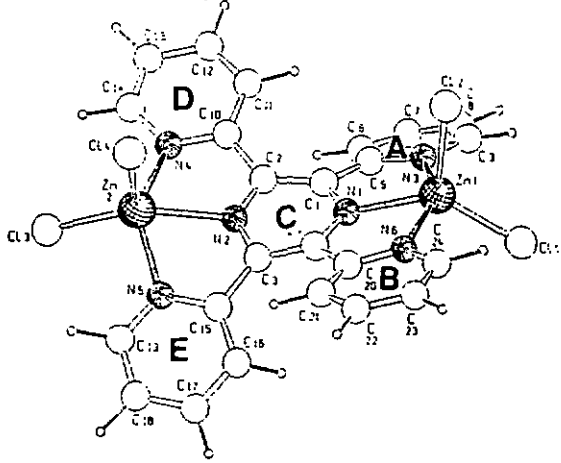

Fig. 34. SCHAKAL plot of $[Zn_2(tppz)Cl_4]$.(17).

Tab. 24. Selected distances (Å) and angles (°) of $[Zn_2(tppz)Cl_4]$ (17)

Zn(1)-N(1)	2.182(5)	Zn(2)-N(2)	2.210(5)
Zn(1)-N(3)	2.147(5)	Zn(2)-N(4)	2.159(6)
Zn(1)-N(6)	2.134(6)	Zn(2)-N(5)	2.153(6)
Zn(1)-Cl(1)	2.2513(19)	Zn(2)-Cl(3)	2.2546(20)
Zn(1)-Cl(2)	2.2757(20)	Zn(2)-Cl(4)	2.2587(20)
Zn(1)-Zn(2)	6.9450(13)		
Cl(1)-Zn(1)-Cl(2)	116.26(8)	Cl(3)-Zn(2)-Cl(4)	111.97(8)
N(1)-Zn(1)-N(3)	73.66(20)	N(2)-Zn(2)-N(4)	72.55(20)
N(1)-Zn(1)-N(6)	73.47(20)	N(2)-Zn(2)-N(5)	73.10(20)
N(1)-Zn(1)-Cl(1)	132.83(16)	N(2)-Zn(2)-Cl(3)	148.90(15)
N(1)-Zn(1)-Cl(2)	110.83(15)	N(2)-Zn(2)-Cl(4)	99.11(15)
N(3)-Zn(1)-N(6)	146.72(20)	N(4)-Zn(2)-N(5)	141.11(21)
N(3)-Zn(1)-Cl(1)	98.82(15)	N(4)-Zn(2)-Cl(3)	99.72(17)
N(3)-Zn(1)-Cl(2)	95.25(16)	N(4)-Zn(2)-Cl(4)	100.71(17)
N(6)-Zn(1)-Cl(1)	99.55(15)	N(5)-Zn(2)-Cl(3)	100.28(16)
N(6)-Zn(1)-Cl(2)	101.12(15)	N(5)-Zn(2)-Cl(4)	102.18(17)

To carry out an exact assignment of the protons a COSY-45 n.m.r. spectrum was recorded, see Fig. 35. Because of the bis(tridentate) coordination mode we observed four signals for the equivalent protons. It can be seen that proton d couples with proton c and b , proton b with a,c and d; proton a with b and c; proton c with b and d, resulting in the proposed assignment. U.v. measurements in water solution shows the two bands of the ligand at 295 and 315 nm. The infrared spectra of the binuclear complex show no significant differences in comparison to the spectra of the mononuclear complex $[Zn(tppz)Cl_2]$. The proposed composition is in agreement with the elemental analysis.

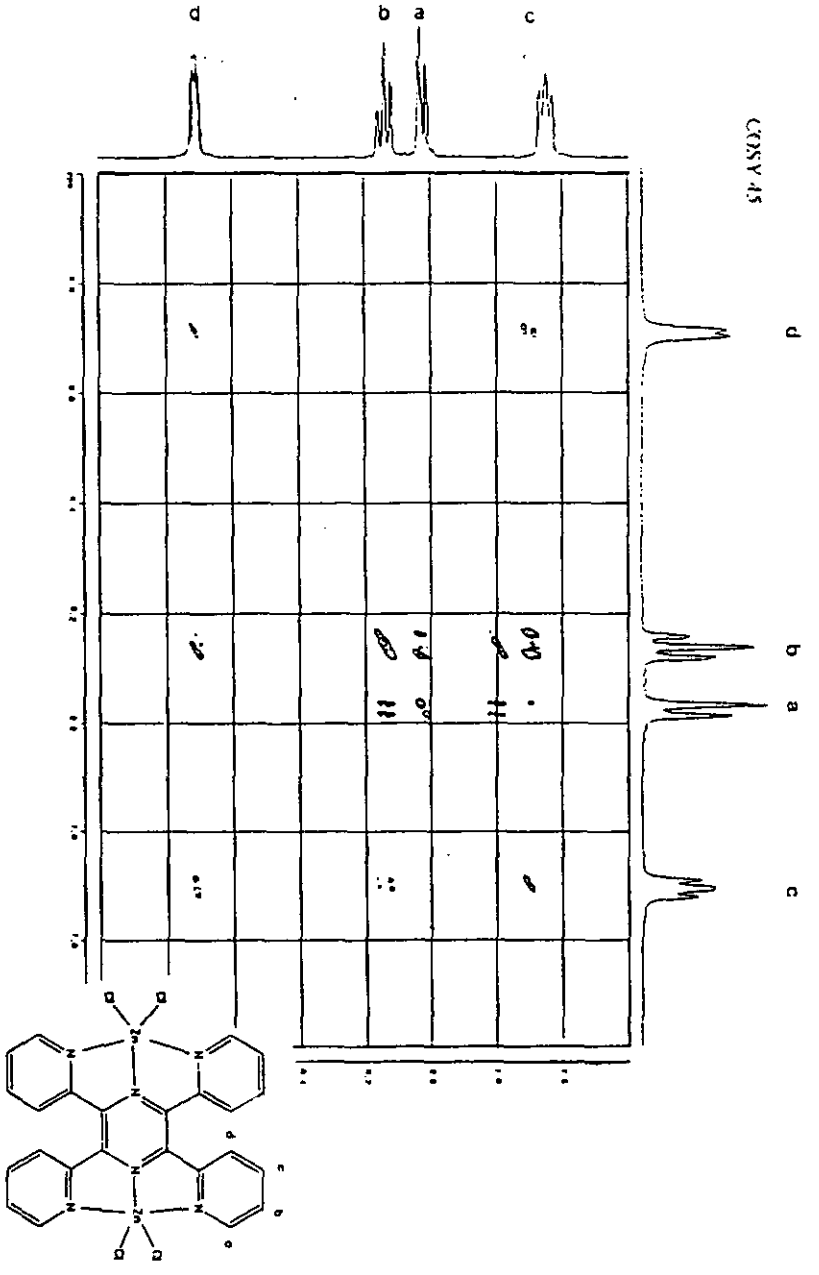

Fig. 35.COSY-45 spectrum of $[Zn_2(tppz)Cl_4]$ (17).

Concerning the coordination behaviour of the Zn(II) ions with tppz we investigated the reaction of $[Zn(tppz)(H_2O)_2](ClO_4)_2$ with a large excess of $ZnCl_2$ in a $EtOH/H_2O$ mixture. By heating for several times and repeated filtration we could isolate after two months well formed yellow prisms. The X-ray diffraction studies of this compound[83] show that it is a very interesting centrosymmetric macrocycle bis-$[Zn_2(\mu\text{-tppz})(H_2O)Cl(\mu\text{-}ZnCl_4)(\mu\text{-}ZnCl_2)(\mu\text{-}ZnCl_3H_2O)]$ (**18**). Two highly twisted dinuclear zinc complexes (C^C"11.6(3)° are linked by no less than 3 Cl-Zn-Cl bridges. Fig. 37a. The macrocycle is neutral possessing 10 zinc atoms and 20 chloride atoms. There are 6 four coordinate, 2 five coordinate and 2 six coordinate Zn-atoms. In the binuclear complex of the macrocycle atom Zn(1) has a trigonal bipyramidal coordination and lies in the plane of atoms N(1), OW(1) and Cl(1) with atoms N(2) and N(3) displaced from the best plane by 2.024(4)Å and -2.059 (4)Å, respectively. Pyridine rings A and B, which are coordinated to Zn(1), are inclined to one another by 7.72(17)° while pyridine rings D and E, coordinated to Zn(2), are inclined to one another by 12.19(18)°. The diagonally oppositing pyridine rings (A, D and B, E) are inclined to one another by 48.61(18) and 35.00(16)°. The adjacent rings A and E are inclined by 41.56(16), whereas B and D are inclined by 41.20(18)°. Atom Zn(1) is linked to Zn(2) by three Cl···Zn···Cl bridges. The average Zn···Cl bridging distance is 2.3239(4)Å and slightly longer than the non-bridging Zn-Cl distances which have an average value of 2.208(6)Å. The macrocycles are linked to one another by longer Zn···Cl···Zn bridging bonds, 2.806(1)Å, involving the Zn atoms of the binuclear complex, Zn(1) and Zn(2), and atom Cl(5), which is directly coordinated to atom Zn(1) of a symmetry related molecule, see Fig.36. There are two coordinated water molecules in the macrocycle, one to Zn(1), Zn(1)-OW(1) 2.090(4)Å, and the other to a bridging zinc atom [Zn(3)-OW(2) 2.004(5)Å]. Within the macrocycle there are two hydrogen bonds involving water OW(1) and atoms Cl(2A) and Cl(3). A third hydrogen bond links the macrocycles and involves water OW(2) and atom Cl(5) of a symmetry related molecule. In Fig.37b a picture of the packing in the crystal is given. Selected bond lengths and angles are given in Table 25.

---

[83]M. Graf, H. Stoeckli-Evans, *Acta Cryst.C.* (1994) 1461.

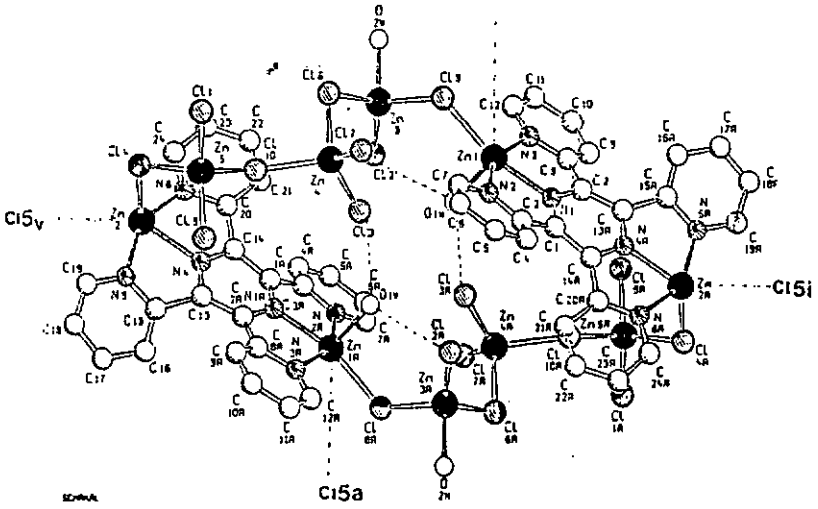

Fig. 36. Perspective view of the macrocycle showing part of the atomic numbering scheme.

(H-atoms are omitted for clearity).

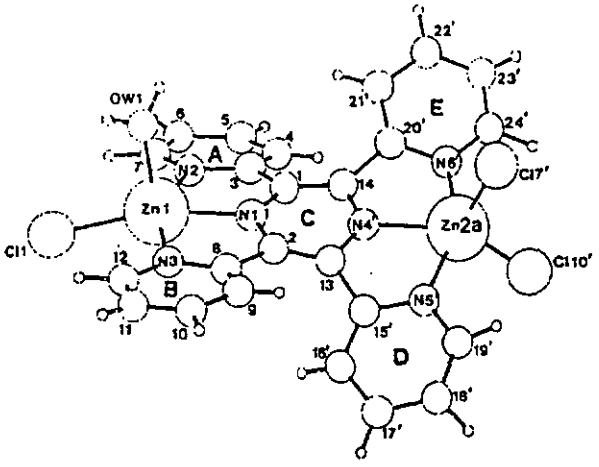

Fig.37a. Perspective view of the binuclear complex showing the atomic numbering scheme.

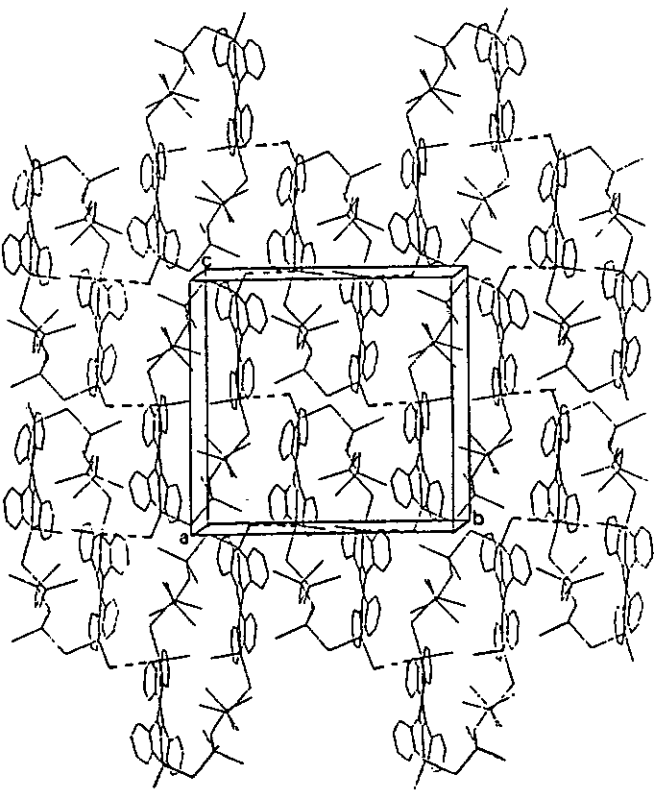

Fig.37b. Crystal packing showing the Zn(5)-Cl(10)···Cl bridging bonds (dashed line) linking the macrocycles.

Tab. 25. Selected bond distances (Å) of (18).

Zn(1)-N(1)	2.123(3)	Zn(2)-N(4)	2.145(3)
Zn(1)-N(2)	2.094(4)	Zn(2)-N(5)	2.117(4)
Zn(1)-N(3)	2.116(4)	Zn(2)-N(6)	2.132(4)
Zn(1)-Cl(5)	2.8061(13)	Zn(2)-Cl(4)	2.3426(13)
Zn(1)-Cl(8)	2.3563(12)	Zn(2)-Cl(5)	2.2894(12)
Zn(1)-OW(1)	2.090(4)		
Zn(3)-Cl(2)	2.1895(14)	Zn(3)-Cl(8)	2.3122(13)
Zn(3)-Cl(6[a])	2.2716(14)	Zn(3)-OW(2[a])	2.004(4)
Zn(4)-Cl(3[b])	2.2353(13)	Zn(4)-Cl(7[c])	2.1950(13)
Zn(4)-Cl(6)	2.3675(13)	Zn(4)-Cl(10[d])	2.3003(15)
Zn(5)-Cl(1)	2.2024(14)	Zn(5)-Cl(9)	2.2198(15)
Zn(5)-Cl(4)	2.3299(13)	Zn(5)-Cl(10)	2.3456(15)
Zn(1)-Zn(2)	4.2698(9)	Zn(4)-Zn(5)	4.3632(9)
Zn(1)-Zn(3)	4.0358(9)	Zn(5)-Zn(2)	3.8173(9)

Symmetry operation: a) x, 0.5-y, -0.5+z, b) 1-x, -0.5+y, 0.5-z, c) x, 0.5-y, 0.5-z, d) 1-x, -y, -z.

Tab. 25a. Hydrogen bonding geometry (Å, °) (18).

D	H	A	D-H	H...A	D...A	D-H...A
OW(1)	HAW1	Cl(2)	0.80(6)	2.41(6)	3.202(4)	168(6)
OW(1)	HBW1	Cl(3)	0.94(8)	2.23(8)	3.091(4)	151(7)
OW(2)[i]	HBW2[i]	Cl(5)	0.75(7)	2.37(7)	3.116(5)	168(7)

Symmetry operation: i) x, 0.5-y, z+0.5.

From n.m.r. and u.v. investigations we get the information that a break of the Zn- Cl bridges occurs in solution. The two bands at 295 and 315 nm were observed at the same wave lengths as for the other $ZnCl_2$-complexes, and an aquo complex is assumed. In the infrared spectrum

for the macrocycle we found that the two characteristic bands are closer together. A separation of 8 cm^{-1} was found and results in a broading of the bands at 1605s, 1597s cm^{-1}. We observed bands in the ν(C=C), ν(C=N) region at 1447w, 1473m, 1456w, 1412s, 1388w, 1304w cm^{-1}.

From a reaction of $Zn(NO_3)_2 \cdot 6H_2O$ with tppz in EtOH/H_2O mixture we isolated deep yellow crystals of 19.

$$2Zn(NO_3)_2 \cdot 6H_2O + tppz + 1.5H_2O \rightarrow [Zn_2(tppz)(H_2O)_6](NO_3)_4 \cdot 1.5H_2O \quad (19)$$

The reaction was carried out at 90°C with a metal to ligand ratio of 6:1. The x-ray structure analysis indicates a binuclear complex with the composition $[Zn_2(tppz)(H_2O)_6](NO_3)_4 \cdot 1.5H_2O$Å[84], the atomic numbering scheme is given in Fig.38.

We found that three molecules of water are coordinated around the Zn atoms to build an octahedral coordination sphere. In the asymmetric unit we found two molecules, discussed in the following context is only molecule A. In the complex the nitrate ions are situated outside of the coordination sphere together with two molecules of water. The central pyrazine rings of both molecules have a twist conformation with a dihedral angle between the plane C and C' of 12.4(5)° (molecule A and B). In comparison to the complex $[Zn(tppz)Cl_2]$ and $[Zn_2(tppz)Cl_4]$ these planes are more strongly twisted. The N(3)-Zn(1)-N(6) angle is 150.7(3)° and similar to the N(4)-Zn(2)-N(5) angle of 148.7(4)°. The found Zn-N(pyrazine) distances of 2.125(6) and 2.127(6)Å are slightly longer than that observed for $[Zn(terpy)Cl_2]$ and smaller than in the mononuclear zinc complex. The values of the Zn-N(pyridine) distances are comparable with those of $[Zn_2(tppz)Cl_4]$, see Table 27. The Zn-O(water) distances are in the range from 1.98 to 2.21Å. The distance Zn(1)-O(2) and Zn(2)-O(6) are the longest. A reason for this could be the formation of hydrogen bridging bonds to two molecules of water of crystallization, O(8) and O(7)g. The pyridine rings A,B,D and E are inclined relative to the central pyrazine ring by 25.2(3), 25.5(3), 23.1(3) and 27.5(3)°, respectively. The pyridine rings C and E are inclined to one another by 27.5(3) and rings B and D by 48.2(3)°. An overview of the dihedral angles of

[84]To be published

the pyridine rings relative to the central pyrazine ring of several complexes is given in Table 26. The shortest intramolecular distance is that between C(6)...C(11) with 3.155(12) and between C(16)...C(21) with 3.155(12)Å. The intramolecular distance of the corresponding protons are 2.4190(6) and 2.5798(6)Å. The Zn...Zn separation of 6.8790(16) is shorter by 0.066Å than the corresponding distance in $[Zn_2(tppz)Cl_4]$.

Tab.26. Overview of dihedral angles (Å) between the central pyrazine ring C and the pyridine rings of Zn^{2+} complexes of tppz

angles	$[Zn(tppz)Cl_2]$	$[Zn_2(tppz)Cl_4]$	macrocycle (18)	$[Zn_2(tppz)(H_2O)_6](NO_3)_4 \cdot 1.5H_2O$ (19)
A^B	13.5(1)	13.13.(23)	7.72(17)	2.2(3)
A^C(C')	7.8(2)	29.62(23)		25.2(3)
B^C(C')	21.0(1)	16.81(23)		25.5(3)
D^E	37.0(1)	14.7(3)	12.19(18)	7.9(3)
D^C"	22.8(2)	14.8(3)		23.1(3)
E^C"	43.9(2)	28.83(24)		27.5(3)
A^D	37.6(1)	44.40(3)	48.61(18)	48.0(3)
A^E	61.9(1)	58.25(24)	41.56(16)	52.6(3)
B^D	50.9(1)	31.60(3)	41.20(18)	48.2(3)
B^E	74(1)	45.17(24)	35.00(16)	53.0(3)
C'^C"	10.6(2)	12.0(5)	11.6(3)	12.4(5)

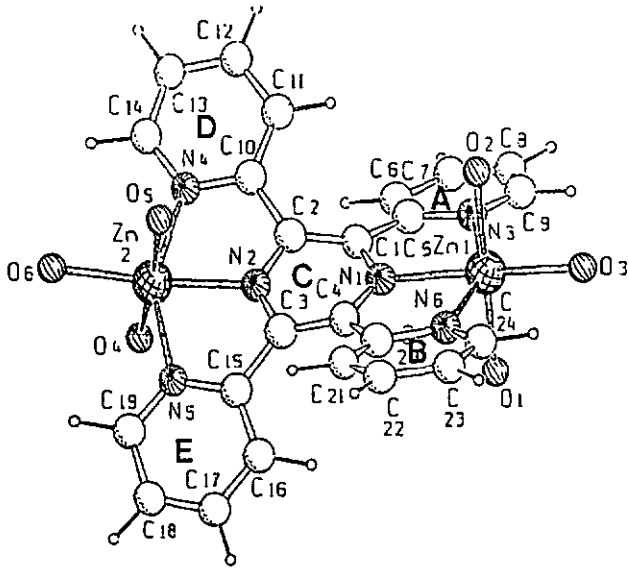

Fig. 38. SCHAKAL plot of $[Zn_2(tppz)(H_2O)_6](NO_3)_4 \cdot 1.5H_2O$(19).

Tab. 27. Selected distances (Å) and angles (°) of $[Zn_2(tppz)(H_2O)_6](NO_3)_4 \cdot 1.5H_2O$(19)

Zn(1)-O(1)	2.136(6)	Zn(1)-N(1)	2.125(6)
Zn(1)-O(2)	2.209(6)	Zn(1)-N(3)	2.155(6)
Zn(1)-O(3)	1.983(5)	Zn(1)-N(6)	2.149(6)
Zn(2)-O(4)	2.070(6)	Zn(2)-N(2)	2.127(6)
Zn(2)-O(5)	1.991(6)	Zn(2)-N(4)	2.137(7)
Zn(2)-O(6)	2.205(7)	Zn(2)-N(5)	2.171(7)
N(1)-Zn(1)-N(3)	75.00(23)	N(3)-Zn(1)-O(1)	92.61(25)
N(1)-Zn(1)-N(6)	75.30(23)	N(3)-Zn(1)-O(2)	89.37(24)
N(1)-Zn(1)-O(1)	87.75(25)	N(6)-Zn(1)-O(1)	88.75(25)
N(1)-Zn(1)-O(2)	93.50(23)	N(6)-Zn(1)-O(2)	89.91(23)
N(1)-Zn(1)-O(3)	176.5(3)	N(6)-Zn(1)-O(3)	107.2(3)
N(2)-Zn(2)-N(4)	98.76(24)	N(4)-Zn(2)-O(5)	105.5(3)

Tab. 27 (continuation)

N(2)-Zn(2)-N(5)	75.00(24)	N(4)-Zn(2)-O(6)	86.7(3)
N(2)-Zn(2)-O(5)	169.1(3)	N(5)-Zn(2)-O(4)	91.74(25)
N(2)-Zn(2)-O(6)	84.9(3)	N(5)-Zn(2)-O(5)	105.1(3)
N(4)-Zn(2)-O(4)	91.38(25)	N(5)-Zn(2)-O(6)	92.1(3)

The proton n.m.r. spectrum measured in $CDCl_3$ (1drop of DMSO) exhibits the four signal groups for the bis(tridentate) coordination mode at δ8.62(m); δ7.76 (m); δ7.66(m); δ7.43 (m). In the infrared spectra a broad band of the ν(N=O) of the nitrate ion covers partially the ligand bands in the ν(C=C), ν(C=N) region. The two characteristic bands were observed at 1595m, 1574w cm^{-1} and this is in agreement with that found for the other zinc complexes. The u.v. spectrum indicates the coordinated ligand at 295 and 320 nm.

To investigate the coordination behaviour towards the pseudohalides SCN^-, $N(CN)_2^-$ and $C(CN)_3^-$ we carried out the same reactions as described for the binuclear nickel complex, in chapter 2.3. From a reaction of the $[Zn_2(tppz)(H_2O)_6](NO_3)_4 \cdot 1.5\ H_2O$ with NH_4NCS (molar ratio 1:2) we obtained a yellow precipitate which was sparingly soluble in all common solvents.

$$[Zn_2(tppz)(H_2O)_6](NO_3)_4 + 2NH_4NCS \rightarrow \underset{(20)}{[Zn(tppz)(SCN)_2]} + Zn(NO_3)_2 \cdot 6H_2O + 2NH_4NO_3$$

Elemental analysis results imply the composition $[Zn(tppz)(SCN)_2]$ for the monomer unit. The infrared spectra (KBr) indicated that one metal is bound to the tppz. This effect of losing one zinc atom to form a new coordination mode (polymer) was also observed in the latter described reaction with dicyanamide and tricyanmethanide, proved in this case by X-ray structure analysis. From the infrared spectrum we obtained the information that the thiocyanate anion acts as bridging ligand (M-SCN-M). The two ν(CN) vibration bands are shifted significantly to higher wave numbers (2080, 2172 cm^{-1}), this is a clear indication for a bidental

coordination behaviour, and for this reason we assume a polymer structure $[Zn(tppz)(SCN)_2]_\infty$ for this compound.

To introduce the bridging ligand $N(CN)_2^-$, we carried out a reaction of $[Zn_2(tppz)(H_2O)_6](NO_3)_4 \cdot 1.5H_2O$ with $KN(CN)_2$ in water solution at 70°C with a molar ratio of 1:1 and 1:2. Interestingly, we found that in one case a coordination of one molecule of dicyanamide takes place and in the other case dicyanamide acts as counterion. From a reaction in a molar ratio of 1:1 we obtained after recrystallization from methanol/water well formed yellow needles of compound 21.

$$[Zn_2(tppz)(H_2O)_6](NO_3)_4 \cdot 1.5H_2O + KN(CN)_2 \rightarrow [Zn(tppz)(N(CN)_2)(NO_3)(H_2O)] \quad (21) + KNO_3 + Zn(NO_3)_2 + 6.5H_2O$$

X-ray structure analysis showed a coordination of one dicyanamide together with a nitrate and a water molecule $[Zn(tppz)(N(CN)_2)(NO_3)(H_2O)]$ (21)[84]. The monomer complex is hydrogen bonded via the protons of the water molecules to the next dicyanamide nitrogen atom [N(9)...O(4) 2.773Å, symmetry operation: x-0.5, 1-y, 1-z]. Furthermore a hydrogen bridging bond was located from the nitrate oxygen to the protons of the water molecule [O(2)...O(4) 2.712Å, symmetry operation x-1, y, z]. A linear hydrogen bridged polymer chain was observed. The coordination of the zinc atom can be described as distorted octahedral. The central Zn-N(pyrazine) distance with 2.098(9)Å is shorter than comparable distances found for the complexes **16**, **17** and **19** and longer as found for **18** and **22**. The Zn-N(pyridine) distances are 2.132(12) and 2.101(12)Å. The Zn-O(nitrate) distance is 2.22(2)Å and the Zn-O(water) bondlength 2.174(12)Å. For the coordinated dicyanamide molecule we observed a distance of Zn-N(7) 1.986(11)Å. The angle N(1)-Zn(1)-N(7) is about 179.1(7)° whereas the angle C(25)-N(8)-C(26) is 120(2)° and the ∠NCN angles are 167(2) and 171(3)°. Jensen et al.[85] found for the salt $KN(CN)_2$ (C-N) distances of 1.155 and 1.156Å as well as (N-C) distances of 1.304 and 1.309Å. Angles were found with ∠CNC 120.3 and ∠NCN 172.8°. Also in this complex

[85]H. Jensen, B. Klewe, E. Tjelta, *Acta Chem. Scand.*, A31 (1977) 151.

the central pyrazine ring is considerably distorted. The dihedral angle between the planes C' and C" is 12.2°. A collection of important bond distances and angles for the complex are given in Tab. 28.

Tab. 28.. Selected distances (Å) and angles (°) of [Zn(tppz)($N(CN)_2$)(NO_3)(H_2O)] (21).

Zn(1)-N(1)	2.098(9)	Zn(1)-O(1)	2.22(2)
Zn(1)-N(3)	2.132(12)	Zn(1)-O(4)	2.174(12)
Zn(1)-N(4)	2.101(12)	Zn(1)-N(7)	1.986(11)
N(7)-C(25)	1.15(2)	C(25)-N(8)	1.30(2)
N(8)-C(26)	1.31(2)	C(26)-N(9)	1.12(2)
N(10)-O(1)	1.12(2)	N(10)-O(3)	1.38(2)
N(10)-O(2)	1.13(2)		
N(1)-Zn(1)-N(7)	179.1(7)	N(3)-Zn(1)-N(7)	104.3(5)
N(1)-Zn(1)-O(1)	92.6(6)	N(4)-Zn(1)-N(7)	104.6(5)
N(1)-Zn(1)-O(4)	88.5(5)	N(3)-Zn(1)-O(1)	80.4(6)
N(1)-Zn(1)-N(4)	76.3(4)	N(4)-Zn(1)-O(1)	96.8(6)
N(1)-Zn(1)-N(3)	74.8(4)	N(3)-Zn(1)-O(4)	91.8(5)
N(4)-Zn(1)-N(3)	150.8(4)	N(4)-Zn(1)-O(4)	91.6(5)
O(1)-Zn(1)-O(4)	171.5(6)	Zn(1)-N(7)-C(25)	170(2)
C(26)-N(8)-C(25)	120(2)	O(1)-N(10)-O(2)	132.2(2)
N(9)-C(26)-N(8)	167(2)	O(1)-N(10)-O(3)	115.3(13)
O(2)-N(10)-O(3)	111.1(14)		

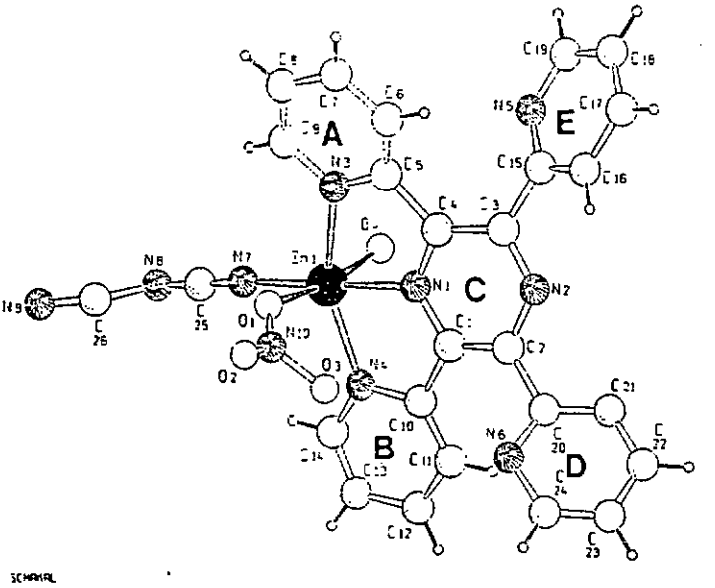

Fig. 39. SCHAKAL plot of $[Zn(tppz)(N(CN)_2)(NO_3)(H_2O)]$ (21).

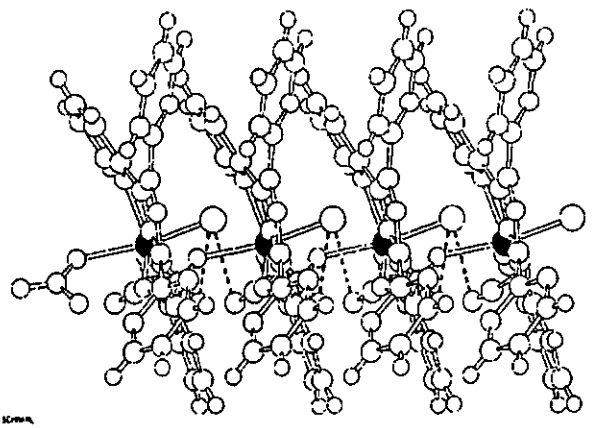

Fig. 39a. SCHAKAL plot of the hydrogen bonded polymer chain.

The infrared spectrum contains the following characteristic bands for the coordinated dicyanamide [$\nu_s+\nu_{as}$(C-N) 2309, ν_{as}(CN) 2241, n_s(CN) 2187 cm^{-1}]. The shift to higher wave numbers indicates clearly the monodentate coordination of $N(CN)_2^-$. The characteristic bands for the ligand are present at 1599m, 1568m, 1468m, 1399m. U.v. measurements in water solution show the two bands for the ligand at 295 and 318 nm. FAB mass spectroscopy results confirm with the determined X-ray crystal structure. The characteristic fragments are listed in Table 29.

Tab. 29. FAB mass spectrum (70 eV) of $[Zn(tppz)(N(CN)_2)(NO_3)(H_2O)]$ (21)

m/e	relative intensity (%)	fragment
518	20	$[Zn(tppz)\{N(CN)_2\}]^+$
452	18	$[Zn(tppz)]^+$

From a reaction in a molar ratio of 1:2 we obtained a new complex arrangement $[Zn(tppz)_2](N(CN)_2)_2 \cdot H_2O$ (22)[86]. Probably because of steric reasons we found for the first time the arrangement $[M(tppz)_2]^{2+}$ in which two molecules of tppz are coordinated around one zinc atom. The large dicyanamide anion acts as counterion in this case. In the structure we found nearly similar Zn-N(pyrazine) distances of 2.10Å which are significant shorter in comparison to the corresponding distances in the mononuclear complex $[Zn(tppz)CL_2]$ [2.156(2)Å]. Usually the Zn-N(pyridine) distances are found to be longer. Here the distance Zn-N(3) is 2.171(7)Å and the Zn-N(4) distance is 0.008Å shorter. The same relation was found for the distances Zn-N(10) which is 2.162(7)Å and shorter by 0.007Å than Zo-N(9) with 2.169(7), see Table 31. Important angles around the Zn atom are N(1)-Zn-N(7), N(3)-Zn-N(4) and N(9)-Zn-N(10) which have the values 177.3(3), 151.4(3) and 150.2(3)°, respectively. A strong deviation from 180° is observed. This is an indication for a distorted octahedral coordination sphere. We found also in this complex that the central pyrazine rings are twisted

[86]To be Published.

by 9.07and 9.02°. The coordinated pyridine rings A and B are inclined to one another by 8.00° and by 18.66 and 18.35° relative to the central pyrazine ring. For A' and B' we found angles of A'^B' = 6.80°, A'^C' = 25.92 and B'^C' = 19.97°.

Tab. 31 Observed dihedral angles (°) of the complexes $[Zn(tppz)_2](N(CN)_2)_2$ (22)

angle	$[Zn(tppz)_2](N(CN)_2)_2$	angle	$[Zn(tppz)_2](N(CN)_2)_2$
A^B	8.00	A'^B'	6.80
A^C	18.66	A'^C'	25.92
B^C	18.35	B'^C'	19.97
D^E	38.04	D'^E'	33.61
D^C	36.47	D'^C"	31.92
E^C	37.08	E'^C"	38.74
A^D	51.80	A'^D'	55.92
A^E	54.49	A'^E'	62.26
B^D	54.33	B'^D'	51.10
B^E	50.52	B'^E'	55.92
C"^C"	9.07	C"^C' "	9.52

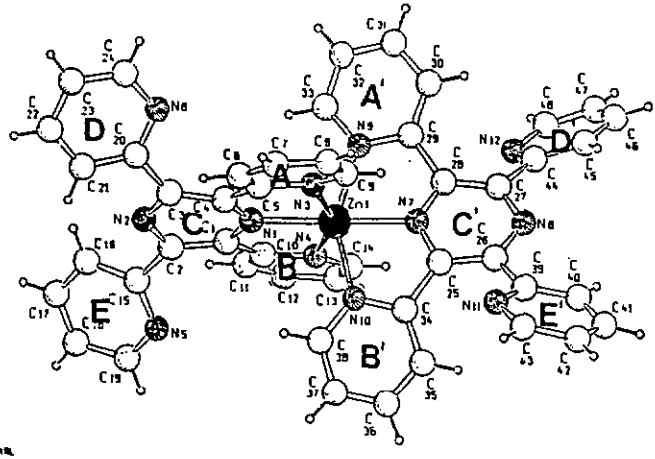

Fig. 40. SCHAKAL plot of $[Zn(tppz)_2]^{2+}$ (22), the anion and water molecules are omitted.

Tab 30. Selected bond distances (Å) and angles (°) for $[Zn(tppz)_2](N(CN)_2)_2 \cdot H_2O$ (22)

Zn-N(1)	2.101(5)	Zn-N(7)	2.100(6)
Zn-N(3)	2.171(7)	Zn-N(9)	2.169(7)
Zn-N(4)	2.163(7)	Zn-N(10)	2.162(7)
N(1)-Zn-N(3)	75.8(3)	N(1)-Zn-N(10)	104.1(3)
N(1)-Zn-N(4)	75.6(3)	N(7)-Zn-N(9)	74.7(3)
N(3)-Zn-N(4)	151.4(3)	N(1)-Zn-N(9)	105.7(3)
N(7)-Zn-N(4)	107.1(3)	N(10)-Zn-N(9)	150.2(3)
N(7)-Zn-N(3)	101.5(3)	N(4)-Zn-N(9)	92.8(3)
N(7)-Zn-N(1)	177.3(3)	N(10)-Zn-N(3)	93.7(3)
N(7)-Zn-N(10)	75.5(3)	N(9)-Zn-N(3)	94.1(3)

The discussion of the pseudohalide anion will be centered in comparison to the known informations about the potassium salt. In the literature is an angle of ∠CNC 120.3° and ∠ NCN of 172.8° observed. This is an indication for a deviation from a planar system. We found for the dicyanamide molecules stronger deviations. The ∠CNC angles of 105(2) and 114(2)° are significantly smaller. The ∠NCN angles are found in a range of 139(7) to 168(2)°, this is a clear indication for a nonplanar system. Generally, the distances and angles of all pseudohalide anions are distorted from their ideal values which here is suffering from coosiderable thermal vibrations. In the infrared spectrum the characteristic bands for the dicyanamide were found at 2128 vs, 2185 m and 2227 m cm^{-1}.

Tab. 31: Selected bond distances (Å) and angles (°) for the dicyanamide counterions in $[Zn(tppz)_2](N(CN)_2)_2 \cdot H_2O$

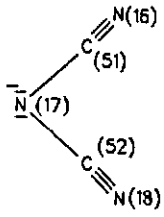

dicyanamide 1

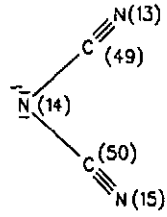

dicyanamide 2

dicyanamide 1		dicyanamide 2	
N(17)-C(51)	1.36(4)	N(14)-C(49)	1.32(2)
N(17)-C(52)	1.25(6)	N(14)-C(50)	1.33(2)
C(51)-N(16)	1.15(3)	C(49)-N(13)	1.09(2)
C(52)-N(18)	1.31(6)	C(50)-N(15)	1.103(14)
C(51)-N(17)-C(52)	105.0(4)	C(50)-N(14)-C(49)	114.0(2)
N(17)-C(52)-N(18)	139(7)	N(14)-C(49)-N(13)	148(3)
N(17)-C(51)-N(16)	158(3)	N(14)-C(50)-N(15)	168(2)

To investigate the coordination behaviour of the pseudohalide tricyanmethanide towards the complex $[Zn_2(tppz)(H_2O)_6](NO_3)_4 \cdot 1.5H_2O$ we carried out a reaction in a molar ratio of 1:1 in water solution at 70 °C. A yellow powder precipitated very quickly. After recrystallization from methanol/water we obtained fine yellow needles. X-ray structure analysis indicates the same arrangement as described above. The binuclear zinc complex loses one zinc atom and two molecules of tppz are arranged around the metal atom in an octahedral coordination sphere $[Zn(tppz)_2](C(CN)_3)_2$ **(23)**[84], the atomic numbering scheme is to see in Fig. 41. We found a highly symmetric molecule with a two-fold axis, on which set atoms Zn, N(1), N(2), N(5), and N(6). The important angles for a description of the coordination polyhedron are N(1)-Zn-N(5) with 180°, N(3)-Zn-N(3)^A with 151.8(4) and N(7)-Zn-N(7)^A with 150.4(4)°. This is comparable to the corresponding angles in compound **22**. We found that the Zn-

N(pyrazine) distances are 2.089(10) and 2.059(9)Å, therefore they are shorter than those observed in 22. Because of the two-fold symmetry in the molecule the Zn-N(pyridine) distances are equal on both sides of the molecule, with values of 2.131(7) and 2.193(6)Å. The central pyrazine rings are twisted by 7.659 and 7.604°. Important bond distances and angles are given in Table 32.

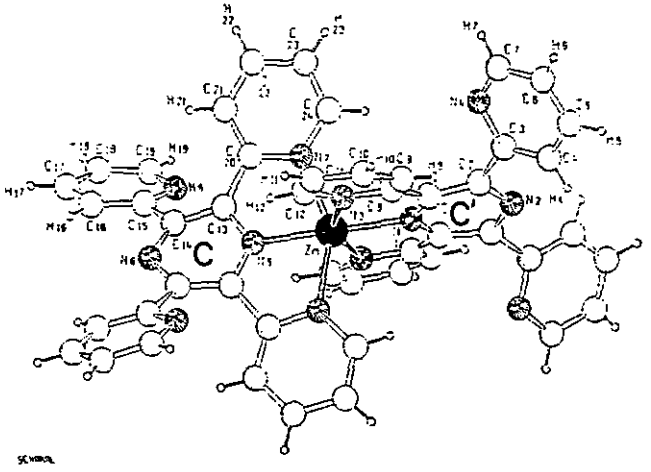

Fig. 41. SCHAKAL plot of $[Zn(tppz)_2](C(CN)_3)_2$ (23), the anions are omitted for clearity.

Tab. 32. Selected bond distances (Å) and angles (°) for $[Zn(tppz)_2](C(CN)_3)_2$ (23)

Zn-N(1)	2.089(10)	Zn-N(5)	2.059(9)
Zn-N(3)	2.131(7)	Zn-N(7)	2.193(6)
Zn-N(3A)	2.131(7)	Zn-N(7A)	2.193(6)
N(1)-Zn-N(5)	179.9	N(3)-Zn-N(7A)	91.6(2)
N(3)-Zn-N(5)	104.1(2)	N(3A)-Zn-N(7A)	95.3(2)
N(3)-Zn-N(1)	75.9(2)	N(5)-Zn-N(7)	75.1(2)
N(3A)-Zn-N(5)	104.1(2)	N(1)-Zn-N(7)	104.9(2)
N(3A)-Zn-N(1)	75.9(2)	N(3)-Zn-N(7)	95.3(2)

Tab.32. (continuoation)

N(3A)-Zn-N(3)	151.7(4)	N(3A)-Zn-N(7)	91.9(2)
N(7A)-Zn-N(5)	75.1(2)	N(7A)-Zn-N(7)	150.2(4)
N(7A)-Zn-N(1)	104.9(2)		

Tab. 32b. Selected bond distances (Å) and angles (°) of the compounds $[Zn(tppz)_2]C(CN)_3)_2$ (23), $[Zn(tppz)_2]N(CN)_2)_2 \cdot H_2O$ (22) and $[Zn(tppz)Cl_2]$ (16)

$[Zn(tppz)Cl_2]$ (16)	$[Zn(tppz)_2](N(CN)_2)_2 \cdot H_2O$ (22)	$[Zn(tppz)_2](C(CN)_3)_2$ (23)
Zn-N(1) 2.156(2)	Zn-N(1) 2.101(5) Zn-N(7) 2.100(6)	Zn-N(1) 2.089(10) Zn-N(5) 2.059(9)
Zn-N(2) 2.204(3)	Zn-N(3) 2.171(7) Zn-N(9) 2.169(7)	Zn-N(3) 2.131(7) Zn-$N(7)^A$ 2.193(6)
Zn-N(3) 2.178(3)	Zn-N(4) 2.136(7) Zn-N(10) 2.162(7)	Zn-$N(3)^A$ 2.141(7) Zn-N(7) 2.193(6)
	N(1)-Zn-N(7) 177.3(3)	N(1)-Zn-N(5) 179.9
	N(3)-Zn-N(4) 151.4(3)	N(3)-Zn-$N(3)^A$ 151.7(4)
	N(9)-Zn-N(10) 150.2(3)	N(7)-Zn-$N(7)^A$ 150.2(4)

The discussion of the pseudohalide anion will be centered on a comparison with the results found for the potassium salt. A strong planarity of the tricyanmethanide molecule was observed for the structure of $KC(CN)_3$[51]. The ∠CCC angles are 119.2, 120.1 and 120.5° as is common for sp^2 hybridized carbon atoms. We observed for 23 ∠CCC angles in the range from 103.5 to 134.1° three ∠CCN angles of 133.5, 174.0 and 178.5°. Atom C(27) and N(10) undergo considerable thermal motion which could explain the poor bond lengths and angles of this group.

Tab. 33: Selected bond distances (Å) and angles (°) for the counterions tricyanmethanide of the complex $[Zn(tppz)_2](C(CN)_3)_2$

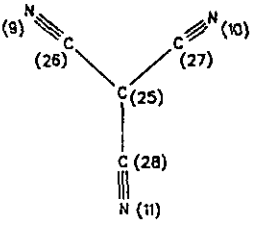

C(26)-N(9)	1.16(2)	C(27)-N(10)	0.93(4)
C(25)-C(26)	1.35(2)	C(25)-C(28)	1.36(2)
C(25)-C(27)	1.63(5)	C(28)-N(11)	1.19(2)
C(26)-C(25)-C(27)	134.1(14)	C(28)-C(25)-C(26)	122.5(2)
C(27)-C(25)-C(28)	103.5(2)		

In the infrared spectrum the characteristic bands for the ligand are present at 1597 m, sh; 1568 m; 1543 w; 1480 m; 1468 m; 1445 m; 1401 s. cm^{-1}. The pattern of bands are shifted in accordance with the dicyanamide complex 22 described above. Elemental analyses agree with the composition found for the structure. The FAB mass spectrum contains the following characteristic fragments, see Table 34.

Tab. 34. FAB- mass spectrum 70 (eV) of $[Zn(tppz)_2](C(CN)_3)_2$ (23)

m/e	rel. intensity (%)	fragment
931	12	$[Zn(tppz)_2(C(CN)_3)]^+$
841	25	$[Zn(tppz)_2]^+$
543	40	$[Zn(tppz)(C(CN)_3)]^+$
453	60	$[Zn(tppz)]^+$

3. Study of the coordination behaviour of 2.4.6-tris(2-pyrimidyl)-1.3.5-triazine

3.1. Introduction

The tris-tridentate ligand 2.4.6-tris(2-pyrimidyl)-1.3.5-triazine (tpymt) was first prepared in small amounts by allowing a solution of 2-cyanopyrimidine to stand for several months[87]. These authors obtained the 2-cyanopyrimidine by the method published by Klötzer[88]. A further method was found by Case and Koft[89]. In the latter work the tpymt was also prepared in low yields by standing 2-cyanopyrimidine for three months. Better yields could be obtained by Lerner and Lippard[90]. They also started from the 2-cyanopyrimidine and stirred this compound for two days in a stoppered flask at 150°C; according to the following reaction scheme:

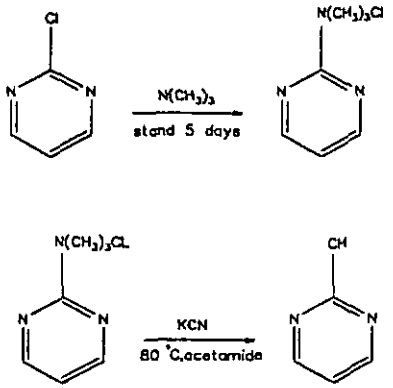

[87]E. Ochiai, H. Yamanaka, *Pharm. Bull. (Jpn.)*, 3 (1955) 173; C.A. 50 7810 e.

[88]W. Klötzer, *Monatsh.* 87 (1956) 526.

[89]F.H. Case, E. Koft, *J. Am. Chem. Soc.*, 81 (1959), 905.

[90]E. I. Lerner, S.J. Lippard, *J. Am. Chem. Soc.*, 98 (1976) 5397.

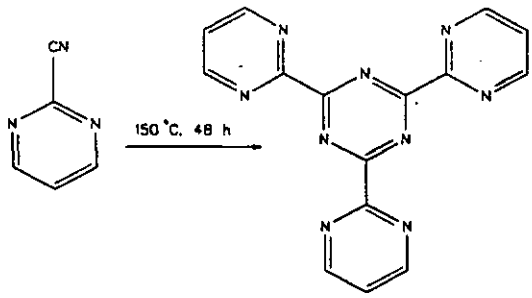

This improved method was also used by us. The difficulty of this synthesis is the relative low yield of the 2-cyanopyrimidine.

The first four metal complexes of this ligand were described in 1976 and the compound $[Pb_2(tpymt)(NO_3)_4(H_2O)_2]$ was crystallographically investigated[91], Fig. 42. The triazine ligand binds two lead atoms in two of its three tridentate sites. These lead atoms are bridged by a nitrate ion and a water molecule to form a polymer chain along the crystallographic b axis. The ring system of the ligand is puckered and a water molecule is hydrogen bonded in the third terpyridine-like site. The geometry around the Pb(1) atom can be described as a distorted cube. One face of the cube comprises nitrogen atoms of the ligand and the oxygen atoms of one bidentate nitrate ion. The opposite face of the cube is comprised of oxygen atoms of the bidentate and the monodentate nitrate ion and O(14) from a water molecule. The Pb(2) atom is eight-coordinated being bound to three nitrogen atoms of the tpymt ligand. Four nitrate oxygen atoms and one oxygen of a water molecule are coordinated to form a pentagonal bipyramid. The individual pyrimidine and pyrazine rings are planar. The Pb(1) atom is 1.199(1)Å below that plane while the Pb(2) atom is 0.826(1)Å above it.

[91]E.I. Lerner, S.J. Lippard, *Inorg. Chem.*, 16 (1977) 1537.

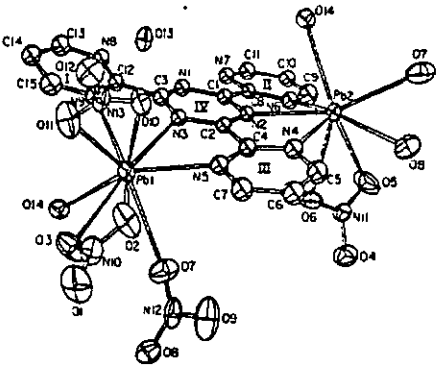

Fig. 42. Molecular structure of $[Pb_2(tpymt)(NO_3)_4(H_2O)_2]$

Furthermore, the complexes $[(UO_2)(tpymt)(NO_3)_2]\cdot 7H_2O$, $[Pb_3(tpymt)Cl_6]\cdot 3H_2O$ and $[Tl_7(tpymt)_2(NO_3)_7]$ were also obtained, but no crystallographic investigations were carried out. The same authors observed hydrolysis reactions of tpymt in the presence of $Cu(NO_3)_2$ [92]. The bis-(2-pyrimidyl)carboximidatotriaquocopper (II) nitrate trihydrate was formed, see Fig.43. Julve and co-workers found with the ligand 2.4.6-tris-(2-pyridyl)-1.3.5-triazine (tptz), in the presence of $[Cu(H_2O)_6](ClO_4)_2$[93], that a hydrolysis reaction also occurs. The complexes formed $[Cu\{(NC_5H_4CO)_2N\}\text{-}(NC_5H_4CONH_2)]\cdot ClO_4\cdot H_2O$ and $(Cu\{(NC_5H_4CO)_2N\})ClO_4$ were isolated and investigated by X-ray analysis[94].

---

[92]E.I. Lerner, S.J. Lippard, *J. Am. Chem. Soc.*,98 (1976) 5397.

[93]E.I. Lerner, S.J. Lippard, *Inorg. Chem.*, 16 (1977) 1546.

[94]A. Cantarero, J.M. Amigo, J. Faus, M. Julve, T. Debaerdemacker, *J. Chem. Soc., Dalton Trans.*, (1988) 2033.

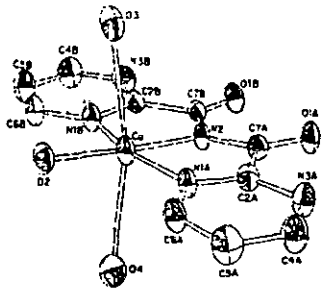

Fig. 43. Molecular structure of the bis-(arylcarbonyl)-aminato copper (II) complex.

For the first time dimeric complexes were found from the reaction of CoI_2 with 2.4.6-tris(2-pyridyl)-1.3.5-triazine. Figgis et al.[95] published the X-ray crystal structure of two different hydrated phases of bis[2.4.6-tris(2-pyridyl)-1.3.5-triazine]cobalt(II)iodide which crystallizes separately from the reaction mixture. A monohydrate and a 3.75-hydrate crystallize in different space groups with one and two independent cations in the asymmetric unit, respectively.

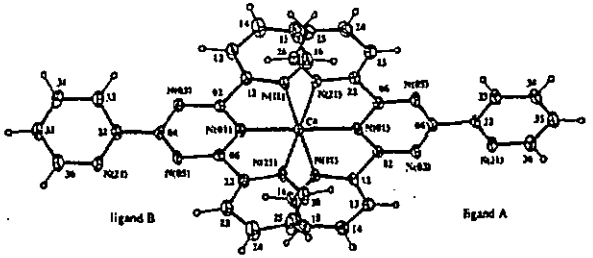

Fig. 44. Molecular structure of bis[2.4.6-tris(2-pyridyl)-1.3.5-triazine]cobalt(II)iodide.

Up to now the coordination behaviour of this ligand was not intensively investigated. For this reason we carried out some reactions with metal salts of the 3d row as well as with Ag^{+}, Cd^{2+}, Hg^{2+} and Tl^{+}.

---

[95]B. Figgis, E.S. Kucharski, S. Mitra, B.W. Skelton, A. H. White, *Aust. J. Chem.*, 43 (1990) 1269.

5.2. Further characterization of the ligand tpymt

From the literature some spectroscopic data were known, e.g. the i.r. and m.s. spectra are reported /89/ and the ^1H n.m.r.[90] spectrum. The latter consists of a doublet (δ9.57, 2H) and a triplet (δ8,39, 1H) in 3M DCl solution (internal standard DSS). These values were also obtained by us. By means of proton n.m.r. measurements the fact was confirmed that the ligand is decomposed by concentrated mineral acids. Standing of a tpymt solution in 3M DCl for three days yields a number of additional signals, ligand: δ9.54 (d); δ8.33 (t), amide: δ9.54 (d); 8.43 (m), cyanide: δ9.09 (d); δ7.86 (t). We recorded also a proton n.m.r. spectrum of tpymt in D_2O/DSS and obtained the following signals: δ9.11(d, 2H $^3J_{(H-H)}$=4.94Hz); δ7.85 (t, 1H, $^3J_{(H-H)}$=4.94Hz). In addition a ^{13}C {^1H} n.m.r. spectrum (D_2O/1drop HCl) was recorded by us. Four singlets for four different carbon atoms were observed:, δ=171.5 (C 7), δ=160.8 (C 3 and C 5), δ=159.1 (C 1), δ=127.4 (C 4).

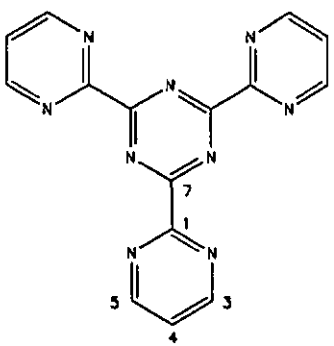

These observations are in accordance with theoretical expectations and with the literature [96] data.

Furthermore, an u.v. spectrum in water was recorded at 25 °C. We obtained one broad absorption band at λ_{max}=250 nm (λ_{min}=210 nm) with ε_{max} = 24 900. Thermogravimetric

---

[96]H.O. Kalinowski, S. Berger, S. Brown, "^{13}C-NMR-Spectroskopie", Georg Thieme Verlag Stuttgart, (1984), 325.

measurements of a sample of the ligand show a loss of mass from 33.3 to 148.3 °C, Δm = 0.33 mg corresponding to 1.8 water molecules. Therefore we assume the composition tpymt·$2H_2O$. Cyclovoltammetric measurements could be carried out only in water solution because of the solubility, therefore only a small range could be studied. A cyclic voltammogram of a 10^{-4} M solution of the ligand at 25°C was recorded. As background electrolyte a 0.1 M KCl solution was used. A platinum working electrode and a calomel electrode were the reference electrodes. In the range from 0 to 0.8 V scanned at 40mV/s a reversible redox process was observed with E_{red} = -0,21 V and E_{ox} = -0,19 V. Probably an one electron redox step occurs on the pyrimidine rings.

A hydrochloride tpymt·4HCl·$2H_2O$ (24) was obtained from a 6 M HCl solution after precipitatioo with acetone. The elemental analysis implies 4 HCl and two molecules of water per molecule. Thermogravimetric measurements show a loss of mass from 121,3 to 155,3 °C ; Δm = 1.66 mg, probably corresponding to 4.5 HCl. A quantitative determination of chloride with $AgNO_3$ agrees with these results. Proton n.m.r. investigations in D_2O show an upfield shift of the signals (δ 8.98 (d), 2 H and δ 7.85 (t), 1 H) but no additional signals were observed in solution because of a protonation. The infrared spectra (KBr) differ in so far that a new pattern of bands in the ν(C=C), ν(C=N) region (1660m, 1595w, 1553vs, 1510w, 1400w and 1373w cm^{-1}) could be observed. This effect was also found in the later described spectra of Ni(II) complexes of tpymt. The u.v. spectrum in water shows a broad band for the ligand at λ_{min} =210 nm, λ_{max} = 250 nm with ε_{max} =22400.

5.3. Reactions of tpymt with 3 d metal salts

To obtain information oo the flexibility of the ligand tpymt, the coordination behaviour towards some metal salts of Fe^{3+}, Co^{2+}, Ni^{2+}, Cu^{2+}, Zn^{2+} were investigated. All reaction attempts were carried out in aqueous solution at 50 °C with a metal to ligand ratio of 3:1. In the presence of several copper(II) salts CuX_2 (X= Cl^-, PF_6^-, NO_3^-, ClO_4^-, SO_4^{2-}) we also observed a hydrolysis reaction as described by Lerner and Lippard [90] for $Cu(NO_3)_2$. The same results were observed in the presence of cobalt compounds (chloride, nitrate and sulphate)

after standing the solutions over a long period (longer than one week). The characterization of the powders obtained indicated the formation of the bis(pyridyl)carboximidato copper or cobalt complexes ($\nu C{=}O{=}1735cm^{-1}$). To have a first indication if the ligand is able to coordinate one, two or three metal centers we synthesized the sparingly soluble perchlorate complexes of Fe^{3+}, Co^{2+}, Ni^{2+} and Zn^{2+} (25a-e) which precipitated very quickly from solution. The elemental analysis results indicated that the metal to ligand ratio in all the formed compounds was 1:1. Uv measurements in water solution show no shift of the characteristic bands of the ligand. By means of proton n.m.r. investigations we also observed that no coordination in solution occured. The infrared spectra (KBr) show slight shifts of the characteristic bands of the ligand, a decomposition was not observed. The anions were changed to hinder a quick precipitation and in some cases defined products could be isolated. In a reaction of the chlorides of $Fe^{3+}$and Zn^{2+} with tpymt (ratio 3:1) yellow crystals were obtained (26) and a white powder (28) respectively. The elemental analysis results indicated in both cases also a metal to ligand ratio of 1:1. The reaction attempts of tpymt with $NiSO_4$ resulted in green solutions which were stable over a long period. Crystals could not be isolated, however a precipitation of the compound with ethanol was possible. The elemental analysis indicated a ligand to metal ratio of 1:2, therefore the composition $[Ni_2(tpymt)(SO_4)_2(H_2O)_4]$ (27) is assumed. The infrared spectra (KBr) show clearly a change of the absorption pattern for the ligand which indicated the coordination. A change of the anions to chloride or nitrate gave no suitable crystals for X-ray diffraction studies. The reflectance spectra exhibit three bands at 9527, 15625 and 25974 cm^{-1}. The bands have been ascribed to d→d transition near to O_h [$^3A_{2g}\rightarrow{}^3T_{2g}$, $^3A_{2g}\rightarrow{}^3T_{1g}(F)$, $^3A_{2g}\rightarrow{}^3T_{1g}(P)$]. An octahedral coordioation sphere for the Ni^{2+} is assumed.

Finally, one can remark that the complexes of tpymt, the free ligand as well as the hydrochloride salt, all exhibit a poor crystallization behaviour. This could be shown in a lot of reaction attempts. Futthermore, in the presence of cobalt and copper metal-assisted hydrolysis reactions of the triazine ring occurs. Here, the metal can act as Lewis acid (electrophile) and catalyses reactions which are not normally acid catalyzed. Mononuclear iron and zinc compounds show, in the infrared spectra (KBr), a small shift of the characteristic C-N vibration

bands which could be a indication for a coordination in the solid state. With nickel salts however we found a two-fold coordination which is clearly seen in the infrared and the reflectance spectra. For this reason we carried out further reaction attempts with metals which are able to form longer metal nitrogen bonds.

5.4. Reaction of tpymt with silver(I) salts and cadmium(II) chloride

From a reaction of tpymt with $AgClO_4$ (metal to ligand ratio 3:1) we obtained an orange precipitate (25e). The elemental analysis results indicated a ligand to metal ratio of 1:2. From a reaction of tpymt with $AgSO_4$ (1:3) after standing for some days we isolated yellow orange crystals (29) which dried out very quickly. The elemental analysis results indicated also a metal to ligand ratio of 2:1. In the infrared spectra of all synthesized compounds bands appeared of the ligand together with the characteristic vibrations of the anions sulphate and perchlorate. Only small shifts of the characteristic ligand bands were found, this was also observed for the lead complexes in the literature mentioned above. From a reaction of tpymt with $CdCl_2$ (molar ratio 1:3) we obtained pale yellow crystals of 30.

$$CdCl_2 \quad +tpymt \quad + \quad 4H_2O \quad \rightarrow \quad [Cd(tpymt)Cl_2(H_2O)]\cdot 3H_2O$$

(30)

The X-ray structure analysis indicates a mononuclear complex $[Cd(tpymt)Cl_2(H_2O)]\cdot 3H_2O$. The geometry around the Cd atom can be described as a distorted octahedron, see Fig.45. Two chloride ions are bound to the cadmium atom with distances of Cd-Cl(1) 2.5254(10) and Cd-Cl(2) 2.4362(9)Å. One molecule of water is coordinated with a distance of 2.5659(24)Å. The Cd-N(triazine) bondlength is 2.3347(19)Å, respectively. The Cd-N(pyrimidine) distances are significantly different with a Cd-N(4) bond length of 2.3930(21)Å whereas the Cd-N(6) distance is 0.092Å longer [2.4852(20)Å]. The same fact was observed for the complex $[Pb_2(tpymt)(NO_4)_4\cdot 2H_2O]$. One Pb-N(pyrimidine) distance of both tridentate sites is longer by 0.08Å. This indicates that the ligand system is not flexible enough to distort the pyrimidine rings relative to the central triazine ring. The dihedral angles show an almost planar ring

system. The structural data of a cadmium complex with terpy are known in the literature. In the complex μ-(2,2':6',2"-terpyridyl-cadmium)-bis(pentacarbonyl-manganese) the coordination of the cadmium atom is best described as a very distorted trigonal bipyramid. The Cd-N(pyridine) bondlength (Cd-N(2) 2.405Å) to the nitrogen of the central pyridine ring is shorter than the distance to the other two nitrogens (Cd-N(1) 2.475, Cd-N(3) 2.493Å). These distances are comparable with the longest distance Cd-N(pyrimidine) in our $[Cd(tpymt)Cl_2(H_2O)]\cdot 3H_2O$.

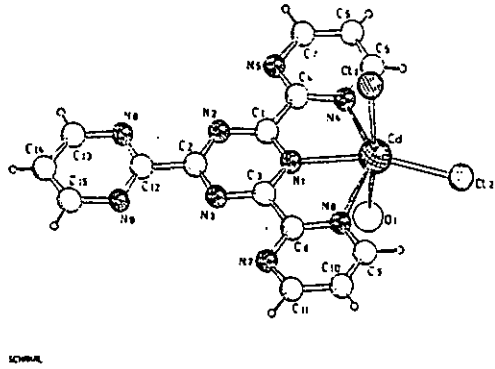

Fig.45. SCHAKAL plot of $[Cd(tpymt)Cl_2)(H_2O)]$ (30)

Tab.35. Selected bondlengths (Å) and angles (°) of $[Cd(tpymt)Cl_2)(H_2O)]\cdot 3H_2O$ (30)

Cd-Cl(1)	2.5254(10)	Cd-N(1)	2.3347(19)
Cd-Cl(2)	2.4363(9)	Cd-N(4)	2.3930(21)
Cd-O(1)	2.5659(24)	Cd-N(6)	2.4852(20)
Cl(1)-Cd-Cl(2)	103.45(3)	Cl(2)-Cd-N(1)	161.31(5)
Cl(2)-Cd-O(1)	85.37(6)	Cl(2)-Cd-N(4)	118.31(6)
Cl(1)-Cd-N(1)	93.49(5)	Cl(2)-Cd-N(6)	102.63(5)
Cl(1)-Cd-N(4)	91.12(5)	O(1)-Cd-N(4)	78.67(7)
Cl(1)-Cd-N(6)	95.78(5)	O(1)-Cd-N(6)	88.69(7)
O(1)-Cd-N(1)	78.85(7)		

The infrared spectrum (KBr) shows the following vibrations in the ν(C=C), ν(C=N) region: 1578s; 1553vs; 1425sh,w; 1374vs cm^{-1}. The vibration at 1578 cm^{-1} is shifted by 10 cm^{-1} in comparison with the free ligand and indicates coordination. ^1H n.m.r. investigations of the complex in D_2O/DSS solution gave two signals at δ9.23 (d, $^3J_{(H-H)}$=4.97Hz) and at δ7.95(t, 1H, $^3J_{(H-H)}$=4.96Hz). For the free ligand we found in the same solvent two signals at δ9.11 and δ7.85. Therefore, we assume an interaction in solution. The direct mononuclear coordination of the cadmium is not indicated in solution, this was also found by means of u.v. measurements.

3.5. Reaction of tpymt with thallium(I)nitrate

Lerner and Lippard obtained from a reaction of tpymt and $TlNO_3$ dark yellow crystals[91]. They proposed by means of elemental analysis results the composition $[Tl_7(tpymt)_2(NO_3)_7]$ (31). We wanted to reproduce this synthesis but we found the reaction was incomplete and after filtering pale yellow needles could be isolated. X-ray structure analysis showed the composition $[tpymt{\cdot}3TlNO_3{\cdot}0.75H_2O]$. The thallium atoms occupy sites near the terpyridine like sides, see Fig 46 and 46a. The Tl-N distances (see Tab 26) are between 2.85 and 3.13Å. These distances are thought to be to long for covalent bonds. In the literature structural data of a 2-pyridyl-cyanoxime-thallium(I) complex is described[97]. The Tl-N bond length is 2.695(12)Å. A similar distance of Tl-N 2.61(1) was observed in the complex tetramethylammonium-(2,2'-bipyridine-N,N')-octacarbonyl-di-iron-thallium and 2.58(1)Å in tetramethylammonium-(2,2'-phenanthroline-N,N')-octacarbonyl-di-iron-thallium[98]. In this case (31) we assume Van der Vaals forces linked this compound or a co-crystallization effect takes place.

---

[97]N.N. Garasimchuk, L. Nagy, H.-G. Schmidt, M. Noltemeyer, R. Bohra, H.W. Roesky, *Z. Naturforsch., B*, 47 (1992) 1741.

[98]J.M. Cassidy, K.H. Whitmire, *Inorg. Chem.*, 28 (1992)1435.

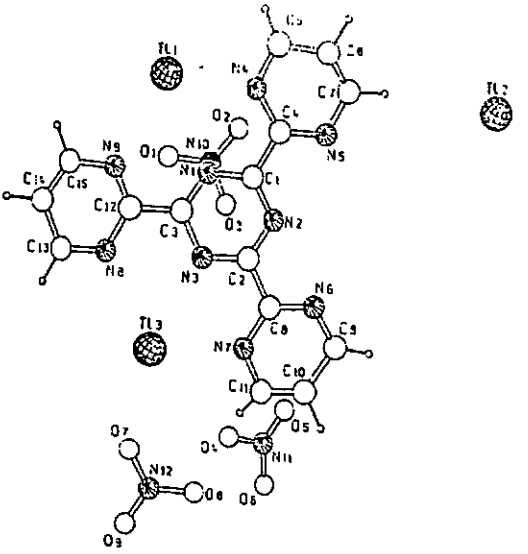

Fig. 46. SCHAKAL plot of tpymt·3$TlNO_3$·0.75H_2O (31)

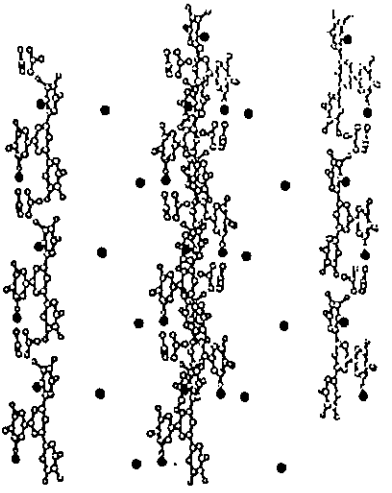

Fig. 46a. SCHAKAL plot of tpymt·3$TlNO_3$·0.75H_2O showing the packing in the crystal.

Tab.26. Important Tl-N distances (Å) of tpymt·3TlNO$_3$·0.75H$_2$O

Tl(1)^c-N(1)	2.934(19)	Tl(2)^d-N(8)	3.132(20)
Tl(1)^c-N(4)	2.946(22)	Tl(3)-N(2)	2.956(18)
Tl(1)^c-N(9)	3.011(21)	Tl(3)-N(5)	2.923(21)
Tl(2)^d-N(3)	3.111(19)	Tl(3)-N(6)	2.851(17)
Tl(2)^d-N(7)	3.063(20)		

Symmetry operations: ^{e} x, -1+y, z; ^{d} 1-x, 2-y, -z.

The aromatic ring system is not as planar as that found for the cadmium complex. A comparison of the dihedral angles of the pyrimidine rings relative to the central triazine ring is given in Table 37. The ligand molecules are stack along the crystallographic c axis.

Tab. 37. Overview of dihedral angles (Å) between the central triazine ring C and the pyrimidine rings of {Cd(tpymt)Cl$_2$(H$_2$O)}·3H$_2$O (**30**) and tpymt·3TlNO$_3$·0.75H$_2$O (**31**).

	{Cd(tpymt)Cl(H$_2$O)}·3H$_2$O (**30**)	tpymt·3TlNO$_3$·0.75H$_2$O (**31**)
A^B	0.41(9)	6.5(9)
A^C	1.04(8)	4.7(8)
A^D	1.16(9)	0.7(12)
B^C	0.69(9)	3.6(9)
B^D	1.39(10)	6.4(10)
C^D	2.08(10)	4.9(8)
C^C'	1.8(3)	

It was found, tpymt is not be able to form three covalent bonds in the terpyridine like sites of the ligand, since the system is not flexible enough to move the pyrimidine rings (nitrogen lone pair interaction).

4. Study of structural, magnetical and conductivity behaviour of coordination polymers containing the ligand pyrazine-2,3,5,6-(tetracarboxylic acid (H_4pztc)

4.1. Introduction

Pyrazine-2,3,5,6-tetracarboxylic acid and its Na^+, K^+, and Ba^{2+} salts as well as its Ag^+ complex have been known since 1893[16,17]. The potential of this bis(tridentate)ligand for the formation of coordination polymers was investigated by Marioni[2]. A series of transition metal salts were reacted with an equimolar amount of H_4pztc at different temperatures and in some cases in the presence of buffer solutions. With divalent metal salts of iron, cobalt and zinc quasi-linear polymers were obtained and the ligand coordinates in a bis(bidentate) manner. The non- coordinated carboxylic groups are rotated by approximately 85° to the plane of the pyrazine ring. In the crystal the linear neutral chains are bridged by hydrogen bonds to the water molecules of crystallization to form a two-dimensional sheet. The first structure of such a quasi-linear polymer from an aqueous solution, namely $[\{Fe(H_2pztc)(H_2O)_2\}\cdot 2H_2O]_x$, was published in 1986[99]. In all reactions neither the metal to ligand ratio nor the temperature had a significant effect on the resulting products, with the exception of Mn^{2+}.

The reaction of $MnSO_4$ in aqueous medium carried out at 50°C gave yellow crystals whose structure proved by X-ray diffraction to be a neutral zig-zag-polymer. It was found that the anion H_2pztc^{2-} coordinates to the manganese, which sits on a two-fold axis and is octa-coordinated. In the crystal the polymer chains run in mutually perpendicular directions, interlacing with one another. In the case of nickel and copper only insoluble precipitates were obtained, therefore no X-ray diffraction studies were possible. If the same reactions were carried out in the presence of a buffer-solution (CH_3CO_2K/CH_3CO_2H, pH~5) all four carboxylic groups were deprotonated and considerable differences were observed, see Fig.47. The ligand is now coordinated in a mono(tridentate)-bis(bidentate) manner. Only one pyrazine N atom is coordinated. At the opposite side of this ligand the carboxylate groups 3 and 5 are

---

[99]P.A. Marioni, H. Stoeckli-Evans, W. Marty, H.U. Güdel, A.F. Williams, *Helv. Chim. Acta*, 69 (1986) 1004.

rotated by almost 85° to the plane of the pyrazine ring. This column type structure is similar to that found for the zinc complex of the pyrazine 2,3-dicarboxylic acid[100].

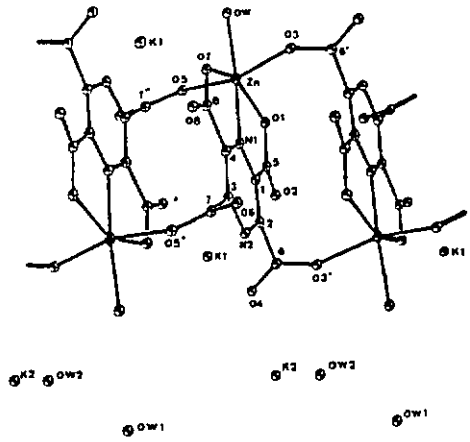

Fig. 47. Molecular structure of $[K_2\{Zn(pztc)(H_2O)\}\cdot 2H_2O)]$.

While carboxylic acid group on C(2) is coordinated to the metal, the adjacent group on C(3) is rotated by almost 85° to the pyrazine ring and coordinates to two symmetry related zinc atoms. This arrangement of two adjacent carboxylic groups which are almost perpendicular to one another on coordination could be exploited in the formatioo of new coordinatioo polymers.

The reaction of $CuCl_2$ with H_4pztc in CH_3CO_2K/CH_3CO_2H buffer solutioo yielded large green crystals which lost water of crystallization very rapidly. Later C. Whitaker reported this reaction not only with the K^+ buffer but also with Cs^+ and Rb^+ buffers. The products were isomorphous and their X-ray analyses revealed an interesting two dimensional polymer structure[101],[102]shown in Fig.48.

---

[100]P. Richard, D. Tran Qui, E.F. Bertaut, *Acta. Cryst.*, 30 (1974) 628.

[101]C. Whitaker, Research report, Université de Neuchâtel, 1990.

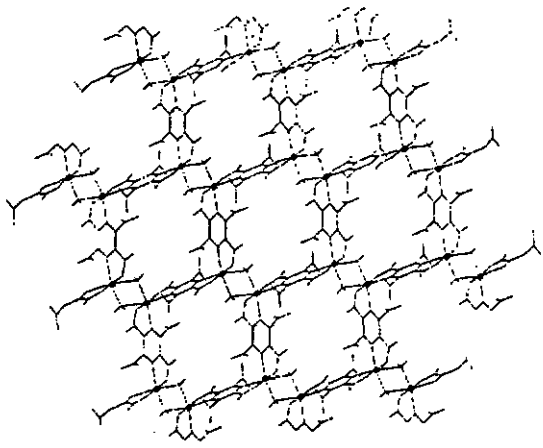

Fig.48. Plot of the two dimensional sheet of $[Cs_4\{Cu_2(pztc)_2(H_2O)_2\}\cdot 9H_2O]_x$, the water molecules of crystallisazion and the Cs atoms have been omitted for clearity.

The copper atom is coordinated differently to the two ligand molecules forming a zig-zag polymer chain, which dimerizes about a center of symmetry forming a two dimensional sheet. The sheets stack up the c- axis and the interlayer space is occupied by water molecules and alkali metal cations.

In 1989 Günther and Thewald[103] described reactions of $[M_2TiCl_2]$ (M=Ti, Zr) with K_4pztc. The reaction of $[Cp_2TiCl_2]$ with K_4pztc in the two phase system of $H_2O/CHCl_3$ giving the tetranuclear complex $[Cp_2Ti(pztc)TiCp_2]_2$, in which two of the titanium atoms are pentacoordinated whereas the other two are tetracoordinated. This compound was obtained as a hydrate (with 12 H_2O) or as a crystalline solvate (with $2H_2O\cdot 2CHCl_3\cdot 3CH_3NO_2$). The reaction of equimolar amounts of $[Cp_2TiCl_2]$ and $[Cp_2ZrCl_2]$ with H_4pztc gives the

---

[102]M. Graf, H. Stoeckli-Evans, C. Whitaker, *Chimia*, 47 (1993) 202.

[103]T. Günther, U. Thewald, *J. Organomet. Chem.*, 43 (1989) 371.

heterometallic complex $[Cp_2Ti(pztc)ZrCp_2]_2$ which crystallized also as a solvate. Jibril et al[104] obtained $[(1,3\text{-}^tBuC_5H_3)TiCl(O_2C\text{-}Pz)_2]$ from a reaction of $(1,3\text{-}^tBuC_5H_3TiCl_3)$ with pyrazine-2-carboxylic acid (molar ratio of 1:1). Surprisingly two molecules of the pyrazine-2-carboxylic acid are coordinated to the titanium atom. Postel and co-workers[105] studied some reactions with various pyridine and pyrazine mono and dicarboxylic acids, respectively, with Bi_2O_3 and characterized the products mainly by infrared methods. From a reaction of pyrazine-2,3-dicarboxylic acid with Bi_2O_3 results a white precipitate which was proposed as polymer $[Bi(O_2C)_2\text{-}pz(OH)]_\infty$. The band found at 470 cm^{-1} was assigned to the Bi-O(H)-Bi vibration and indicates the presence of Bi-O(H)-Bi bridges in the polymer network.

Sanyal and Garai[106] synthesized complexes of Co^{2+}, Ni^{2+}, Cu^{2+}, Fe^{2+}, Zn^{2+}, Cd^{2+}, and $Hg^{2+}$with pyrazine-2,3-dicarboxylic acid dihydrazide. The characterization was undertaken by elemental analysis, spectral and magnetic moment data. The copper and mercury complexes are chloride bridged dimers, the coordination is realized by a hetero-N-atom, along with a carboxyl-O in the former and an enolized hydrazide-O in the latter. The $[CuLCl]_2$ complex shows a subnormal value of $\mu_{eff.}$=0.84 BM which is perhaps due to antiferromagnetic interactions between two Cu^{2+} centers through chloride bridges.

---

[104]I. Jibril, S. Abu-Orabi, S.A. Klaib, W. Imhof, G. Huttner, *J.. Organomet. Chem.*, 433 (1992) 253.

[105]T. Zevaco, N. Guilhaume, M. Postel, *New. J. Chem.*, 15 (1991) 927.

[106]G.S. Sanyal, S. Garai, *Indian J. Chem.*, 30 (1991) 554.

4.2. Improvement of the synthesis of pyrazine-2,3,4,5-tetracarboxylic acid (32)

Marioni[2] synthesized the ligand according to the method of Chattaway and Humphrey[107]. The reaction pathway consists of two steps. The first is a condensation reaction of o-phenylendiamine with the disodium salt of the dihydroxytartric acid yielding the quinoxaline-2,3-dicarboxylic acid. The second step is the oxidation of the latter compound by means of $KMnO_4$ under basic conditions. In contrast to this time consuming synthesis it was our goal to find a more efficient way to isolate the acid in one reaction step in acceptable yields. We started according to the synthesis of Wolff[16], i.e. oxidation of 2,3,5,6-tetramethylpyrazine under basic conditions. In the literature no details of the reaction conditions were described. Preliminary experiments indicated that this special oxidation is a very sensitive reaction and occurs only under carefully defined conditions. The difficulties consist in the following: if the conditions are too mild incomplete oxidation of the methyl groups occurs; if the conditions are too drastic a partial decarboxylation can take place. After many attempts we improved and optimized the synthesis (for details see experimental part). The 2,3,4,5-tetramethylpyrazine is oxidized by a large excess of $KMnO_4$ at 90°C in an alkaline aqueous medium. The permanganate must be added slowly in small portions and the reaction temperature should not exceed 90°C. For the recrystallization of the free acid from hot water it is important that the temperature does not exceed 70°C because of the possibility of decarboxylation. The determined melting point of 196°C and the elemental analysis are indications for the purity of the obtained product. In the n.m.r. spectrum we can see that all the methyl groups were oxidized. The signal for the equivalent acid protons lies at 9.25 ppm in $CDCl_3$ as solvent. The infrared spectrum exhibits an intense characteristic band at 1746 cm^{-1} for the $\nu_{as}(COO)$ of the carboxylic group.

---

[107]F. D. Chattaway, W.G. Humphray, *J. Chem. Soc.* (1929) 645.

4.3. Synthesis of coordination polymers of Cu(II) and Mn(II) with H_4pztc by introduction of divalent cations

The following reactions were carried out in each case under the same reaction conditions. The metal salt was dissolved in water at 50°C under nitrogen. To this solution was added an equimolar amount of H_4pztc and the corresponding 2M magnesium or uranyl buffer solution to bringing the pH to 4.8-5.0. The solution was stirred and allowed to cool to room temperature (see experimental part). From a reaction of $MnCl_2$ with H_4pztc in the presence of a 2M Mg-acetate buffer we obtained a yellow powder which was insoluble in all common solvents.

$$MnCl_2 + H_4pztc \xrightarrow[(CH_3CO_2)_2Mg/CH_3CO_2H]{50\ ^\circ C,\ H_2O,\ N_2} [Mg(H_2O)_6\{Mn(pztc)(H_2O)_2\}\cdot 3H_2O]_x \qquad (33)$$

It was impossible to obtain crystals of this compound. The product was characterized by infrared spectra, elemental analysis and thermogravimetric measurements. Its infrared spectrum exhibits characteristic bands at 1656 cm^{-1} ν_{as}(COO) , 1605 cm^{-1} ν(C=N) and at 1320 cm^{-1} the ν_s (C=O). In the literature[108, 109, 110, 111] similar values are given for complexes of the pyrazine 2,3- or 2,5-dicarboxylic acid. A broad intensive band at 3407 cm^{-1} ν (OH) is present and we assume an associative water molecule. By means of elemental analysis we propose the composition $[Mg(H_2O)_6\{Mn(pztc)(H_2O)_2\}\cdot 3H_2O]_x$. Thermogravimetric measurements (DTG) show a peak at 51.3 °C, a loss of mass corresponding to 11 molecules of water is assumed.

---

[108] T. Zevaco, N. Guilhaume, M. Postel, *New. J. Chem.*, 15 (1991) 927.

[109] R.W. Matthews, R.A. Walton, *Inorg. Chem.*, 10 (1971) 1433.

[110] S.B. Brown, M.J.S., Dewar, *Inorg. Chim. Acta*, 34 (1979) 221.

[111] G.S. Sanyal, S. Garai, *Indian Jour. Chem.*, 30 (1991) 554.

From a reaction of $CuCl_2$ with H_4pztc in the presence of Mg-acetat buffer we obtained well formed green crystals which were suitable for X-ray diffraction studies.

$$CuCl_2 + H_4pztc \xrightarrow[(CH_3CO_2)_2Mg/CH_3CO_2H]{50\ ^\circ C,\ H_2O,\ N_2} [Mg(H_2O)_6\{Cu(pztc)(H_2O)_2\}.2H_2O]_n \qquad (34)$$

The characterization by infrared methods also gave the expected bands at 1645 cm^{-1} for $\nu as(COO)$ and 1307 cm^{-1} for $\nu s(C=O)$. A determination of the (C=N) vibration is impossible because of the overlapping of the broad absorption of the ν_{as} (COO) in the ν(C=N) region. The broad intense band at 3409 cm^{-1} ν(OH) indicates associative water molecules. Thermogravimetric measurements (DTG) indicate a loss of mass at 85°C which could be responsable for a loss of 10 molecules of water. The structure of this polymer is given in Fig.49 and Fig. 50. This quasi linear polymer structure is very similar to that found for the neutral Fe^{2+} polymer of Marioni[2]. The basic unit consists of a copper atom, located on a center of symmetry, coordinated to the pyrazine N-atom and an oxygen of one carboxylic group on either side of a square plane. The coordination of the copper atom is square planar with the Cu atom lying in the best plane through atoms N1, O1, N1' and O1', with atom OW1 and OW1' occupying positions ± 2.373(2)Å from the square plane. The non-coordinated carboxylic groups, involving O3 and O4, are inclined by -85.5(2)° to the best plane trough the pyrazine ring. The polymer chains run parallel to the b axis and are separated by the magnesium hexahydrate cations and the water molecules of crystallization, Fig. 50. The whole assembly is linked by an extensive hydrogen bonding network involving the water molecules of the cation $[Mg(H_2O)_6]^{2+}$ (OW1, OW2, OW3), the coordinated water molecules OW4, the water molecules of crystallization OW5, and the O-atoms of the coordinated and non-coordinated carboxylic groups, O2, O3, and O4. Selected bond lengths and bond angles are given in Tab. 38.

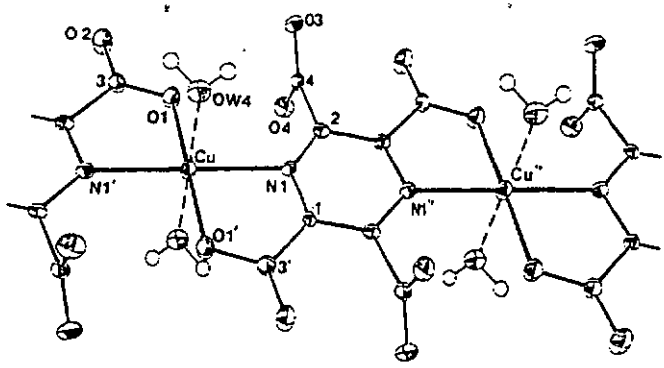

Fig. 49. ORTEP view of $[Mg(H_2O)_6\{Cu(pztc)\cdot 2H_2O\}\cdot 2H_2O]_x$ (34)

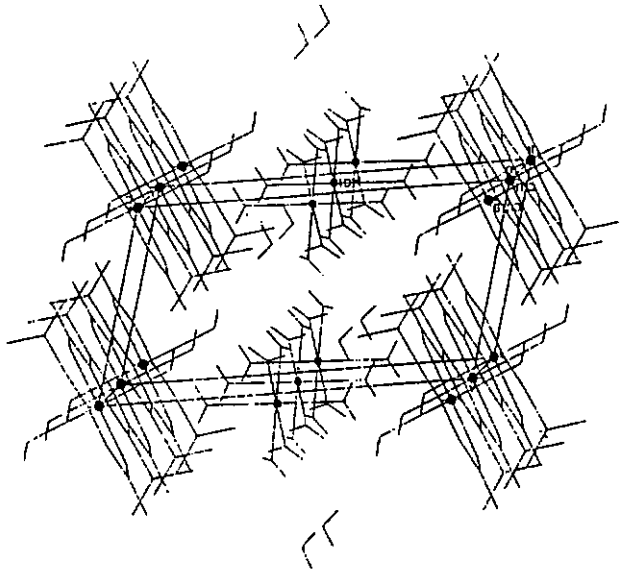

Fig. 50. PLUTO plot of the packing in $[Mg(H_2O)_6\{Cu(pztc)\cdot 2H_2O\}\cdot 2H_2O]_x$ (34)

● Cu-atoms, ■ Mg-atoms.

Tab.38. Important bond distances (Å) and bond angles (°) for $[Mg(H_2O)_6\{Cu(pztc)(H_2O)_2\}\cdot 2H_2O]_x$ (34)

Cu-O(1)	1.901(1)	O(1)-Cu-O(W4)	88.43(6)
Cu-N(1)	2.140(2)	N(1)-Cu-O(1')	81.39(6)
Cu-O(W4)	2.376(2)	N(1)-Cu-N(1')	180.00
O(1)-Cu-N(1)	98.61(6)	N(1)-Cu-O(W4)	92.59(6)
O(1)-Cu-O(1')	180.00		

A Cu-N(pyrazine) distance of 2.139(3)Å for $[Cs_4\{Cu_2(pztc)_2(H_2O)_2\}\cdot 9H_2O]_x$[100] polymer was observed. The same distance for the corresponding polymers containing $K^+$and Rb^+ are 2.127(2)Å and 2.123(2)Å, respectively and for the $[Mg(H_2O)_6\{Cu(pztc)\}(H_2O)_2\cdot 2\ H_2O]_x$ polymer a distance of 2.140(2)Å was observed. They are significantly longer than the standard average value of 2.024Å[112] or those values observed for the mono-and dinuclear copper complexes formed with tppz, were the same distances are 1.943(4) and 1.962(3)Å, respectively[113]. However a similar distance, 2.135(5)Å, was observed recently in a Cu^{2+} mononuclear complex of the new ligand 2,5-dimethylcarboxylate-3,6-dimethylpyrazine[114]. To introduce a further large cation we carried out the reaction of H_4pztc with $MnCl_2$ in the presence of uranyl-acetat buffer. After slow evaporation in air we obtained a yellow insoluble precipitate which was characterized by infrared spectra, elemental analysis and thermogravimetric measurements.

[112]A.G. Orpen, L. Brammer, F.H. Allen, O. Kennard, D.G. Watson, R. Taylor, *J. Chem. Soc., Dalton. Trans.*, (1989) 1.

[113]M. Graf, B. Greaves, H. Stoeckli-Evans, *Inorg. Chim. Acta*, 204 (1993) 239.

[114]Y. Wang, H. Stoeckli-Evans, to be published.

$$MnCl_2 + H_4pztc \xrightarrow[(CH_3CO_2)_2UO_2/CH_3CO_2H]{50\ ^\circ C,\ H_2O,\ N_2} [UO_2\{Mn(pztc)(H_2O)_2\}.15H_2O]_x \quad (35)$$

The infrared spectrum shows the typical pattern for the coordinated ligand. We found bands ν_{as} (CO) at 1666 cm^{-1} the ν(C=N) at 1635 cm^{-1} and the νs(C=O) at 1322 cm^{-1}. The broad band at 3333cm^{-1} ν(OH) indicates associative water molecules. The characteristic vibration for the ν(U=O) is described in the literature[115] at 933 cm^{-1} and we found this band at 931 cm^{-1} with a strong intensity. Thermogravimetric measurements (OTG) show a loss of mass at 50.2 °C which could be responsable for a loss of 17 molecules of water which is in agreement with the elemental analysis. Therefore we propose the following composition $[UO_2\{Mn(pztc)\}(H_2O)_2\}\cdot 15\ H_2O]_x$.

The reaction of H_4pztc with $CuCl_2$ and UO_2-acetat buffer results in a green precipitate which is also insoluble and similar to the previously described compounds.

$$CuCl_2 + H_4pztc \xrightarrow[(CH_3CO_2)_2UO_2/CH_3CO_2H]{50\ ^\circ C,\ H_2O,\ N_2} [UO_2\{Cu(pztc)(H_2O)_2\}.14H_2O]_x \quad (36)$$

The infrared spectrum exhibits the characteristic bands at 1684 cm^{-1} ν_{as} (COO), 1651 cm^{-1}, ν (C=N) and 1314 cm^{-1} ν_s(C=O). The strong band for the ν(U=O) is present at 931 cm^{-1}. The broad intensive band at 3348 cm^{-1} ν(OH) is assigned to associative water molecules. Thermogravimetric measurements (DTG) show a peak at 56.8°C which could be responsable for a loss of 16 molecules of water. The elemental analysis is in agreement with this result. No crystals were obtained from a reaction in a UO_2-buffer medium. The pH of this reaction mixtures was lower than 4.8-5.0, probably by reason of protolysis equilibriums ($UO_2^{2+} + H_2O \rightarrow UO_2(OH)^+ + H^+$). This fact could cause the relatively quick precipitation.

---

[115] M. Hesse, H. Meier, B. Zeeh "Spektroskopische Methoden in der Chemie", Georg Thieme Verlag Stuttgart, (1991).

Reaction attempts with Ca^{2+}, Sr^{2+} and Ba^{2+} with H_4pztc in the presence of Cu^{2+} resulted in white insoluble powders of H_4pztc containing no Cu^{2+} cations.

4.4. Electrical conductivity measurements of some polymers of H_4pztc

The following investigated polymers crystallize in a defined arrangement[4] and they have anisotropic character. To obtain conclusions between structural and conducting properties single crystal resistivity measurements are the most precise analytical methods. The crystal must be stable, well formed, and large enough for these investigations. The polymers of H_4pztc do not satisfy this condition. They loose water very quickly and therefore a structural change results. For this reason we dried the polymers over P_4O_{10} to avoid complicating effects due to the presence of water during the conductivity measurements. The presence of water was controlled by thermogravimetric measurements. A partial tempering of the compounds was necessarily. To have a good sample to handle we pressed discs (KBr power press for infrared) of all the polymers under a defined pressure of 125 bar. After this the discs were connected by tin-wire onto silver-painted electrodes. A scheme of the temperature dependence measurements is given in Fig. 51.

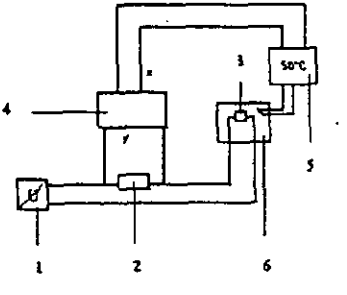

Fig. 51. Scheme of the temperature dependence measurements:
1 voltage supply; 2 resistor (10KΩ); 3 sample; 4 xy-recorder(x=T, y=U_R);
5 thermostat, 6 temperature controlled heater

Tab. 39. The room temperature measured specific resistivities for the polymers: $[K_4\{Cu_2(pztc)_2(H_2O)_2\}\cdot 9H_2O]_x$ (KCu); $[Rb_4\{Cu_2(pztc)_2(H_2O)_2\}\cdot 9H_2O]_x$ (RbCu), measured after tempering; $[Cs_4\{Cu_2(pztc)_2(H_2O)_2\}\cdot 9H_2O]_x$ (CsCu); $[Mg(H_2O)_6\{Cu(pztc)(H_2O)_2\}\cdot 2H_2O]_x$ (MgCu), measured after tempering. All samples were dried over P_4O_{10}. $\rho = R\cdot A/l$ in Ωcm with ρ = electrical resistivity, R= resistance; A= surface of the conductor; l= thickness of the conductor

polymer	U in V	I in A	A in cm	l in cm	R in Ω	ρ in $\Omega\cdot$cm
KCu	300	0.1	0.12	0.01	$3000\cdot 10^6$	$3.6\cdot 10^{10}$
RbCu	30	3.5	0.78	0.026	$300\cdot 10^6$	$9.00\cdot 10^9$
CsCu	30	0.12	0.78	0.035	$250\cdot 10^6$	$5.36\cdot 10^9$
MgCu	30	1.7	0.2	0.009	$300\cdot 10^6$	$6.66\cdot 10^9$

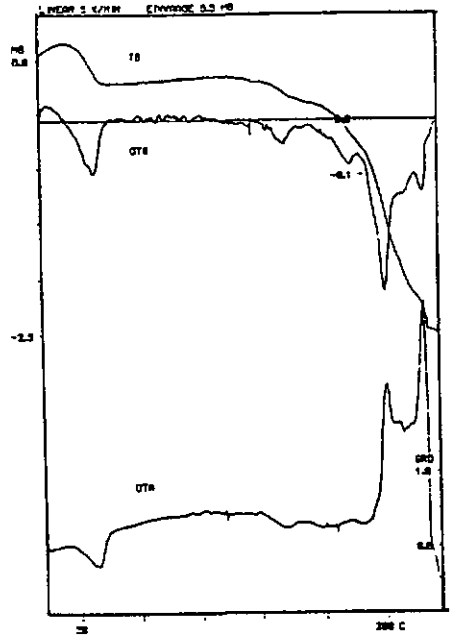

Fig. 52a Thermogram of the RbCu-polymer

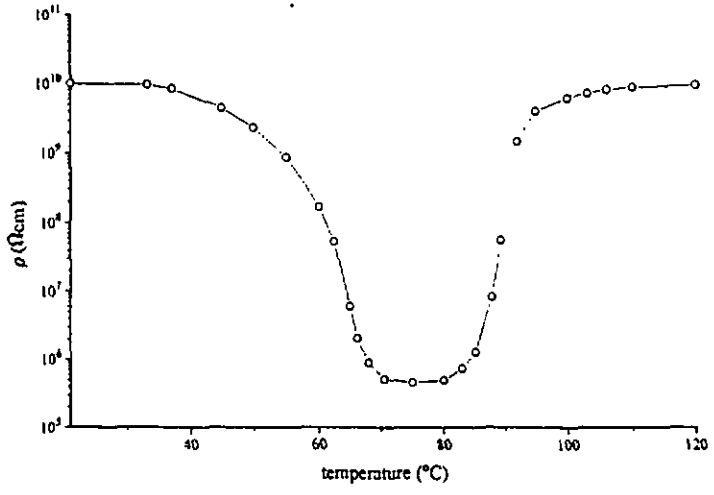

Fig.52b. Tempering curve of tbe RbCu-polymer in the temperature range from 20 to 200°C.

The RbCu-polymer contained, after drying over P_4O_{10}, about four to five molecules of water (DTG shows a loss of mass of 5.6% between 42 and 79°C, Fig. 52a). The resistivity reaches a value of $2.57 \cdot 10^8$ Ω cm. The tempering curve of this compound was recorded. An enormous increase of the conductivity with increasing temperature was observed. This effect could be due to the presence of water molecules, see Fig. 52b. The constant resistance after tempering ($300 \cdot 10^6$ Ω) is comparable with the resistivities of the MgCu-polymer in a temperature range from 21 to 200°C.. The resistivity of the CsCu-polymer is a little bit smaller and for the KCu-polymer ten times higher, see Tab.39.

Brown et al.[116] prepared transition metal complexes and coordination polymers of the pyrazine-2,5-dicarboxylic acid. They obtained an anhydrous Cu^{2+} polymer as well as hygroscopic Ni^{2+} and Co^{2+} polymers. Electrical conductivity measurements were undertaken. The global values for all the polymers was $> 10^{12}\Omega$; whether the material was hydrated or not

[116]B. Brown, M.J.S. Dewar, *Inorg. Chim. Acta*, 34 (1979) 221.

is not stated. The effect of the presence of water was also discussed and found to be very complicated for these measurements. We have determined the resistivity under defined conditions and found that the Cu^{2+}-polymers of H_4pztc have a resistance of nearly $10^6\Omega$. The voltage dependence of the samples in a range from 0 to 30V indicates a linear curve like an ohmic resistor. The spezific resistivities of nylon or phenoplastics are in the same range as found for these semiconducting polymers.

5. Summary

One object of the present work was the investigation of the coordination behaviour of the ligand tppz towards transition metal salts of Co^{2+}, Ni^{2+}, Cu^{2+} and Zn^{2+}. Bock and co-workers[21] investigated the monoclinic form (tppz-II) by means of X-ray structure analysis. During the present work the monoclinic form of the free ligand, recrystallized from CH_2Cl_2, was obtained with identical results. From an equimolar reaction of tppz with $ZnCl_2$ in $EtOH/H_2O$ the complex $[Zn(tppz)Cl_2]$ and a new tetragonal form of the free ligand (tppz-I) was isolated. ^{15}N n.m.r. investigations show a temperature dependent behaviour for tppz. A movemeot of the pyridine rings is assumed at elevated temperatures. Therefore, there were indications that the ligand could be flexible but it depends on the solvent used and the temperature. For further characterization the question of the different hydrochlorides was of interest. Bock and co-workers[21] obtained, in a reaction of tppz in 1M HCL, a two-fold hydrochloride after recrystallization from CH_3CN. Contrarily we obtained a four-fold hydrochloride $tppz{\cdot}4HCl{\cdot}2H_2O$ (1)[40] from a reaction with 2M HCl. Interestingly in this centrosymmetric molecule two chloride ions are situated near the protonated nitrogens of the pyridine rings and two are situated far away, probably because of crystal packing reasons. Goodwin and Lions[18] investigated for the first time the coordination behaviour of tppz in 1959. By means of elemental analysis results of the complexes obtained they assumed only a mono(tridentate) coordination. In this context they noted that the pyrazine nucleus was unable to have both its nitrogen atoms acting simultaneously as docors. Since a number of complexes containing tppz have been prepared but oo structural proof for a bis(tridentate) coordination behaviour, or a bridging coordination mode together with further ligands, was obtained. Therefore we carried out reactions of tppz with an excess of metal salts in ethanol/water mixtures at 90°C to obtain crystals suitable for X-ray diffraction studies, whicb could be important for the discussion of the resulting physical properties.

We could isolate the complex $[Ni_2(tppz)(H_2O)_6](NO_3)_4{\cdot}3H_2O$ (4) with tppz in a bis(tridentate) coordination mode[48]. The central pyrazine ring in this molecule is twisted. The dihedral angle between plane C'[C(1), N(1), C(4)] and C"[C(2), N(2), C(3)] is C'^C" = 10.9°.

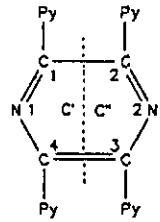

Three molecules of water are coordinated around each nickel atom to give an octahedral coordination sphere; the nitrates act as counterions. The Ni(1)...Ni(2) separation in this molecule is 6.6446(18) Å. From the reaction of 4 with the complex $[Mn(H_2O)_4(sqacH)_2]$ a hydrogen bonded three-dimensional polymeric network was obtained. The manganese complex decomposed in solution and a counterion exchange occured to form the complex $[Ni_2(tppz)(H_2O)_6](sqac)_2{\cdot}2.5H_2O$ (9)[48]. We found a very compact hydrogen bonded network of oxygen atoms from the squaric acid molecule to the protons of the coordinated water molecules around the nickel atoms. Additionally, the water molecules of crystallization are also hydrogen bonded to each other and to the squaric acid oxygen molecules. The central pyrazine ring in the complex also has a twisted conformation, the dihedral angle C'^C" is 10.7(3)°. The intramolecular Ni...Ni separation is 7.488(19)Å and the distance to other nickel atoms in the crystal is in the range from 6.63 to 8.46Å. The pseudohalides thiocyanate and dicyanamide could also coordinate in nickel complexes. $[Ni_2(tppz)(SCN)_4(H_2O)_2]$ (6) and $[Ni_2(tppz)(N(CN)_2)_2(H_2O)_4](NO_3)_2$ (7) were characterized by means of elemental analysis, infrared and electronic absorption spectra. A new coordination mode was found for the complex $[Ni(tppz)_2](C(CN)_3)_2$ (8). The large anion tricyanmethanide forces a decomposition of the binuclear complex to build a geometry like $[M(tppz)_2]^{2+}$. Here two ligand molecules are coordinated around the Ni atom.

From reactions of tppz with $Cu(ClO_4)_2{\cdot}6H_2O$ and $CuCl_2{\cdot}2H_2O$ we also obtained binuclear complexes. The coordination sphere of the copper atoms in the complexes $[Cu_2(tppz)(H_2O)_4](ClO_4)_4{\cdot}2H_2O$ (10)[62] and $[Cu_2(tppz)Cl_4]{\cdot}5H_2O$ (12)[73] is in each case a distorted square pyramid. The central pyrazine ring in **10** is planar and in **12** distorted by 10.18(24)°. Magnetic investigations show a very strong antiferromagnetic behaviour. The

value 2J was determined to be -61.1 cm^{-1} for 10 and -34.2 cm^{-1} for 12. These are high values which were found for the first time for pyrazine ligands. It is proposed that the superexchange mechanism is propagated through the σ-system of the ligand.

From a reaction of tppz with $Cu(ClO_4)\cdot 6H_2O$, in the presence of hydrochloric acid the chloride bridged complex $[Cu(tppzH)Cl]_2(ClO_4)_4$ (11) was obtained[62]. In this complex very short Cu(1)...Cu(1^a) and Cu(1)...Cu(1^b) distances of 3.446(3) and 3.854(4)Å were observed. Magnetic investigations indicate a ferromagnetic behaviour. Cyclovoltammetric measurements show a stepwise reduction from Cu^{2+}-Cu^{2+} to a Cu^{2+}-Cu^{+} and lastly to a Cu^{+}-Cu^{+} species. For the oxidation we found only one wave which is less pronounced than the other waves.

From reactions of $[Cu_2(tppz)(H_2O)_4](ClO_4)_4\cdot 2H_2O$ with bridging ligands like oxalate and pyrazine 2.3.5.6-tetracarboxylic acid we assume polymer structures $[\{Cu_2(tppz)(ox)(H_2O)_2\}(ClO_4)_2]_x$ (13) and $[\{Cu_2(tppz)(H_2pztc)(H_2O)_2\}(ClO_4)_2]_x$ (15). The e.p.r. measurements of 13 indicate an axial spectrum with Cu-Cu interactions in the solid state. In the electronic reflectance spectra we found one band at 14671 cm^{-1} and a d→d transition $^2E_g \rightarrow {}^2T_{2g}$ is assumed for an octahedral coordination sphere. The same transition was observed for 15 at 13935 cm^{-1}.

We found, that the chemistry concerning the zinc complexes is very productive. A lot of coordination possibilities were observed. From reactions with $ZnCl_2$ and $Zn(NO_3)_2\cdot 6H_2O$ we obtained binuclear complexes. The coordination spbere around the zinc atoms in the complex $[Zn_2(tppz)Cl_2]$ (17) can be described as a strongly distorted square pyramid. The central pyrazine ring is twisted by an angle of C'^C" of 12.0(5)° and this is greater than found for 12 and smaller than found for 4. In the complex $[Zn_2(tppz)(H_2O)_6](NO_3)_4\cdot 1.5H_2O$ (19) we found a dihedral angle of C'^C" of 12.4(5)° [84]. In this complex three molecules of water are coordinated around the zinc atom in an octahedral coordination sphere, the nitrates act as counterions. From a reactioo of 19 with KSCN a new mononuclear compound was obtained. It is nearly insoluble in all commoo solvents and we assume a polymer structure $[\{Zn(tppz)(SCN)\}]_x$ (20). The infrared spectra shows a significant shift of the characteristic bands to higher wave numbers indicating a bridging mode for the thiocyanate. By an equimolar reaction of 19 with dicyanamide the complex looses one zinc atom. The X-ray structure

determination yielded the composition $[Zn(tppz)(N(CN)_2)(NO_3)(H_2O)]$ (**21**)[84]. The protons of the coordinated water molecule in the monomer unit are hydrogen bonded to a symmetry related molecule so forming a linear polymer chain structure. From a reaction with the molar ratio of 1:2 we found the composition $[Zn(tppz)_2](N(CN)_2)_2 \cdot H_2O$ (**22**)[86]. The coordination mode of the zinc atom in the centrosymmetric structure is octahedral. We found also that in this case the central pyrazine rings are distorted by 9.52 and 9.07° The same structure type was observed for the compound $[Zn(tppz)_2](C(CN)_3)_2$ (**23**), obtained from a reaction of **19** with the pseudohalide tricyanmethanide[86]. The dihedral angles in this case are 7.65 and 7.60°. Concerning the coordination behaviour of Zn^{2+} ions with tppz we investigated the reaction of $[Zn(tppz)(H_2O)_3](ClO_4)_2$ with a large excess of $ZnCl_2$ in an ethanol/water mixture by heating for several times. The X-ray crystal structure analysis indicates an interesting centrosymmetric macrocycle[83] (**18**). Two highly twisted binuclear zinc complexes are bridged by three Cl-Zn-Cl bridges. The macrocycle is neutral possessing 10 Zn atoms and 20 Cl atoms. There are two coordinated water molecules in the macrocycle, one to Zn(1) and the other to a bridging Zn(3) atom. Within the macrocycle there are two hydrogen bonds involving water OW(1) and atoms Cl(2) and Cl(3A). A third hydrogen bond links the macrocycle and involves water OW(2) and atom Cl(5) of a symmetry related molecule which forms a three-dimensional network. Furthermore, the mononuclear complexes $[Co(tppz)Cl]Cl \cdot 2H_2O$ (**2**), $[Co(tppz)(ma)(H_2O)] \cdot 4H_2O$ (**3**), $[Ni(tppz)(ox)(H_2O)] \cdot 5H_2O$ (**5**) and $[Zn(tppz)Cl_2]$ (**16**) were prepared and investigated by means of X-ray crystal structure analysis.

To summarize, we found that the ligand tppz is flexible enough to coordinate two metals in a bis(tridentate) coordination mode, depending on the temperature and the solvents used. The conclusions of Goodwin and Lions that the pyrazine nucleus was unable to have both its nitrogen atoms acting simultaneously as donors, is herewith refuted. Nevertheless tppz is a sterically hindered ligand and we found that the central pyrazine ring was distorted in several complexes. Distortion angles in the range from 8 to 13° were observed, an overview is given in Table 40. Only the centrosymmetric compound **10** has a planar pyrazine ring. The ligand is able to form coordination polymers and hydrogen bonded polymer networks after introducing further bridging ligands. The tppz alone does not form polymers with metal salts.

Tab. 40. Overview of the distortion angles(°) between plane C'^C"of the central pyrazine ring in various complexes containing tppz

bis(tridentate) complexes	C'^C"	mono(tridentate) complexes	C'^C"
$[Ni_2(tppz)(H_2O)_6](NO_3)_4 \cdot 3H_2O$ (4)	10.9(4)	$[Co(tppz)(ma)(H_2O)] \cdot 4H_2O$ (3)	9.4(6)
$[Ni_2(tppz)(H_2O)_6](sqac)_2 \cdot 2.5H_2O$ (9)	10.7(3)	$[Ni(tppz)(ox)(H_2O)] \cdot 5H_2O$ (5)	9.0(4)
$[Cu_2(tppz)(H_2O)_4](ClO_4)_4 \cdot 2H_2O$ (10)	0	$[Cu(tppzH)Cl]_2(ClO_4)_4$ (11)	8.0(2)
$[Cu_2(tppz)Cl_4] \cdot 5H_2O$ (12)	10.18(24)	$[Zn(tppz)Cl_2]$ (16)	10.6(2)
$[Zn_2(tppz)Cl_4]$ (17)	12.0(5)	$[Zn(tppz)(N(CN)_2)(NO_3)(H_2O)]$ (21)	12.2
$[Zn_2(tppz)(H_2O)_6](NO_3)_4 \cdot 1.5H_2O$ (19)	12.4(5)	$[Zn(tppz)_2](N(CN)_2)_2$ (22)	9.52, 9.07
$[Zn_{10}(tppz)_2Cl_{20}(H_2O)_4]$(18)	11.6(3)	$[Zn(tppz)_2](C(CN)_3)_2$ (23)	7.65, 7.60

Another object of this work was the investigation of the coordination behaviour of the ligand tpymt which could offer the possibility to coordinate three metals in a tris(tridentate) fashion. Unfortunately, several copper and cobalt salts induced hydrolysis reactions of this ligand. From a reaction of tpymt with $NiSO_4 \cdot 6H_2O$ we obtained the binuclear complex $[Ni_2(tpymt)(SO_4)_2] \cdot H_2O$ (27) which gave a characteristic infrared spectra for the coordinated ligand. Reactions with Fe^{3+} and Zn^{2+} salts yielded only mononuclear complexes. The crystallization behaviour of compounds containing this ligand is very poor. Many attempts under different conditions gave no suitable crystals for X-ray crystal studies. Furthermore, we investigated reactions of tpymt with metal salts containing elements which can form longer metal-nitrogen bonds. With silver(I) salts we obtained products by using of metal to ligand

ratios of 2:1. For the first time we could determine the structure of a complex containing tpymt. In $[Cd(tpymt)Cl_2(H_2O)]\cdot 3H_2O$ (30) tpymt is mono(tridentate) and the coordination sphere around the cadmium atom can be described as a distorted octahedron. The two Cd-N(pyrimidine) distances are very different, the Cd-N(6) bond length is 0.92Å longer than distance Cd-N(4) of 2.393(21)Å. This could be an indication, that the ligand system is not flexible enough to distort the pyrimidine rings relative to the central planar triazine ring. Lerner and Lippard[91] prepared by reaction of tpymt with $TlNO_3$ (molar ratio 1:3) a compound with the composition $[Tl_7(tpymt)_2(NO_3)_7]$. They characterized this product by means of elemental analysis. We reproduced this reaction and isolated yellow needles suitable for X-ray diffraction. We found a thallium complex with the composition $tpymt\cdot 3TlNO_3\cdot 0.75H_2O$. The thallium atoms are situated in the terpyridine like site, however the distances to the donor nitrogens are too long (2.85-2.95Å) to assume coordinative bonds.

The ligand tpymt can coordinate at most two metal ions. The crystallization behaviour of compounds containing this ligand is very poor. The aim to obtain three-dimensional networks could not be realized with this ligand.

The coordination behaviour of the third ligand H_4pztc towards divalent cations was investigated by Marioni[2] for the first time. From a reaction of H_4pztc with $CuCl_2$ in a $(CH_3COO)_2Mg/CH_3COOH$ buffer medium the quasi linear coordination polymer $[Mg(H_2O)_6\{Cu(pztc)(H_2O)_2\}\cdot 2H_2O]_x$ (34) was obtained[102]. The basic unit consists of a copper atom located on a center of symmetry which is coordinated to the pyrazine N-atom and an oxygen of one carboxylic group on either side of a square plane. The non-coordinated carboxylate groups are inclined by 85.5(2)° to the best plane through the pyrazine ring. The polymer chains run parallel to the b axis and are separated by the magnesium hexahydrate cations and the water molecules of crystallization. In the same buffer medium we carried out a reaction of H_4pztc with $MnCl_2$ and obtained the polymer $[Mg(H_2O)_6\{Mn(pztc)(H_2O)_2\}\cdot 3H_2O]_x$ (33). Furthermore, we made attempts to introduce the divalent cation UO_2^{2+} in the buffer system to obtain new ordered polymer systems. We could isolate compounds like $[UO_2\{Cu(pztc)(H_2O)_2\}\cdot 14H_2O]_x$ (36) and $[UO_2\{Mn(pztc)(H_2O)_2\}\cdot 15H_2O]_x$ (35). With the polymers

$[M^{I}_4\{Cu_2(pztc)_2(H_2O)_2\}\cdot 9H_2O]_x$ (M = K, Rb, Cs)[102] , and with 34, for the first time solid state conductivity investigations were made. All these polymers loose water very quickly and a structural change occurs. This fact has a strong influence on the conductivity and therefore it was necessary to dry rigorously to have defined conditions. The pressed discs were connected by tin-wire onto silver painted electrodes. The determined resistances of the copper polymers are about $10^6\Omega$. We can infer that the polymers of H_4pztc have better conducting properties than found for the polymers of the 2.5-dicarboxylic acid by Brown[116].

6. Conclusion

The main work was carry out with the ligand tppz. Only a few structural informations of compounds containing this ligand were known. For the first time we found that the ligand tppz is flexible enough to coordinate two metals in a bis(tridentate) coordination mode. Structural proofs for some binuclear nickel, copper and zinc complexes were given. We found that tppz is a sterically hindered ligand, in several complexes the central pyrazine ring is distorted. Generally we observed the tendence that the twist angles (C^C') of the bis(tridentate) complexes are greater than the same in mono(tridentate) complexes with the exeption of compounds **10**, **16** and **21**. In all the crystallographically investigated copper and nickel complexes the metal- nitrogen (pyrazine) distance are shorter than the metal- nitrogen (pyridine) distances. For the zinc complexes we observed no such tendance. In compound **16**, **19**, **21**, **22** and **23** the Zn-N(pyrazine) bondlength is shorter than the Zn-N(pyridine) bondlength wehreas in the complexes **17** and **18** it is the reverse. We observed that the dihedral angle of the coordinated pyridine rings relative to the central pyrazine ring is smaller than the same angle of the uncoordinated pyridine rings in all of the mononuclear complexes. Because of ring tention a opening of the back chelate takes place. In the dinuclear complexes the tension is reflected in the high ring distorsion with exception of compound **10**. To obtain coordination polymers it is neccessary to introduce further flexible bridging ligands which are able to coordinate to bis(tridentate) complexes.

It would be useful to test the following bridging ligands, because of their ability to act as bridging ligand with the complex units $[Ni_2(tppz)(H_2O)_6]^{4+}$, $[Cu_2(tppz)(H_2O)_4]^{4+}$ and $[Zn_2(tppz)(H_2O)_6]^{4+}$ to form eventually coordination polymers: N_3^-, OCN^-, croconic acid, 2,5-dichlor-3,6-dihydroxy-1,4-benzochinone. The resulting magnetic and electric properties of these compounds could be of interest to complete the informations of this substance class.

We worked again with the ligand H_4pztc and could introduce divalent cations like Mg^{2+} and UO_2^{2+} together with manganese and copper as second metal. With various polymers containing copper conductivity measurements were undertaken. All newly synthesized polymers lose water during heating or standing in air. A structural change in this compounds is

assumed and these fact has a strong influence on the properties. The determination of the resistances, under defined conditions, show resistivities of about $10^6\Omega$, one can discuss it as a semiconducting material.

The ligand tpymt which was furthermore investigated can coordinate at most two metal ions. The aim to obtain three dimensional networks could not be realized with this ligand. The fixed tris(tridentate) sides are too inflexible, because of this reason a ligand such 2.4.6-tris(4-pyridyl)-1.3.5-triazine leads to more interesting results. Furthermore it would be interesting to obtain mixed valence complexes with this ligand to investigate the resulting photochemical and magnetic properties.

7. Experimental

7.1. Starting materials

ammonia (> 99.8%, Fulka)

ammonium acetate (> 99, Fluka)

ammonium thiocyanate (> 99%, Fluka)

2-chlor-pyrimidine (> 97%, Fluka)

potassium dicyanamide /54, 55/

hydrochloric acid (~ 99.8%, Fluka)

acetic acid (> 99.5%, Fluka)

potassium cyanide (> 99%, Fluka)

potassium hydroxide (> 87%, Fluka)

potassium permanganate (> 99%, Fluka)

magnesium acetate tetrahydrate (> 99.5%, Fluka)

malonic acid disodium salt (> 99%, Fluka)

metal salts (Fluka)

sodium oxalate (> 99,5%, Fluka)

perchloric acid (20%, Fluka)

pyridine (> 99%, Fluka)

α-pyridoine (~ 99%, Aldrich)

2,3,5,6-tetramethyl-pyrazine (> 98%, Fluka)

potassium tricyan methanide /57/

trimethylamine (> 98%, ampulle, Fluka)

uranylacetate dihydrate (> 99%, Fluka)

7.2. Analytical methods

7.2.1. Infrared spectroscopy

IR spectra were recorded on a Perkin-Elmer FT-IR 1720 X spectrometer using KBr pellets. The absorption bands were determined in wave numbers (cm^{-1}). The abbreviation for the described intensities are : vs = very strong, s = strong, m = medium, w = weak, sh = shoulder.

7.2.2. Nuclear magnetic resonance spectroscopy

The n.m.r. spectra were recorded on a Bruker WP-200 or a Bruker AMX-400. The shift at the scale is declared in ppm. The abbreviation for the multiplicities are: s = singlet, d = doublet, t = triplet, m = multiplet, b = broad. The deuterated solvents were commercially available from ICN (99.8%).

7.2.3. Ultraviolet (u.v.) visibel (v.i.s.) spectroscopy

U.v.-vis spectra were recorded on a UVIKON 810/820; detector: Photomultiplier R 446 (standard). Quarz dust-plates (1 cm) were used for all measurements in solution. Electronic absorption spectra were recorded on a Perkin Elmer, LAMBDA 19.

5.2.4. Thermogravimetric measurements

TG measurements were carried out on a Mettler TA-3000 with processor TC 10, a TG 50 relay and a microbalance Mettler M 3. About 10 mg were used for each sample.

7.2.5. E.p.r.-measurements

The spectra were recorded on a e.p.r.-spectrometer Varian E 9 and a Brucker ESP 300 E spectrophotometer in a 300-4 k range.

7.2.6. Mass spectroscopy

The spectra were recorded on a Hitachi Perkin Elmer RMU 6 , Nermag R 30-10.

7.2.7. Magnetic measurements

The magnetic measurements were carried out with a pendulum type magnetometer (MANICS DSM 8) equipped with a helium continous-flow cryostat, working in the temperature range from 300 to 4 K with a Bruker BE15 electromagnet. The magnetic field was approximately 15000 G. Calibration of the instrument was made by magnetization measurement of a standard strontium ferrite. Diamagnetic corrections were estimated from Pascal's tables.

7.2.8. Cyclovoltammetric measurements

The voltammetry equipment, controlled by a personal computer, consists of a potentiostat connected with a programmable digital analog converter (12 Bit x 2kByte) used as a function generator and a fast transient recorder for data storage. The timing of each experiment was precisely controlled by a programmable counter timer circuit. The working electrodes were platinum microelectrodes with diameters of 50µm and 60µm (Leye Kunze GmbH, Leipzig). The surface were careful polished. A Ag/0.01 $AgNO_3$ reference electrode was used, the determined halve-wave potential for ferrocene was $E_{1/2(ferrocene)}$ = 0.91 V/s. The background electrolyte was a 0.1 M solution of TBAP in acetonitrile.

7.2.9. X-ray structure analysis

Intensity data were collected at room temperature on a "Stoe AED" 4-circle diffractometer using MoKα graphite monochromated radiation. A numerical absorption correction were applied using SHELX-76[117]. The structures were solved by direct methods or Patterson and difference Fourier syntheses using the SHELXS[118] or the NRCVAX[119] system.

---

[117]G. M. Sheldrick, SHELX-76, Program for Crystal Structure Determination, University of Cambridge, UK, (1976).

[118]Sheldrick, SHELXL-93, Program for the Refinement of Crystal Structures, University of Göttingen, Germany (1993).

[119]E. J. Gabe, Y. Le Page, J. P. Charland, F. L. Lee, NRCVAX- an Interactive Program System for structure Analysis, J. Appl. Crystallogr. 22. (1989) 384.

The refinement was carried out usy NRCVAX[119] or SHELXL-93[120]. Neutral complex-atom scattering factors in NRCVAX are from international tables for X-ray crystallography[121].The majority of the H-atoms were located from difference maps, the rest was included in calculated positions. They were either refined isotropically or held fixed, while the nonhydrogen atoms were refined anisotropically, using weighted fullmatrix least-squares. Crystal data, details of data collection and structure refinement for the different compounds are given in chapter 8.. The atomic numbering schemes used are illustrated in ORTEP-II[122], PLUTO[123] or SCHAKAL[124] plots.

7.2.10. Electrical conductivity measurements

The schematic equipment is described in chapter 4.5.

7.2.11. Elemental analysis

Elemental analyses were determined in the laboratory of the ETH-Zürich and the laboratory for microanalysis of Ciba Geigy in Basel as well as in the laboratories of the department of chemistry and pharmacy and the university of Halle/Wittenberg.

---

[120]SHELDRICK, SHELX-86, Program for solving crystal structures, Uni versity Göttingen (1986).

[121]Kynoch, International Tables for X-ray Crystallography, Vol.IV, Birmingham, UK, (1974).

[122]C. K. Johnson, ORTEP-II, Report 5138, OaK Ridge National Laboratory, Oak Ridge, Tenessee, USA (1976).

[123]W. D. Motherwell and W. Cleg, PLUTO, Program for Plotting Molecular and Crystal Structures, University of Cambridge, UK, (1978).

[124]E. Keller, Schakal-88, a Fortran Program for the Graphical Representation of Crystallographic Models, University of Freiburg, Germany, (1988).

7.3. Syntheses of the new compounds containing tppz

7.3.1. Synthesis of tppz

This compound was prepared by the method of Goodwin and Lions, analytical data are published in[15].

7.3.2. Synthesis of tppz·4 HCl·2H_2O (1)

Tppz (100 mg, 0.26 mmol) was dissolved in 20 ml of conc. HCl and stirred at room temperature for 30 min. The solution was evaporated under reduced pressure and the residue recrystallized from water.

Anal.calcd.: C 50.52, H 4.20, N 14.73; found: C 50.03, H 3.99, N 14.88.

IR (KBr, cm^{-1}); ν(C=C), ν(C=N): 1612 vs; 1543 s; 1461 s; 1428 s; 1379 vs.

UV (H_2O, nm): λ_{1max}=297; λ_{2max}=320; ε_1=6168; ε_1=6168.

^{1}H-n.m.r (D_2O, DSS): δ=8.74 (m); δ8.34 (m); δ8.19 (m); δ7.94(m).

7.3.3. Synthesis of [Co(tppz)Cl]Cl·2H_2O (2)

$CoCl_2 \cdot 6H_2O$ (371 mg, 1.56 mmol) was dissolved in 20 ml of water in a 100 ml Erlenmeyer flask. Tppz (100mg, 0.26 mmol) was added and the mixture was stirred at 70 °C for 30 min. EtOH (10 ml) was added to dissolve the remaining solid of tppz. The resulting red solution was stirred at 90 °C for 4 hour, cooled to room temperature and evaporated to dryness. After crystallisation from EtOH red fine needles were obtained. The product was allowed to dry over P_4O_{10}. Yield: 28%.

Anal.calcd.: C 51.98, H 3.61, N 15.16; found: C 52.08, H 3.42, N 15.18.

IR (KBr, cm^{-1}); ν(C=C), ν(C=N):1636 s; 1597 s; 1543 w; 1510 w; 1472 m; 1456 m; 1416 m; 1386 m.

UV: (H_2O, nm) λ_{1max}=295; λ_{2max}=325; ε_1= 6586 ; ε_1=6230.

FAB-mass spectrum (70 eV) $[Co(tppz)Cl]Cl{\cdot}2H_2O$.

m/e	relative intensity (%)	fragment
482	100	$[Co(tppz)Cl]^+$
446	55	$[Cu(tppz)]^+$

7.3.4. Synthesis of $[Co(tppz)(ma)(H_2O)]{\cdot}4H_2O$ (3)

$CoCl_2{\cdot}6H_2O$ (123 mg, 0.52 mmol) was dissolved in 20 ml of water in a 100 ml Erlenmeyer flask. Tppz (100 mg, 0.26 mmol) was added and the mixture was stirred at 90 °C for 30 min. EtOH (10 ml) was added to dissolve the remaining solid of tppz. To the resulting red solution (38 mg, 0.26mmol) of Na-malonate was added and stirred at 90 °C for 1 h. The solution was cooled to room temperature and filtered into a 100 ml Erlenmeyer flask. After slow evaporation in air red crystals were obtained. The product was allowed to dry over P_4O_{10}. Yield: 52%.

Anal.calcd.: C 50.66, H 4.37, N 13.13; found: C 49.98, H 4.14, N 12.62. IR (KBr, cm^{-1}); ν(C=C), ν(C=N): 1573 vs,sh; 1477 m; 1400 vs,sh; 1386 m.. UV (H_2O, nm): λ_{1max}=300; λ_{2max}=320; ε_1=4405; ε_1=4405.

7.3.5. Synthesis of $[Ni_2(tppz)(H_2O)_6](NO_3)_4{\cdot}3H_2O$ (4)

$Ni(NO_3)_2$ x $6H_2O$ (453 mg, 1.56 mmol) was dissolved in 20 ml of water in a 100 ml Erlenmeyer flask. Tppz (100 mg, 0.26 mmol) was added and the mixture was stirred at 90 °C for 30 min. EtOH (10 ml) was added to dissolve the remaining solid of tppz. The resulting red brown solution was stirred at 90 °C for 4 h, cooled to room temperature and filtered into a 100 ml Erlenmeyer flask. After several days large red brown needles were obtained. The product was allowed to dry over P_4O_{10}. Yield: 38%.

Anal.calcd.: C 31.44, H 3.71, N 15.28 found: C 31.39, H 3.65, N 14.98. IR (KBr, cm^{-1}); ν(C=C), ν(C=N): 1600 m; 1573 m; 1546 w; 1477 m; 1385 vs,sh.

UV (H_2O, nm): λ_{1max}=295; λ_{2max}=350; ε_1=23080; ε_1=22890.

7.3.6. Synthesis of $[Ni(tppz)(ox)(H_2O)]\cdot 5H_2O$ (5)

Ni-oxalate 227 mg (1.56 mmol) was dissolved in 20 ml of water in a 100 ml Erlenmeyer flask. tppz 100 mg (0.26 mmol) was added and the mixture was stirred at 90 °C for 30 min. EtOH (10 ml) was added to dissolve the remaining solid of tppz. The resulting red brown solution was stirred at 90 °C for 4 h, cooled to room temperature and filtered into a 100 ml Erlenmeyer flask and evaporated slowly in air. After several days red brown needles were obtained. the product was allowed to dry over P_4O_{10}. Yield:45%.

Anal.calcd.: C 48.50, H 4.35, N 13.05; found: C 48.33, H 4.33, N 13.09.

IR (KBr, cm^{-1}); ν(C=C), ν(C=N): 1635 vs,sh; 1600 s; 1569 s,sh; 1479 w; 1466 w;1403s.

UV (H_2O, nm): λ_{1max}=290; λ_{2max}=350; ε_1=9786; ε_1=8514.

7.3.7. Synthesis of $[Ni_2(tppz)(SCN)_4(H_2O)_2]$ (6)

NH_4NCS (25 mg, 0.33 mmol) was dissolved in 20 ml of water in a 100 ml Erlenmeyer flask. $[Ni_2(tppz)(H_2O)_6](NO_3)_4\cdot 3H_2O$ (100 mg, 0.11 mmol) was added and the resulting solution was stirred at 70 °C for 1 h and cooled to room temperature. An orange precipitate was obtained. After recrystallization from 40 ml water fine crystals were isolated. The product was allowed to dry over P_4O_{10}. Yield: 66%.

Anal.calcd.: C 41.32, H 2.21, N 17.22; found: C 41.82, H 2.22, N 17.41.

IR (KBr, cm^{-1}): 3362 br; 2099 vs, sh; 1634 m; 1597 s; 1477 m; 1386 s,sh.

7.3.8. Synthesis of $[\{Ni_2(tppz)(N(CN)_2)_2(H_2O)_4\}(NO_3)_2]_x$ (7)

$KN(CN)_2$ (18 mg, 0.16 mmol) was dissolved in 20 ml of water in a 100 ml Erlenmeyer flask. $[Ni_2(tppz)(H_2O)_6](NO_3)_4\cdot 3H_2O$ (150 mg, 0.16 mmol) was added and the resulting solution was stirred at 70 °C for 30 min., cooled to room temperature and filtered into a 100 ml

Erlenmeyer flask. Very fine orange crystals were obtained. The product was washed which water, recrystallized from a water/MeOH mixture (1:1) and allowed to dry over P_4O_{10}. Yield:48%.

Anal.calcd.: C 40.33, H 2.88, N 20.16; found: C 41.08, H 3.55, N 20.21. IR (KBr, cm^{-1}): 3242 br; 2309 m; 2240 m; 2187 vs; 1661 m; 1599 m; 1568 m; 1468 m; 1399 vs, sh; 1321 vs, sh.

7.3.9. Synthesis of $[Ni_2(tppz)_2](C(CN)_3)_2 \cdot 2H_2O$ (8)

$KC(CN)_3$ (28 mg, 0.22 mmol) was dissolved in 20 ml of water in a 100 ml Erlenmeyer flask. $[Ni_2(tppz)(H_2O)_4](NO_3)_4 \cdot 3H_2O$ (100 mg, 0.11 mmol) was added and the resulting solution was stirred at 70 °C for 30 min., cooled to room temperature and filtered off. The orange precipitate was washed whith water and allowed to dry over P_4O_{10}. After recrystallization from a methanol/water solution fine orange plates could be isolated. Yield:61%.

Anal.calcd.: C 63.95, H 1.90, N 23.98; found: C 63.55, H 2.25, N 23.50. IR (KBr, cm^{-1}); ν(C=C), ν(C=N): 1599 m, sh; 1569 m; 1542 w; 1480 m; 1469m; 1446m and 1403s; ν(CN) 2157vs, sh.

FAB mass spectrum (70 eV) of $[Ni(tppz)_2](C(CN)_3)_2 \cdot 2H_2O$.

m/e	rel. intensity (%)	fragment
925	28	$[\{Ni(tppz)_2\}\ (C(CN)_3)]^+$
835	45	$[Ni(tppz)_2]^+$
447	98	$[Ni(tppz)]^+$

7.3.10. Synthesis of $[Ni_2(tppz)(H_2O)_6](sqac)_2 \cdot 1.5H_2O$ (9)

$[Mn(H_2O)_4(sqacH)_2$ (57 mg, 0.16 mmol) was dissolved in 20 ml of water in a 100 ml Erlenmeyer flask. $[Ni_2(tppz)(H_2O)_6](NO_3)_4 \cdot 3H_2O$ (150 mg, 0.16 mmol) was added and the

resulting solution was stirred at 70 °C for 30 min., cooled to room temperature and filtered into a 100 ml Erlenmeyer flask. Very fine orange crystals were obtained. The product was washed with water, recrystallized from a water/MeOH mixture (1:1) and allowed to dry over P_4O_{10}. Yield:75%.

Anal.calcd.: C 43.61, H 4.28, N 10.90; found: C 43.90, H 4.56, N 11.05. IR (KBr, cm^{-1}): 1631m; 1597m; 1473br, sh, vs; 1303m. UV (H_2O, nm): λ_{1max}=295; λ_{2max}=350; ε_1=22120; ε_1=20650.

7.3.11. Synthesis of $[Cu_2(tppz)(H_2O)_4](ClO_4)_4 \cdot 2H_2O$ (10)

$Cu(ClO_4)_2$ x $6H_2O$ (184 mg, 0.52 mmol) was dissolved in 20 ml of water in a 100 ml Erlenmeyer flask. Tppz (100 mg, 0.26 mmol) was added and the mixture was stirred at 90 °C for 30 min. EtOH (10 ml) was added to dissolve the remaining solid of tppz. The resulting green solution was stirred at 90 °C for 4 h, cooled to room temperature and filtered into a 100 ml Erlenmeyer flask. After slow evaporation in air deep green crystals were obtained. (A better crystallization occurs with a small excess of $Cu(ClO_4)_2 \cdot 6H_2O$). Yield: 58%.

Anal.calcd.: C 28.20, H 2.74, N 8.22; found: C 27.93, H 3.01, N 8.18. IR (KBr, cm^{-1}); ν C=C, ν C=N: 1626 m; 1599 m; 1495 m; 1477 w; 1424 m; 1390 w. UV (H_2O, nm): λ_{1max}=300; λ_{2max}=362; ε_1=23340; ε_1=20830.

7.3.12. Synthesis of $[Cu(tppzH)Cl]_2(ClO_4)_4$ (11)

$Cu(ClO_4)_2 \cdot 6H_2O$ (95 mg, 0.26 mmol) was dissolved in 20 ml of water in a 100 ml Erlenmeyer flask. tppz (100 mg; 0.26 mmol) was added and the mixture was stirred at 90 °C for 30 min. EtOH (10 ml) and 1M HCl were added to dissolve the remaining solid of tppz. The resulting green solution was stirred at 90 °C for 45 min., cooled to room temperature and filtered into a 100 ml Erlenmeyer flask. This compound was also obtained by the reaction of $CuCl_2 \cdot 2H_2O$ with tppz (molar ratio 1:1) and with 1M $HClO_4$ under the same conditions. Yield: 73%.

Anal.calcd.: C 41.77, H 2.79, N 12.20; found: C 41.94, H 2.49, N 12.23. IR (KBr, cm^{-1}); ν(C=C), ν(C=N): 1626 m; 1614 m; 1601 m; 1589 w,sh; 1571 w; 1549 w; 1533 m; 1469 m; 1460 m; 1442 m; 1403 m; 1383 m; 1344 w; 1300 m. UV (H_2O, nm): λ_{1max}=300; λ_{2max}=360; ε_1=28380; ε_1=26050.

FAB-mass spectrum (70 eV) of $[Cu(tppzH)Cl]_2(ClO_4)_4$.

m/e	relative intensity (%)	fragment
551	5	$[Cu(tppz)H]^+$
486	6	$[Cu(tppz)Cl]^+$

7.3.13. Synthesis of $[Cu_2(tppz)Cl_4]\cdot 5H_2O$ (12)

$CuCl_2\cdot 2H_2O$ (257 mg, 1.56 mmol) was dissolved in 20 ml of water in a 100 ml Erlenmeyer flask. tppz (100 mg, 0.26 mmol) was added and the mixture was stirred at 90 °C for 30 min. EtOH (10 ml) was added to dissolve the remaining solid of tppz. The resulting green solution was stirred at 90 °C for 4 h, cooled to room temperature and filtered into a 100 ml Erlenmeyer flask. After several days dark green block like crystals were obtained, washed with a small amount of water and allowed to dry over P_4O_{10}. Yield: 53%.

Anal.calcd.: C 38.53, H 3.47, N 11.23; found: C 38.43, H 3.38, N 11.08. IR (KBr, cm^{-1}); ν C=C, ν C=N: 1635 m; 1595 m; 1542 w; 1474 m; 1420 s; 1385 m. UV (H_2O, nm): λ_{1max}=306; λ_{2max}=363; ε_1=23430; ε_2=20420.

FAB-mass spectrum (70eV) of $[Cu_2(tppz)Cl_4]\cdot 5H_2O$.

m/e	relative intensity (%)	fragment
584	5	$[Cu_2(tppz)Cl_2]^+$
549	5	$[Cu_2(tppz)Cl]^+$
514	5	$[Cu(tppz)]^+$
486	12	$[Cu_2(tppz)Cl]^+$

7.3.14. Synthesis of $[\{Cu_2(tppz)(ox)(H_2O)_2\}(ClO_4)_2]_x$ (13)

Na-oxalate (26 mg, 0.19 mmol) was dissolved in 20 ml of water in a 100 ml Erlenmeyer flask. $[Cu_2(tppz)(H_2O)_4](ClO_4)_4$ (100 mg, 0.19 mmol) was added and the resulting green solution was stirred at 70 °C for 4 h, cooled to room temperature and filtered into a 100 ml Erlenmeyer flask. After one day very fine green needles were obtained. The product was washed with water and allowed to dry over P_4O_{10}. Yield:61%.

Anal.calcd.: C 37.18, H 2.38, N 10.01; found: C 37.23, H 2.41, N 9.98.

IR (KBr, cm^{-1}); ν(C=C), ν(C=N): 1659 vs; 1605 m; 1569 m; 1542 m; 1482 m; 1472 m; 1446 m; 1404 s.

UV (H_2O, nm): λ_{1max}=300; λ_{2max}=363; ε_1=8965; ε_1=7782.

FAB-mass spectrum (70eV) of $[\{Cu_2(tppz)(ox)(H_2O)_2\}(ClO_4)_2]_x$.

m/e	rel. intensity (%)	fragment
836	38	$[Cu_2(tppz)(ox)(H_2O)_2](ClO_4)_2^+$
800	10	$[Cu_2(tppz)(ox)](ClO_4)_2]^+$
602	18	$[Cu_2(tppz)(ox)]^+$
514	50	$[Cu_2(tppz)]^+$
451	72	$[Cu(tppz)]^+$

7.3.15. Synthesis of $\{(Cu(tppz)Cu(terpy)(H_2O)_2\}(ClO_4)_2\}_x$ (14)

2,2':6',2"-terpyridine (44.3 mg, 0.19 mmol) was dissolved in 20 ml of EtOH in a 100 ml Erlenmeyer flask. $[Cu_2(tppz)(H_2O)_4](ClO_4)_4$ (100 mg, 0.19 mmol) was added and the resulting green solution was stirred at 70 °C for 4 h, cooled to room temperature and filtered into a 100 ml Erlenmeyer flask. After one day very fine plates were obtained. The product is sparingly soluble in all common solvents and was washed with water and allowed to dry over P_4O_{10}. Yield:28%.

IR (KBr, cm^{-1}); ν(C=C), ν(C=N): 1598 m, 1578 m, 1500 w, 1476 m, 1452 m, 1395 m, 1323m.

FAB mass spectrum (70eV) of $[Cu(H_2O)_2(tppz)Cu(terpy)](ClO_4)_4$:

m/e	rel. intensity (%)	fragment
783	12	$[Cu(H_2O)_2(tppz)Cu(terpy)]^+$
684	45	$[(terpy)Cu(tppz)]^+$
550	98	$[Cu(tppz)(ClO_4)]^+$
529	35	$[(terpy)Cu(terpy)]^+$
451	80	$[Cu(tppz)]^+$
296	88	$[Cu(terpy)]^+$

7.3.16. Synthesis of $[\{Cu_2(tppz)(H_2pztc)(H_2O)_2\}(ClO_4)_2]_x$ (15)

Pyrazine-2,3,5,6-tetracarboxylic acid (48.6 mg, 0.19 mmol) was dissolved in 20 ml of water in a 100 ml Erlenmeyer flask. $[Cu_2(tppz)(H_2O)_4](ClO_4)_4$ (100 mg, 0.19 mmol) was added and the resulting green solution was stirred at 60 °C for 1 h, cooled to room temperature and the green precipitate was filtered off. The product was washed several times with water and allowed to dry over P_4O_{10}.Yield: 71%.

Anal.calcd.: C 38.13, H 2.18, N 11.12 Cu 12.6; found: C 38.48, H 3.16, N 11.32 Cu 13.2.

IR (KBr, cm^{-1}); ν(C=C), ν(C=N): 1720 s; 1656 vs; 1598 s; 1495 m; 1478 w; 1424 s; 1405.

7.3.17. Synthesis of $[Zn(tppz)Cl_2]$ (16)

$ZnCl_2$ (140 mg, 1.04 mmol) was dissolved in 20 ml of water in a 100 ml Erlenmeyer flask. tppz (200 mg, 0.52 mmol) was added and the mixture was stirred at 70 °C for 30 min. EtOH (5 ml) was added to dissolve the remaining solid of tppz. The resulting yellow solution was stirred at 70 °C for 4 h, cooled to room temperature and filtered into a 100 ml Erlenmeyer

flask. After standing for one day pale yellow crystals were formed. The product was allowed to dry over P_4O_{10}. Yield: 38%.

Anal.calcd.: C 54.88, H 3.07, N 16.00; found: C 53.51, H 3.54, N 15.52. IR (KBr, cm^{-1}); ν(C=C), ν(C=N): 1597 vs; 1573 sh; 1540 m; 1475 m; 1456 m; 1444 w; 1405 vs; 1305 m.

UV (H_2O, nm): λ_{1max}=295; λ_{2max}=315; ε_1=2329; ε_2=2263. ^{1}H-n.m.r. (CD_2Cl_2): δ9.12(m); δ8.68(m); δ8.25(m), δ8.06(m); δ7.76(m); δ7.64(m); δ7.57(m); δ7.31(m).

7.3.18. Synthesis of [Zn_2(tppz)Cl_4] (17)

In a 100 ml Erlenmeyer flask, $ZnCl_2$ (420 mg, 3.12 mmol) was dissolved in 20 ml of a water/alcohol (1:1) solution. Tppz (200 mg, 0.52 mmol) was added and the mixture stirred at 90 °C for one hour and repeated for several times.. The resulting yellow solution was cooled to room temperature and filtered into a 100 ml Erlenmeyer flask. After several days a deep yellow precipitate was obtained. The product was allowed to dry over P_4O_{10}. Yield: 68%.

Anal.calcd.: C 43.61, H 2.44, N 12.71; found: C 42.93, H 2.67, N 12.51. IR (KBr, cm^{-1}); ν(C=C), ν(C=N): 1594 s; 1575 w; 1475 m; 1456 w; 1407 s; 1388 m. UV (H_2O, nm): λ_{1max}=295; λ_{2max}=315; ε_1=5772; ε_2=5562. ^{1}H-NMR (D_2O, DSS): δ=8.70 (m); δ8.21 (m); δ8.02 (m); δ7.69(m).

7.3.19. Synthesis of bis[Zn_2(μ-tppz)H_2OCl(μ-$ZnCl_4$)(μ-$ZnCl_2$)(μ-$ZnCl_3H_2O$)] (18)

$Zn(ClO_4)_2$ (68.3 mg, 0.26 mmol) and tppz (100 mg, 0.26 mmol) were dissolved in 30 ml of a water/alcohol (1:1) solution and stirred at 90 °C for one hour. The resulting solution was allowed to stand for three days at room temperature. The obtained yellow precipitate was filtered and dried over P_4O_{10}. It was identified as the mononuclear $Zn(ClO_4)_2$ complex. 50 mg of this complex [Zn(tppz)(H_2O)$_2$](ClO_4) and 2.03 g $ZnCl_2$ were dissolved in 15 ml of water/alcohol (1:1) and the resulting solution was stirred at 90 °C for one hour. A significant

color change from slight yellow to deeper yellow was observed. After several days a white precipitate was obtained and filtered off. The filtrate was allowed to stand in a closed crystallizer for two months, deep yellow crystals were obtained. The product was allowed to dry over P_4O_{10}.

IR (KBr, cm^{-1}); ν(C=C), ν(C=N): 1605 s; 1597 s; 1547 w; 1473 m; 1456 w; 1412 s; 1388 w.

UV (H_2O, nm): λ_{1max}=295; λ_{2max}=315.

^{1}H-n.m.r. (D_2O, DSS): δ=8.70 (m); δ8.21 (m); δ8.02 (m); δ7.69(m).

7.3.20. $[Zn_2(tppz)(H_2O)_6](NO_3)_4 \cdot 1.5H_2O$ (19)

In a 100 ml Erlenmeyer flask, $Zn(NO_3)$ x 6 H_2O (460 mg, 1.56 mmol) was dissolved in 20 ml of a water/alcohol (1:1) solution. tppz (100 mg, 0.26 mmol) was added and the mixture stirred at 90 °C for one hour. The resulting yellow solution was cooled to room temperature and filtered into a 100 ml Erlenmeyer flask. After several days, deep yellow crystals were obtained. The product was allowed to dry over P_4O_{10}. Yield: 42%.

Anal.calcd.: C 30.84, H 3.85, N 14.99; found: C 29.53, H 3.64, N 14.98.

IR (KBr, cm^{-1}); ν(C=C), ν(C=N): 1595 m; 1574 w; 1538 w; 1476 m; 1385 vs.

UV (H_2O, nm): λ_{1max}=295; λ_{2max}=320; ε_1=4060; ε_2=3880.

^{1}H-n.m.r. ($CDCl_3$ 1 drop DMSO): δ8.62(m); δ7.76(m) δ7.66(m); δ7.43 (m).

7.3.21. Synthesis of $[\{Zn(tppz)(SCN)_2\}]_x$ (20)

NH_4NCS (16 mg, 0.22 mmol) was dissolved in 20 ml of water in a 100 ml Erlenmeyer flask. $[Zn_2(tppz)(H_2O)_6](NO_3)_4 \cdot 1.5H_2O$ (100 mg, 0.11 mmol) was added and the resulting solution was stirred at 70 °C for 30 min., cooled to room temperature and filtered off. The yellow precipitate was washed whith water and allowed to dry over P_4O_{10}. Yield:62%.

Anal.calcd.: C 54.79, H 2.81, N 19.67; found: C 54.60, H 2.98, N 19.59.

IR (KBr, cm^{-1}); ν(C=C), ν(C=N): 2171s, 2080 sh,s, 1598m, 1574m, 1563m, 1545w, 1540m, 1500m, 1463m, 1452m, 1440m, 1423m, 1398m.

Tab. FAB-mass spectrum (70 eV) of $[\{Zn(tppz)(SCN)_2\}]_x$.

m/e	rel. intensity (%)	fragment
511	25	$[Zn(tppz)(SCN)]^+$
569	15	$[Zn(tppz)(SCN)_2]^+$

7.3.22. Synthesis of $[Zn(tppz)(N(CN)_2)(H_2O)(NO_3)]$ (21)

$KN(CN)_2$ (25 mg, 0.24 mmol) was dissolved in 20 ml of water in a 100 ml Erlenmeyer flask. $[Zn_2(TPPZ)(H_2O)_6](NO_3)_4 \cdot 1.5H_2O$ (150 mg, 0.16 mmol) was added and the resulting solution was stirred at 70 °C for 30 min, cooled to room temperature and filtered into a 100 ml Erlenmeyer flask. After one day very fine yellow crystals were obtained. The product was washed whith water and allowed to dry over P_4O_{10}. Yield:61%.

Anal.calcd.: C 52.08, H 3.00, N 23.37; found: C 52.38, H 3.13, N 23.40.

IR (KBr, cm^{-1}): 3245 br; 2309 m; 2241 m; 2187 vs; 1599 m; 1568 m; 1468 m; 1399 m.

Tab. FAB-mass spectrum (70 eV) of $[Zn(tppz)(N(CN)_2)(H_2O)(NO_3)]$.

m/e	rel. intensity (%)	fragment
453	18	$[Zn(tppz)]^+$
519	20	$[Zn(tppz)(N(CN)_2)]^+$

7.3.23. Synthesis of $[Zn(tppz)_2](N(CN)_2)_2 \cdot H_2O$ (22)

$KN(CN)_2$ (50 mg, 0.49 mmol) was dissolved in 20 ml of water in a 100 ml Erlenmeyer flask. $[Zn_2(tppz)(H_2O)_6](NO_3)_4 \cdot 1.5H_2O$ (150 mg, 0.16 mmol) was added and the resulting solution was stirred at 70 °C for 30 min, cooled to room temperature and filtered into a 100 ml Erlenmeyer flask. After recrystallization from a water/MeOH mixture very fine yellow needles were obtained. The product was washed whith water and allowed to dry over P_4O_{10}. Yield:56%.

Anal.calcd.: C 60.03, H 3.27, N 24.24; found: C 60.55, H 3.11, N 24.15.

IR (KBr, cm^{-1}): 3776b; 2300w; 2277m; 2165m; 2128vs; 1597m; 1544m; 1470m; 1444m; 1401s;

UV (H_2O, nm): λ_{1max}=298; λ_{2max}=318; ε_1=4560; ε_2=4080.

7.3.24. Synthesis of $[Zn(tppz)_2](C(CN)_3)_2$ (23)

$KC(CN)_3$ (14 mg, 0.11 mmol) was dissolved in 20 ml of water in a 100 ml Erlenmeyer flask. $[Zn_2(tppz)(H_2O)_6](NO_3)_4 \cdot 1.5H_2O$ 100 mg (0.11 mmol) was added and the resulting green solution was stirred at 70 °C for 4 h, cooled to room temperature and filtered into a 100 ml Erlenmeyer flask. After one day very fine green needles were obtained. The product was washed with water and allowed to dry over P_4O_{10}. Yield:61%.

Anal. calcd.: C 61.46, H 2.19, N 23.04; found: C 61.24, H 3.41, N 22.43.

IR (KBr, cm^{-1}): 2128 vs, 2185 m and 2227m; 1597 m, sh; 1568 m; 1543 w; 1480 m; 1468 m; 1445 m; 1401 s.

UV (H_2O, nm): λ_{1max}=298; λ_{2max}=318; ε_1=3990; ε_2=3690.

Tab. FAB-mass spectrum (70 eV) of $[Zn(tppz)_2](C(CN)_3)_2$.

m/e	rel. intensity (%)	fragment
931	12	$[Zn(tppz)_2(C(CN)_3)]^+$
841	25	$[Zn(tppz)_2]^+$
543	40	$[Zn(tppz)(C(CN)_3)]^+$
453	60	$[Zn(tppz)]^+$

7.4.1. Synthesis of tpymt

This ligand was prepared according to the literature procedure /16/.

IR (KBr, cm^{-1}); ν(C=C), ν(C=N): 1568m, 1536s, 1445s, 1430m, 1378s. ^{1}H-n.m.r. (D_2O/DSS): δ9.11(d, 2H, $^3J_{(H-H)}$=4.94Hz); δ7.85 (t, 1H, $^3J_{(H-H)}$=4.94Hz).

7.4.2. Synthesis of tpymt·4HCl·2H_2O (24)

Tpymt (100 mg, 0.31 mmol) was dissolved in 20 ml of conc. HCl and stirred at room temperature for 30 min. After addition of acetone a precipitation of the hydrochloride salt occurs. The product was allowed to dry over P_4O_{10}.

Anal. calcd.: C 36.23, H 3.01,N 25.36; found: C 35.65, H 2.89, N 25.30.

IR (KBr, cm^{-1}); ν((C=C), ν(C=N): 1660m, 1595w, 1553vs, 1510w, 1400w and 1373w. ^{1}H-n.m.r. (D_2O/DSS): δ8.98 (d, 2H, $^3J_{(H-H)}$=4.85Hz); δ7.85 (t, 1H, $^3J_{(H-H)}$=4.86Hz).

7.4.3. Synthesis of complexes with tpymt and M-perchlorate salts with M= Fe(II), Co(II), Ni(II), Zn(II) and Ag(I) (25a-e)

A 100 ml erlenmmeyer flask is charged with a magnetic stirrbar and (200 mg, 0,63 mmol) tpymt in 20 ml of water was added. After heating the solution up to 60 °C (1.90 mmol) of the corresponding perchlorate salt was added. The reaction mixture was stirred at 60 °C for one hour. The solution was allowed to stand for 24 h. The precipitate was filtered off and washed several times with water and dried over P_4O_{10}.

complex	colour	elemental analyses 1=calc.;2=fnd.;C,H,N	yield in %	infrared C=C, C=N
$[Fe(tpymt)(H_2O)_3](ClO_4)_3]$ (a)	red powder	1: 26.91, 1.35, 18.83 2: 25.30, 1.80, 17.43	54	
$[Co(tpymt)(H_2O)](ClO_4)_2$ (b)	orange powder	1: 31.44, 1.58, 22.00 2: 31.78, 2.00, 22.11	48	1656 m 1586 s 1480 m 1407 s 1376 sh, w
$[Ni(tpymt)(H_2O)_3](ClO_4)_2 \cdot 3H_2O$ (c)	green powder	1: 29.56, 2.13, 20.69 2: 29.83, 2.56, 20.50	62	1657 s 1567 vs 1419 m 1407 s
$[Zn(tpymt)(H_2O)_2](ClO_4)_2] \cdot 2H_2O$ (d)	yellow crystals	1: 27.64, 2.61, 19.34 2: 27.73, 2.51, 19.34	59	1660 m 1558 vs 1484 m 1440 vs 1386 w

$[Ag_2(tpymt)\cdot(ClO_4)_2]$ (e)	orange powder	1: 24.65, 1.23, 17.26 2: 27.90, 1.59, 18.81 Ag_{aas}=27.26%	72	1537 sh, vs 1430 w 1374 sh, s

7.5.4. Synthesis of $[Fe(tpymt)Cl_3]$ (26)

A 100 ml Erlenmeyer flask was charged with a magnetic stirrbar and (200 mg, 0,63 mmol) of tpymt in 20 ml of water was added. After heating the solution up to 60°C (514 mg, 1,9 mmol) of $FeCl_3\cdot 6\ H_2O$ was added. The reaction mixture was stirred at 60°C for one hour. After cooling to room temperature the solution was allowed to stand for several weeks; yellow crystals were obtained. The product was allowed to dry over P_4O_{10}. Yield. 65%.

Anal. calcd.: C 37.73, H 1.9, 26.4; found: C 37.43, H 2.16, N 25.57.

IR (KBr, cm^{-1}); ν(C=C), ν(C=N): 1578m; 1561w; 1539sh,vs; 1428w; 1374s.

7.4.5. Synthesis of $[Ni_2(tpymt)(SO_4)_2]\cdot 2H_2O$ (27)

A 100 ml Erlenmeyer flask is charged with a magnetic stirrbar and (100 mg, 0.32 mmol) tpymt in 20 ml of water was added. After heating the solution up to 60 °C (260 mg, 0.96 mmol) of $NiSO_4\cdot 6H_2O$ was added. The reaction mixture was stirred at 60 °C for one hour. The solution was allowed to stand for 24 h and precipitated with EtOH. The product was allowed to dry over P_4O_{10}. Yield: 65%.

Anal. calcd.: C 25.21, H 2.66, N 17.62, Ni 16.4; found: C 24.99, H 2.99, N 17.21, Ni 16.3.

IR (KBr,cm^{-1}); ν(C=C), ν(C=N): 1590s; 1566m; 1497w; 1412s; 1385m.

7.4.6. Synthesis of $[Zn(tpymt)Cl_2]$ (28)

A 100 ml Erlenmeyer flask is charged with a magnetic stirrbar and (200 mg, 0.63 mmol) TPymT in 20 ml of water was added. After heating the solution up to 60 °C (259 mg, 1.9 mmol) of $ZnCl_2$ was added. The reaction mixture was stirred at 60 °C for one hour. After

cooling to room temperature the solution was allowed to stand for several weeks; a yellow precipitate was obtained. The product was allowed to dry over P_4O_{10}. Yield: 32%.

Anal. calcd.: C 27.64, H 2.61, N 19.34; found: C 27.73, H 2.51, N 19.43.

IR (KBr,cm^{-1}); ν(C=C), ν(C=N): 1660m; 1558vs; 1484m; 1440vs; 1386w.

1H-n.m.r. (D_2O,DSS): δ905(d, 2H, $^3J_{(H-H)}$=4.93Hz); δ7.80 (t, 1H, $^3J_{(H-H)}$=4.93Hz).

7.4.7. Synthesis of $[Ag_2(tpymt)(H_2O)_2]SO_4$ (29)

A 100 ml Erlenmeyer flask is charged with a magnetic stirrbar and (100 mg, 0.32 mmol) tpymt in 20 ml of water was added. After heating the solution up to 60 °C (297 mg, 0.96 mmol) of Ag_2SO_4 was added. The reaction mixture was stirred at 60 °C for one hour. The formed orange solution was filtered and evaporated at room temperature. After several weeks orange crystals were obtained. The product was allowed to dry over P_4O_{10}. Yield: 56 %.

Anal. calcd.: C 27.15, H 1.96, N 19.00; found: C 27.65 H 1.59 N 18.96.

IR (KBr, cm^{-1}); ν(C=C), ν(C=N): 1577w; 1537vs,sh; 1428w; 1374s.

^{1}H-n.m.r. (D_2O/DSS): δ9.26(d, 2H, $^3J_{(H-H)}$=4.4Hz); δ8.03(t, 1H, $^3J_{(H-H)}$=5.2Hz).

7.4.8 Synthesis of $[Cd(tpymt)Cl_2(H_2O)] \times 3\ H_2O$ (30)

A 100 ml Erlenmeyer flask is charged with a magnetic stirrbar and (200 mg, 0.63 mmol) tpymt in 20 ml of water was added. After heating the solution up to 60°C (330 mg, 1.90 mmol) of $CdCl_2$ was added. The reaction mixture was stirred at 60°C for one hour. After cooling to room temperature the solution was allowed to stand for several weeks; yellow cream needles were obtained. Yield: 46 %.

Anal. calcd.: C 34.88, H 2.13, N 24.4; found: C 34.57, H 1.91, N 23.89.

IR (KBr,cm-^{1}); ν(C=C), ν(C=N): 1578s; 1553vs; 1425sh,w; 1374vs.

^{1}H -n.m.r. (D_2O/DSS): δ9.23 (d, 2H, $^3J_{(H-H)}$=4.97Hz); δ7.95(t, 1H, $^3J_{(H=H)}$=4.96Hz).

7.4.9. Synthesis of tpymt x $3TlNO_3 \cdot 0.75H_2O$ (31)

A 200 ml round bottom flask is charged with a magnetic stirring bar and (200 mg, 0,63 mmol) of tpymt and (507 mg, 0,63 mmol) of $TlNO_3$ dissolved in 100 ml of water were added. The reaction mixture was refluxed three times for 8 hours. The ligand was partially dissolved. After filtering the pink solution it was left to evaporate at room temperature. After several weeks pink needles were obtained. The product was allowed to dry over P_4O_{10}. Yield: 42%.

Anal. calcd.: C 16.17, H 0.80, N 15.09; found: C 15.93, H 0.95, N 14.89.

IR (KBr cm^{-1}); ν(C=C), ν(C=N): 1534vs; 1430m; 1373s.

^{1}H-n.m.r. (D_2O/DSS): δ9.05(d, 2H, ^{3}J(H-H)=4.93Hz); δ7.80(t, 1H, ^{3}J(H-H)=4.93Hz).

7.5. Synthesis of new polymers containing H_4pztc

7.5.1. Synthesis of pyrazine-2,3,5,6-tetracarboxylic acid (32)

In a 2 l three necked round bottom flask equipped with reflux condenser, thermometer and mechanical stirrer (4.4g, 0.032 mol) of 2,3,5,6-tetramethylpyrazine and 10g of KOH was dissolved in 1.4 l deionized water at 90°C. $KMnO_4$ (130g, 0.16 mol) was then added in 5g portions over a period of three hours, each subsequent addition of $KMnO_4$ being made after the violet color of the solution disappeared. The mixture was refluxed for an additional hour. The reaction mixture was cooled to 70°C and three portions of 5ml ethanol was slowly added to destroy any excess of $KMnO_4$. The mixture was filtered and the brown precipitate of MnO_2 was washed with three portions of hot water (250 ml), such that the filtrate gave no violet color upon addition of a $FeSO_4$ solution. The filtrate and washings were concentrated to 250 ml under reduced pressure at 40°C. 16% HCl was slowly added to the solution until a pH of 4-5 was obtained. The solution was cooled to 0°C and a white precipitate of the corresponding potassium salt of tetracarboxypyrazine was formed. The precipitate was recrystallized from 20% HCl (at 70°C) resulting in a white solid, identified as pyrazine-2.3.5.6-tetracarboxylic acid. Yield 64%; melting point 196°C.

IR (KBr, cm^{-1}): 1276s; 1339s; 1386s; 1455s; 1746vs; 3220b; 3456b ^{1}H-n.m.r.: ($CDCl_3$) δ5.25 (s, b); u.v.: (H_2O, nm) $\lambda_{(max)}$ = 292.

7.5.2. Synthesis of $[Mg(H_2O)_6\{Mn(pztc)(H_2O)_2\}\cdot 3H_2O]$ (33)

To a solution of $MnCl_2$ (244 mg, 1.94 mmol) dissolved in 20 ml of H_2O a solution of tetracarboxypyrazine (500 mg, 1.94 mmol) in 20 ml of water was added. The reaction mixture was stirred at 50°C under N_2. To this 30 ml of a 2 M acetic acid/ magnesium acetate buffer (equimolar) was added bringing pH to 4.8 - 5.0. The resulting yellow solution was stirred for 15 min and cooled to room temperature. The solution was filtered and allowed to evaporate slowly in air. A yellow precipitate was obtained.

Anal. calcd.: C 18.77; H 3.91; N 5.47 found: C 18.87; H 3.80; N 5.46.

IR (KBr, cm^{-1}): 1181s; 1214s; 1320s; 1427s,sh; 1605s; 1656s; 3407b.

7.2.3. Synthesis of the $[Mg(H_2O)_6\{Cu(pztc)(H_2O)_2\}\cdot 2H_2O]_x$ (34)

To a solution of $CuCl_2$ (260mg, 1.94 mmol) dissolved in 20 ml of H_2O a solution of tetracarboxypyrazine (500 mg, 1.94 mmol) in 20 ml of water was added. The reaction mixture was stirred at 50°C under N_2.To this 30 ml of a 2 M acetic acid/ magnesium acetate - buffer (equimolar) was added , bringing pH to 4.8 - 5.0. The resulting green solution was stirred for 15 min and cooled to room temperature. The solutioo was filtered several times and allowed to evaporate slowly in air. After a few of weeks green crystals were obtained.

Anal. calcd.: C 18.46; H 3.84; N 5.38; found: C 18.28; H 3.54; N 5.40.

IR (KBr cm^{-1}): 1150s; 1175s; 1307s,sh; 1416s,sh; 1645br,s 3409b.

7.5.4. Synthesis of $[UO_2\{Mo(pztc)(H_2O)_2\}\cdot 15H_2O]_x$ (35)

To a solution of $MnCl_2$ (240 mg, 1.94 mmol) dissolved in 20 ml of H_2O a solution of tetracarboxypyrazine (500 mg, 1,94 mmol) in 20 ml of water was added. The reaction mixture

was stirred at 50°C under N_2. To this 30 ml of a 2 M $UO_2(CH_3COO)_2/CH_3COOH$ buffer (equimolar) was added , bringing pH to 4.8 - 5.0. The resulting yellow solution was stirred for 15 minutes and cooled to room temperature. The solution was filtered and allowed to evaporate slowly in air. A green precipitate was obtained.

Anal. calcd.: C 10.87; H 3.85; N 3.17; found: C 11.9; H 1.42; N 3.15.

IR (KBr, cm^{-1}): 1190m; 1322m; 1346m; 1398s; 1635s; 1666s; 3333b.

7.5.6. Synthesis of $\{(UO2)Cu(pztc)(H_2O)_2\}\cdot 14H_2O]_x$ (36)

To a solution of $CuCl_2$ (260 mg, 1.94 mmol) dissolved in 20 ml of H_2O a solution of tetracarboxypyrazine (500 mg, 1.94 mmol) in 20 ml of water was added. The reaction mixture was stirred at 50°C under N_2. To this 30 ml of a 2 M $UO_2(CH_3COO)_2/CH_3COOH$ buffer (equimolar) was added , bringing pH to 4.8 - 5.0. The resulting yellow solution was stirred for 15 min and cooled to room temperature. The solution was filtered and allowed to evaporate slowly in air. After a few of weeks, a yellow precipitate was obtained.

Anal. calcd.: C 10.97; H 3.66; N 3.21; found: C 11.05; H 2.69, N 3.15.

IR (KBr, cm^{-1}): 1156s; 1211w; 1314m; 1344m; 1392s; 1651s; 1684s; 3348b.

Overview of all oew synthesized complexes of tppz